Functional plasticity in the brain. Neuronal integration of ES cell-derived neurons in the hippocampus and the influence of the endocannabinoid system on synaptic plasticity

Von der Fakultät für Lebenswissenschaften

der Technischen Universität Carolo-Wilhelmina

zu Braunschweig

zur Erlangung des Grades eines

Doktors der Naturwissenschaften

(Dr. rer. nat.)

genehmigte

D i s s e r t a t i o n

von Martin Polack
aus Wolfenbüttel

1. Referentin oder Referent: Professor Dr. Martin Korte
2. Referentin oder Referent: Professor Dr. Reinhard Köster
eingereicht am: 21.12.2011
mündliche Prüfung (Disputation) am: 06.03.2012

Druckjahr 2012

VORVERÖFFENTLICHUNGEN DER DISSERTATION

Teilergebnisse aus dieser Arbeit wurden mit Genehmigung der Fakultät für Lebenswissenschaften, vertreten durch den Mentor der Arbeit, in folgenden Beiträgen vorab veröffentlicht:

Tagungsbeiträge

Polack, M., Steinke, L., Lutz, B., Korte, M. *Role of CB1 expression in hippocampal excitatory versus inhibitory neurons in regulating activity-dependent synaptic plasticity.* 7th Forum of European Neuroscience; 3.-10. Juli 2010, Amsterdam, NL.

Polack, M., Steinke, L., Lutz, B., Korte, M. *Role of CB1 expression in hippocampal excitatory versus inhibitory neurons in regulating activity-dependent synaptic plasticity.* The 9th Göttingen Meeting of the German Neuroscience Society; 23.-27. März 2011, Göttingen, DE.

Every man must decide

whether he will walk in the light of creative altruism

or in the darkness of destructive selfishness

- Martin Luther King Jr.

Table of contents

Abstract

Learning and memory processes challenge the neuronal network in the brain to be highly plastic during embryonic development until high ages. At the subcellular level, those processes are involved in structural as well as functional plasticity at synapses. In hippocampal pyramidal neurons of the CA1 region strengthening of these neuronal connections is known as long-term potentiation (LTP), while weakening is called long-term depression (LTD). The cellular processes involved in LTP and LTD are widely investigated but already from the beginning on additional modulators of plasticity were found. One potential candidate for modulating plasticity is the endocannabinoid receptor 1 (CB1R). Indeed, strong evidence exists for its influence on behavior, anxiety, short-term plasticity and long-term plasticity. Using two different mouse lines lacking the CB1R on either glutamatergic or GABAergic axon terminals in the hippocampus, I was able to show the influence of the CB1R on functional synaptic plasticity in the hippocampal neuronal network. My findings support the ambivalent character of the endocannabinoid system demonstrated in previous experiments by revealing increased LTP in animals deficient of the CB1R in glutamatergic neurons, and, in contrast to this a decreased LTP in animals deficient of the CB1R in GABAergic neurons. These results may support the endocannabinoids' influence on homeostasis in excitatory circuits.

In a second project the influence of synaptic plasticity and the potential predefined fate of transplanted ES-cell derived neurons (ESNs) on the final cell type were investigated during adult neurogenesis. Since this process continues during adult life in the dentate gyrus of the hippocampus, it is assumed that newly generated neurons may integrate into a pre-existing circuit. A previous study elucidated maturation as well as integration of transplanted ESNs in organotypic hippocampal slices using a morphological approach. Thus, based on the same transplantation system the functional integration of ESNs into pre-existing circuits by electrophysiological experiments was investigated. As a result, I found that transplanted ESNs mature and integrate into the pre-existing neuronal network. Basically, ESNs showed electrophysiological qualities (such as action potentials and miniature excitatory postsynaptic currents) of neighboring intrinsic pyramidal neurons. Moreover, I was able to provide evidence for neuronal electrical connections between the ESNs and intrinsic cells as well as AMPAR mediated currents but the absence of NMDAR mediated currents in ESNs of the hippocampal CA3 region throughout stimulation in the CA1 region.

Zusammenfassung

Lern- und Gedächtnissvorgänge fordern vom neuronalen Netzwerk in unserem Gehirn Plastizität von der embryonalen Entwicklung an bis ins hohe Alter. Diese Prozesse sind auf subzellulärer Ebene an Veränderungen funktionaler und struktureller Plastizität der Synapsen gebunden. Unter anderem in hippokampalen Neuronen der CA1 Region wird die Verstärkung der synaptischen Verbindung Langzeitpotenzierung (LTP) genannt, während im Gegensatz dazu die Abschwächung als Langzeitdepression bekannt ist. Die zellulären Prozesse, welche LTP und LTD unterliegen, sind zwar umfassend untersucht, allerdings wurden schon früh verschiedene Modulatoren synaptischer Plastizität identifiziert. Ein potentieller Kandidat ist der Endocannabinoid Rezeptor 1 (CB1R). Vieles deutet darauf, dass er Einfluss auf Verhalten, Angstzustände, Kurzzeitplastizität und Langzeitplastizität nimmt.

Mit Hilfe zweier Mauslinien, denen entweder der CB1R vollständig in allen glutamatergen Axonterminalen oder GABAergen Axonterminalen fehlte, war es mir möglich den Einfluss vom CB1R auf funktionelle synaptische Plastizität im hippokampalen Netzwerk zu untersuchen. Meine Ergebnisse unterstützen zudem den ambivalenten Charakter des endocannabinoiden Systems, der bereits in früheren Experimenten gezeigt wurde. Das LTP in Mäusen mit fehlendem CB1R in glutamatergen Neuronen im Hippokampus wies eine signifikante Erhöhung auf, während hingegen das LTP in Mäusen mit fehlendem CB1R in GABAergen Neuronen signifikant reduziert war. Diese Ergebnisse deuten auf eine Rolle des endocannabinoiden Systems für die Homöostase in erregenden Netzwerken hin.

Ein zweites Projekt untersuchte die funktionelle Plastizität transplantierter embryonaler Mausstammzellen (ES-Zellen) während adulter Neurogenese, da diese im *Gyrus dentatus* des Hippokampus bis ins hohe Alter stattfindet. Dies deutet darauf hin, dass sich neu gebildete Neurone in das bereits existierende Netzwerk integrieren können. Eine Studie zeigte dies auf morphologischer Ebene in organotypischen hippokampalen Schnittkulturen. Unter Nutzung derselben Transplantationsmethode konnte ich mit Hilfe von elektrophysiologischen Experimenten zeigen, dass transplantierte ES-Zellen vorwiegend typische elektrophysiologische Parameter besitzen. Außerdem sind sie in das neuronale Netzwerk zwischen der CA1 und CA3 Region eingebunden und zeigen durch AMPA- aber nicht durch NMDA-Rezeptoren induzierte Ströme.

1. Introduction

Approximately 100 billion neurons in the human brain are connected via 15 trillion synapses. The complexity of this neuronal network underlies numerous processes involved in neurogenesis, maturation, maintenance and plasticity. Over 50 years it is now known, that the brain is able to create new neurons in two areas in the brain throughout embryonic development. The fact that adult neurogenesis is present in the brain added a new flavor to plasticity, maturation and maintenance in pre-existing networks. Longer than adult neurogenesis another form of plasticity in neuronal circuits is known. Synaptic plasticity is the ability for strengthening and weakening of synaptic connections between neurons. Synaptic plasticity is nowadays an accepted model for the cellular processes of learning and memory. Besides this, there are various modulators known which directly or indirectly influence both directions of synaptic plasticity.

1.1 Adult neurogenesis

The exigency for neurogenesis in a developing embryonic neuronal network is increasingly accepted since the beginning of investigations in medicine and neuroscience. In contrast, the adult central nervous system was for a long time thought to be static and not able to renew or repair itself. With rising knowledge about the complexity of the architecture of the neuronal network and the mechanisms on cellular level debates started how a newly born neuron may integrate into pre-existing circuits.

For the first time, studies in the 1960s provided evidence for adult neurogenesis by investigations of the telencephalon (Altman and Das, 1965) in rats first and in monkeys afterwards (Kornack and Rakic, 1999). Until today two regions were identified which possess the ability to generate neurons until adulthood: the subgranular zone (SGZ) in the dentate gyrus (DG) of the human hippocampus (Eriksson et al., 1998;Gage et al., 1995;Kuhn et al., 1996) as well as the subventricular zone (SVZ) of the lateral ventricles (Lois and Alvarez-Buylla, 1993). In fact, the fate of those new born neurons is well-known for both regions. Whereas stem cells of the SVZ migrate to the olfactory bulb along the rostral migratory stream and consequently differentiate into interneurons, cells of the SGZ develop to granule

cells in the dentate gyrus. During maturation stem cells of the SGZ pass different developmental stages shown in Figure 1.

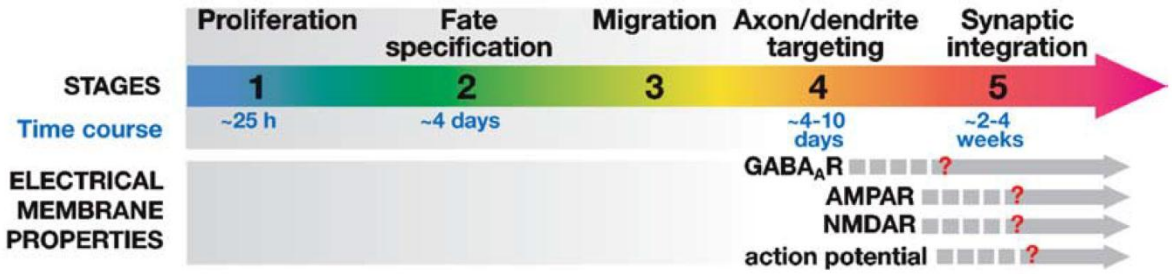

Figure 1: Schematic time course of adult neurogenesis in the dentate gyrus of the hippocampus (modified from (Ming and Song, 2005).

Along these stages typical neuronal characteristics and criteria were found. Furthermore, studies showed axons extending in the CA3 region (Hastings and Gould, 1999;Stanfield and Trice, 1988) and cells which receive synaptic input (Kaplan and Hinds, 1977). Adult born granule cells were shown to carry not only excitatory (van et al., 2002) but also inhibitory (Liu et al., 2005) synapses. In addition, morphological (Zhao et al., 2006) and electrophysiological (Ambrogini et al., 2004;Esposito et al., 2005;Liu et al., 1996) studies have elegantly confirmed that the adult brain is still able to provide the environment for a specific development of new-born neurons.

Attention is now turning on the mechanisms responsible for integration of new born neurons into pre-existing circuits. There is evidence that γ-aminobutyric acid (GABA) and inhibiting input from GABAergic interneurons mediates integration on the synaptic level (Ge et al., 2006). In the hippocampus, which is important in the context of learning and memory, the NMDA receptor plays a crucial role for functional synaptic plasticity. Interestingly, new findings indicate an additional role of NMDA receptors for synaptic integration of new born neurons (Tashiro et al., 2006).

1.2 The endocannabinoid system

The eponymous agriculture plant *cannabis sativa,* known for 2500 years, was utilized in ancient medicine to treat pain and epilepsy (Adams and Martin, 1996). The group of the cannabinoids is the main active component and includes the nowadays prominent psychoactive Δ^9-tetrahydrocannabinol (THC). In 1964 its chemical structure was identified and research continued to uncover the first high affine binding site for cannabinoids in the cortical membrane (Devane et al., 1988). These findings were further supplemented by studies elucidated that two g-protein coupled receptors in the mammalian brain are capable to bind to endogenous cannabinoids (Matsuda et al., 1990;Munro et al., 1993).

1.2.1 Endocannabinoids

Endogenous cannabinoids (endocannabinoids) are part of a class of eicosanoids and derivatives of the arachidonic acid conjugated with ethanolamine or glycerol (Lutz, 2007;Lopez-Rodriguez et al., 2001). Since endocannabinoids are lipid-signaling molecules with a hydrophobic character it is not possible to use vesicles for secretion. Besides, their precursors are located directly in the cell membrane. This assures a rapid synthesis and release during fast timing actions in the brain and supports the endocannabinoids as potential candidates in modulating the transient short-term synaptic transmission (Piomelli, 2003).

The first identified endocannabinoid was N-Arachidonoylethanolamine (Anandamid, AEA) exhibiting a pharmacological similarity to THC but a different molecular structure (Devane et al., 1992). AEA is synthesized in relatively low levels from its phospholipid precursor N-arachidonolyl-phosphatidylethanolamin (N-ArPE) via phospholipase C (PLC), phospholipase A2 or NAPE-phospholipase D (Wang and Ueda, 2009). N-ArPE by itself is synthesized through N-acyltransferase (NAT) by adding arachidonic acid to cephalin (Natarajan et al., 1982;Cadas et al., 1997). Next, synthesis of N-ArPE by NAT is Ca^{2+} and cAMP dependent and regulated by phosphorylation of NAT. This phosphorylation on the other hand is mediated by the cAMP dependent activity of the protein kinase A (PKA) (Piomelli, 2003;Cadas et al., 1996). Finally, the last and most important step concerning synaptic plasticity is the processing of AEA via

the N-acyl phosphatidylethanolamin (NAPE)-specific phospholipase D (NAPE-PLD) and the subsequent release of AEA. The activity pattern of NAPE-PLD is related to depolarization of the cell, activity of the NMDAR and the α7 nicotinic receptors in cortical neurons (Stella and Piomelli, 2001) as well as metabotropic receptors for dopamine, acetylcholine and glutamate (Stella and Piomelli, 2001;Giuffrida et al., 1999;Varma et al., 2001). AEA has various effects in the body mediated primarily by the endocannabinoid receptor 1 (CB1R) in the central nervous system and the endocannabinoid receptor 2 (CB2R) in the immune system (Pacher et al., 2006).

Another important endocannabinoid which is able to bind to the CB1R is known as 2-arachidonoylglycerol (2-AG). In contrast to AEA, it consists of an ester synthesized from omega-6 fatty acid arachidonic acid as well as glycerol and is apparent at relatively high levels in the central nervous system (CNS) under the influence of the PLC. It is likely that activation of metabotropic receptors is important for the initiation of the synthesis as metabotropic receptors are associated with phosphatidyl-inositol-specific PLC and diacylglycerollipase (DGL) signaling (Stella et al., 1997).

However, other identified endocannabinoids are palmitoylethanolamide (PEA), 2-arachidonyl glyceryl ether, N-arachidonoyl-dopamine (NADA) and virodhamine (OAE) (Pacher et al., 2006;Turu et al., 2009;Freund et al., 2003a). It is well established that the endocannabinoid system (ECS) is mainly composed of the CB1R, its ligands (basically AEA and 2-AG) as well as ana-and catabolic enzymes (Hill et al., 2009).

The degradation of AEA and 2-AG is mediated by two specific enzymes: the fatty acid amide hydrolase (FAAH) (Hillard and Jarrahian, 2000;Di, V and Deutsch, 1998;Maccarrone et al., 1998;Cravatt et al., 1996) and the monoacylglycerol lipase (MAGL) (Basavarajappa, 2007). FAAH is responsible for the degradation of AEA, MAGL hydrolyzes 2-AG by ~85% (Savinainen et al., 2011).

1.2.2 The cannabinoid receptors

To our knowledge, there exist two cannabinoid receptors termed CB1- and CB2 receptor (Pacher et al., 2006), but there is accumulating evidence for the existence of more receptors (Begg et al., 2005). The CB2R is primarily expressed in peripheral tissues of the immune system (Galiegue et al., 1995) and can be found exclusively in microglia of the CNS (Pertwee, 2006) or in low density distribution (Onaivi, 2006).

CB1 receptors were found mainly on the presynaptic site of GABAergic axon terminals (Herkenham, 1991;Davies et al., 2002) with surprisingly up to 450 receptors in one axon terminal. Importantly, the receptor density is 10-50 times higher than classical transmitter-receptors like dopamine and opioids (Howlett et al., 2002;Herkenham et al., 1991).

The CB1R is a G protein-coupled receptor which contains seven transmembrane domains connected by three extracellular and three intracellular loops, an intracellular C-terminal and an extracellular N-terminal tail (Elphick and Egertova, 2001). It is important to note that the CB1R plays a key role in the modulation of transmitter release and synaptic communication in the CNS. Hence, the CB1R can be widely found on glutamatergic- and GABAergic neurons of the hippocampus and is therefore a crucial modulator of the reversible suppression of excitatory and inhibitory neurotransmitter release (Heifets and Castillo, 2009;Katona et al., 2000).

1.2.3 The endocannabinoid system and synaptic plasticity

Synaptic plasticity is assumed as activity-dependent modifications respectively the ability of modulating synaptic efficacy (see 1.4). In fact, the endocannabinoid system is a known modulator of activity-dependent plasticity and its active components can be found in plasticity related regions of the brain (Katona et al., 1999). As the CB1R is expressed in excitatory as well as inhibitory neurons of the hippocampus, it appears to be an additional player in the complex network of short-term and long-term synaptic plasticity.

Activation of the postsynaptic cell induces the post-synaptical synthesis of endocannabinoids, which consequently diffuse retrogradely to the presynaptic membrane

and bind to the CB1R. As a result, the neurotransmitter release of the presynaptic cell is inhibited. Despite the fact that this pathway is well described (Steiner et al., 2008), there is also evidence for self-inhibition of the cell which synthesized the endocannabinoid itself (Bacci et al., 2004).

Short-term synaptic plasticity

After a brief depolarization of cells, the retrograde transport of endocannabinoids is only transient and the following inhibition of GABAergic synaptic input was therefore termed depolarization-induced suppression of inhibition (DSI) (Llano et al., 1991;Pitler and Alger, 1992). Besides that, a similar effect was found in the cerebellum where endocannabinoids suppress excitatory signaling (DSE) (Kreitzer and Regehr, 2001b) and DSI (Kreitzer and Regehr, 2001a). Evidence for the influence of endocannabinoids in short-term synaptic plasticity was strengthened by findings that specific stimulation patterns induce either DSI or DSE, which is mediated by endocannabinoids in different areas of the brain (Brown et al., 2003;Maejima et al., 2001) and hippocampus (Isokawa and Alger, 2005;Ohno-Shosaku et al., 2002b). Taken together, these findings were termed eCB-STD.

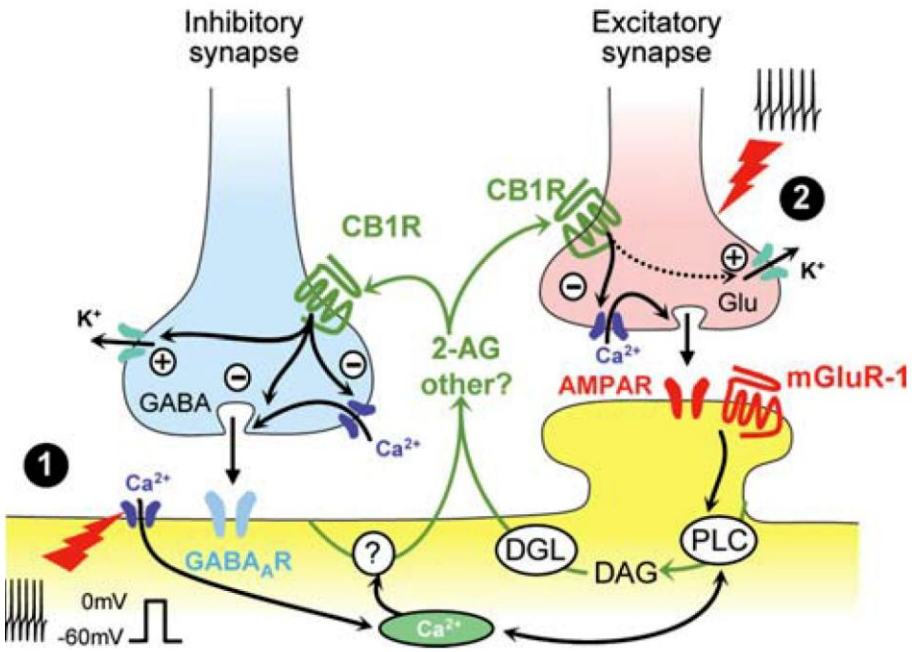

Figure 2: Schematic model of two pathways of endocannabinoid release and eCB-STD. (1) Postsynaptic step depolarization triggers influx of Ca^{2+} via voltage gated channels into the postsynaptic cell, but it is still unknown how this promotes the release of endocannabinoids. **(2)** PLC, DGL and upstream mGluR are necessary for DSI, implicating the synthesis of 2-AG. Both pathways are autonomous, but increased Ca^{2+} levels enhance PLC activity. Interaction of the synthesized endocannabinoids mediates inhibition of presynaptic Ca^{2+} channels and/or activation K^{+} channels.

In eCB-STD the release of endocannabinoids depends on two different actions. Firstly, influx of Ca^{2+} into the postsynaptic membrane is crucial (Ohno-Shosaku et al., 2002b;Llano et al., 1991;Brenowitz and Regehr, 2003), even if it is achieved by uncaging (Wang and Zucker, 2001). Secondly, activation of postsynaptic metabotropic glutamate receptors (mGluR1) (see Fig. 2) is required in the hippocampus (Ohno-Shosaku et al., 2002a;Varma et al., 2001). Next, coeval increased intracellular Ca^{2+} levels facilitate PLC activation by mGluR1. In this model, PLC acts as a coincidence factor (Hashimotodani et al., 2005). Thus, DGL is required downstream of the PLC indicating the synthesis of 2-AG for endocannabinoid mediated short-term plasticity.

Long-term synaptic plasticity

Long-term plasticity was shown in both excitatory (Safo and Regehr, 2005;Sjostrom et al., 2003) and inhibitory synapses (Chevaleyre and Castillo, 2003). Similar to the processes in short-term plasticity all forms of long-term plasticity in the endocannabinoid system are depressive (eCB-LTD). Homosynaptic eCB-LTD was shown in striatum with mostly similar mechanisms found in eCB-STD (Ronesi et al., 2004). In addition, heterosynaptic eCB-LTD in inhibitory inputs (I-LTD) was found in hippocampus by repetitive activation of glutamatergic inputs in the *stratum radiatum* of the CA1 region (Chevaleyre and Castillo, 2003).

1.3 The hippocampus

Since adult neurogenesis occurs in the DG of the hippocampus and crucial members of the endocannabinoid system also play a role in the hippocampal network, the hippocampus becomes a topic of investigation in this study. The hippocampus is involved in processes of learning and memory. This could be primary found by removing parts of both medial temporal lobes (and therefore approximately two-thirds of both hippocampi) in the patient Henry Gustav Molaison. After surgery, the patient suffered from anterograde amnesia: although his working memory and procedural memory were intact, new information was not stored any longer in the long-term memory (Scoville and Milner, 1957). Later on more details about the role of the hippocampus as a mediator and transmitter for information which is devolved from short-term to long-term memory were revealed (Alvarez et al., 1994). Because the hippocampus is formed by the involuted medial wall of the cortex, it is

anatomically part of the archicortex and resides under the neocortex. From the 18th century on neuroanatomists like Santiango Ramòn y Cajal (1911) and Camillo Golgi (1886) described its laminar structure. The hippocampus can be separated in the following three different regions: dentate gyrus (DG), Cornu ammonis (CA) and Subiculum (Fig. 3). The medial of the three layers forms the cell body layer in all three regions, which is called *stratum granulare* in the DG as it consists of granula cells. In the cornu ammonis and subiculum the medial layer forms the *stratum pyramidale* where pyramidal cells are predominant. In the *cornu ammonis* (CA) it is possible to distingish four different subregions due to morphological differences of the pyramidal cells starting from CA1 to DG in clockwise direction: CA1, CA2, CA3 and CA4. In these regions the apical dendrites of the pyramidal neurons form the *stratum radiatum* whereas the basal dendrites of the pyramidal neurons form the *stratum oriens*.

The projection pattern inside the hippocampus is unique and the intrinsic projections can be conserved by using transversal slices (Skrede and Westgaard, 1971). In a set of experiments I performed, slice cultures were done using a vibratome to minimize disturbances in the hippocampal circuitry (Fig. 3). The hippocampus and the entorhinal cortex (EC) form a functional unit, which is called hippocampus-formation. The EC has reciprocal projections with all primary and secondary layers in the cerebral cortex and

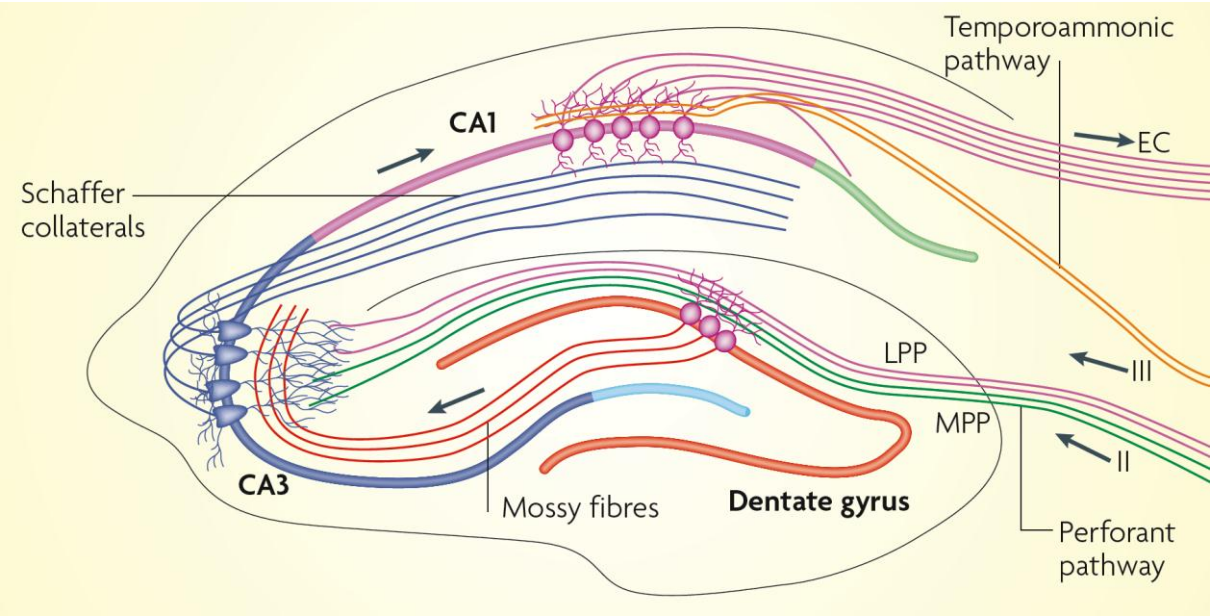

Figure 3: Schematic projections inside the hippocampus. Details see 1.3 (Adjusted after Deng et al., 2010).

projects via the *tractus perforans* (LPP/MPP) to the first member of the trisynaptic pathway, namely the granule cells in the *stratum moleculare* of the DG. The axons of those granule

cells are called mossy fibers (red) and project to the pyramidal cells in the CA3 region (dark blue). Axons of those pyramidal cells project via the S*chaffer collaterals* (blue) to the apical dendrites in pyramidal cells in the CA1 region. From here the fibers project to the contralateral hippocampus and then back to the entorhinal cortex. Along this circled pathway glutamate is the main excitatory neurotransmitter. This pathway is excitatory in general, but modifications are possible by inhibitory interneurons via GABA. Pyramidal excitatory neurons in the CA1 region receive powerful inhibitory input of local GABAergic interneurons located or projecting to all layers of the CA1 region (Chevaleyre et al., 2006). The signal oscillates along the pathway under modification of the synaptic connections of the pyramidal cells. The general modification of signaling strength through neuronal connections between cells (synapses) is called *synaptic plasticity*. The detailed mechanisms will be described in the next chapter.

1.4 Synaptic plasticity

After more than 50 years of the first appearance of the term *synaptic plasticity* by William James, Donald O. Hebb postulated in 1949 the following:

> *„When an axon of cell A … exite(s) cell B and repeatedly and*
> *persistently takes part of firing it, some growth processes*
> *or metabolic changes takes place in one or both cells so that*
> *A´s efficiency as one of the cells firing B is increased. “*

This means for strengthening of a connection between two cells, this connection must be stimulated pre- and postsynaptically at the same time. Hebb defined criteria which can be found today in widely accepted paradigms of synaptic plasticity and later in this work.

1.4.1 Long-term potentiation and long-term depression

In the last decades a large variance of different forms of synaptic plasticity was found. Besides short-term potentiating events like paired-pulse facilitation (PPF; 200 ms), augmentation (10 sec) and post-tetanic potentiation (one min); long term potentiating short-term potentiation (15 min) and long-term potentiation (LTP; > 30 min) are known (Maass and Zador, 1999). In contrast to this, depressing events like short paired-pulse depression (PPD; 200 ms), depletion (10 sec) and long-term depression (LTD; > 30 min) are able to modulate the strength of a cellular response (Maass and Zador, 1999). Due to these antagonistic effects it is possible to define positive and negative synaptic plasticity. In the hippocampus, LTP was found first and it was shown that especially LTP and LTD are two mechanisms concerning synaptic plasticity (Bliss and Lomo, 1973;Dudek and Bear, 1993). LTP and LTD, respectively synaptic plasticity, are nowadays regarded as cellular correlates for learning and memory (Martin et al., 2000;Pastalkova et al., 2006;Whitlock et al., 2006).

The model of Bienenstock (Bienenstock et al., 1982) defines for the induction of LTP and LTD the following principles: above a specific stimulus frequency positive plasticity respectively LTP is generated. This is a long lasting strengthening of the conductance efficiency between neurons. At frequencies below this stimulus frequency LTD is induced. One of Hebb's criteria, namely cooperation, can be confirmed by high-frequent stimuli reaching enough synapses to depolarize the post-synapse. Hebb´s input-specificity describes the requirement that inactive synapses at the same postsynaptic membrane are not potentiated. Synapses are potentiated when receiving input of different sources at the same time (associativity). Most of these effects are based on coincident events at the same post-synapse. Due to its cellular attributes the NMDA receptor (N-methyl-D-aspartate) (NMDAR) is able to detect this coincidence and plays a key role in NMDAR dependent synaptic plasticity. Besides this there are NMDAR independent forms of LTP and LTD: mossy fiber LTP (Johnston et al., 1992) and m-GluR dependent LTD (Bolshakov and Siegelbaum, 1994).

1.4.2 The NMDA receptor

The ionotropic NMDAR is one of two types of glutamate receptors at the synapse and located in the postsynaptic membrane of pyramidal neurons in the CA1 region. Despite its permeability for Ca^{2+} and Na^{+}, it is not important for basal synaptic transmission, which is overall mediated by the AMPA (α-amino-3-hydroxy-5-methyl-4-isoxazolepropionic acid) receptors (AMPAR). The AMPAR (Honore et al., 1982) is an ionotropic transmembrane glutamate receptor which is permeable for Na^{+} and K^{+} and mediates at resting membrane potential the majority of glutamate induced excitatory postsynaptic potentials (EPSPs) at

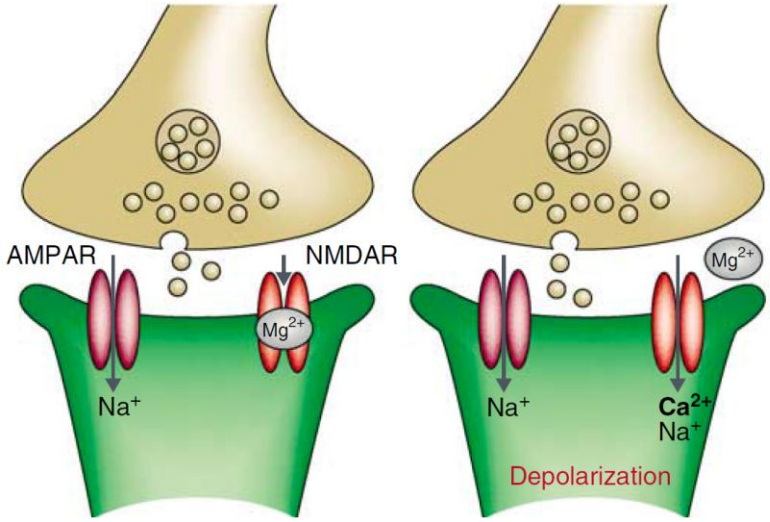

Figure 4: Comparison of synaptic transmission at a synapse before (left) and after (right) glutamate mediated depolarization of the postsynaptic cell. For details see text. (Citri and Malenka , 2008)

basal synaptic transmission. The AMPAR is a tetramer consisting of the four subunits GluR1-4. Conductance, selective ion permeability and open probability are modified by different compositions of these subunits; the GluR2 subunit is responsible for the non-permeability of the NMDAR for Ca^{2+}. This fact is important to understand the cellular mechanism of synaptic plasticity. Two components are necessary for the induction of LTP: presynaptic release of glutamate and at the same time postsynaptic depolarization. The glutamate binds to the AMPAR and NMDAR but opens only the NMDAR and depolarizes the postsynaptic cell via the influx of Na^{+}. Opposing this, the NMDAR does not open immediately after binding of glutamate, because at resting membrane potential the pores of the NMDAR are occluded by Mg^{2+} (Nowak et al., 1984). A contemporary depolarization via the AMPAR mediates the delocalization of the Mg^{2+} (Mayer et al., 1984). Next, the influx of Ca^{2+} is possible and at the same time means the crucial step in the induction of LTP and LTD. In general the influx

pattern is important to mediate these two contrary forms of synaptic plasticity. For LTP a high-frequent train of stimuli is given (Bliss and Lomo, 1973) to assure the ongoing constant depolarization and the release of the Mg^{2+} out of the NMDAR while the next release of glutamate is triggered to bind to both glutamate receptors and results in a fast and massive influx of Ca^{2+}. By modifying the stimulus pattern, the influx of Ca^{2+} can be controlled between rapid massive or tonic but moderate influx profiles. Depending on the influx profile different downstream cascades in the postsynaptic cell are activated to mediate different forms of synaptic plasticity (Malenka et al., 1988;Cummings et al., 1996a;Lisman, 1989).

A short but massive influx of Ca^{2+} is crucial for the induction of LTP, resulting in activation of mainly kinases (Lynch, 2004) such as the Calcium/Calmodulin-dependent protein kinase II (CamKII) which is - except for a short postnatal interval (Yasuda et al., 2003) - essential (Lisman et al., 2002;Malenka et al., 1989;Malinow et al., 1989) for the induction of LTP. Fast strengthening of the synapse transmission can be explained by the induction of CamKII to insert new AMPARs into the postsynaptic membrane by fast vesicle release of intracellular reservoirs and lateral diffusion and the ability of CamKII to phosphorylate AMPARs, thereby increasing their single-channel conductance (Malinow and Malenka, 2002;Malenka and Nicoll, 1999).

Besides these fast and mostly transient changes in synaptic transmission, which is independent from protein-synthesis, the maintenance of long lasting synaptic strengthening for hours or days requires the downstream initiation of gene expression of plasticity-related proteins (Frey et al., 1988a;Krug et al., 1984;Otani and Abraham, 1989). Here, one important mediator is the protein kinase C (PKC) (Bliss and Collingridge, 1993) respectively its isozyme PKMζ, which is highly activated after LTP induction and which deletion or inhibition blocks the long-term maintenance of LTP (Hrabetova and Sacktor, 1996;Ling et al., 2002;Sajikumar et al., 2005a;Sajikumar et al., 2005b;Pastalkova et al., 2006). One key role in synaptic plasticity related gene expression is played by the transcription-factor cyclic-AMP response element-binding protein (CREB) and its phosphorylating protein kinase A (Brindle and Montminy, 1992;Mayr and Montminy, 2001).

Although in this study LTD experiments were not performed, the molecular background will be explained briefly. Due to the higher affinity of phosphatases for Ca^{2+} (Mulkey et al., 1993), a long but moderate influx of Ca^{2+} results in activation of phosphatases which finally induces

a long-term depression (LTD) (Lisman, 1989;Cummings et al., 1996b) with opposing effects to LTP (Kauderer and Kandel, 2000;Manahan-Vaughan et al., 2000;Malinow and Malenka, 2002;Kelleher, III et al., 2004).

Additionally, activity-depending changes in the transport of AMPAR are important for the induction of LTP and LTD (Bredt and Nicoll, 2003;Malenka, 2003).

Functional changes are important at the synapse, especially at synaptic spines, for changes in transient and fast transmission but also in the maintenance of long-lasting synaptic transmission. Regarding the fact that specific memories are often available for a whole lifetime more stable changes must happen in addition. Morphological changes of the highly differentiated neuronal cell are shown in different compartments. The highly dynamic synaptic spines are able to form new synapses or retract from existing neuronal connections and are themselves able to modulate their shape. These morphological changes are in consensus with the previous described bipolar effects: while after LTP inducing stimuli the number and head volume of spines increases (Yuste and Bonhoeffer, 2001), LTD inducing stimuli triggers the opposing effects (Nagerl et al., 2004;Zhou et al., 2004).

.

1.5 Action potentials and excitatory postsynaptic potentials

The fundamental principle of a neuronal network is rooted in its plastic connectivity. Nevertheless, even the best network is not working properly without a solid language for the forwarded information over short and long distances. As neurons are, like the majority of cells, electrically active two important potentials will be introduced, which are widely used in the CNS.

Excitatory postsynaptic potentials

An excitatory postsynaptic potential (EPSP) is a transient depolarization of the postsynaptic membrane mediated by the influx of positive charged ions via ligand-sensitive ion channels or ionotropic receptors into the postsynaptic cell. In this study, excitatory cells were examined where mainly Na^+ is involved in the influx via the glutamate receptors AMPAR and

NMDAR. EPSPs can accumulate at the membrane. If several EPSPs occur at the same patch of the membrane at the same time the summation of the depolarization is elevated. This summation of EPSPs is responsible for the induction of action potentials after obtaining a threshold.

One subclass of EPSPs is the miniature EPSP (mEPSP). Even without stimulation of the presynaptic cell occasionally a single neurotransmitter-filled vesicle will be released into the synaptic cleft and trigger EPSPs at the post-membrane, these are called mEPSPs. In 1951, Bernard Katz revealed the quantal nature of synaptic transmission (Vautrin and Barker, 2003).

The action potential

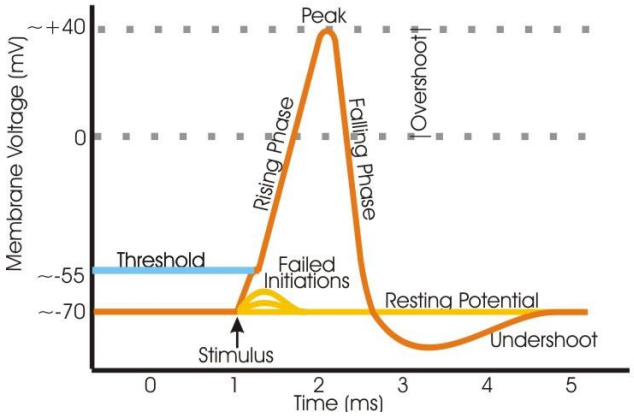

Figure 6: Schematic action potential with described stages in text. (Creative common license)

The action potential (AP) is a short-lasting event where the membrane potential is highly depolarized and hyperpolarized at the postsynaptic membrane in a short time window firstly described in the mathematical Hodgkin-Huxley-model (Hodgkin and Huxley, 1952). The general course of an AP begins with the stable resting membrane potential of the neuron. In this stage almost all Na^+ are closed with only a subset of K^+ channels being open, but these K^+ define the specific resting membrane potential. Excitatory input at the synapses results in EPSPs which are can accumulate and trigger action potentials if the depolarization reaches the threshold at the sensitive axon hillock. Due to the low concentration of Na^+ inside the neuron and the decreasing opening of voltage-gated Na^+ channels an influx of Na^+ begins. The more the membrane depolarizes the more Na^+ channels will open. At the AP threshold of the membrane this positive-feedback loop results in the opening of almost all Na^+ channels and a massive influx and depolarization with a short overshoot where the membrane is positively charged. During the overshoot voltage-gated K^+ channels begin to open and voltage-gated Na^+ channels start to close, this initiates the repolarization of the membrane. While approaching the resting membrane potential during the repolarization the voltage-gated K^+ channels close with a resting increased K^+ conductance. This mediates an undershoot with a hyperpolarized membrane in comparison to the resting membrane potential. During this last stage the axon is not excitable until the resting membrane potential is recovered and the voltage-gated Na^+ are reactivated to ensure the unidirectional character of AP transmission.

1.6 Aim of this study

In this study two different forms of plasticity in the central nervous system were examined. In the first approach I was interested in functional synaptic plasticity in the hippocampus. There exists strong evidence for the hippocampus being involved in processes of learning and memory. Long-term potentiation (LTP) is nowadays an accepted cellular correlate for positive plasticity, while long-term depression (LTD) is used in context of negative plasticity (Dudek and Bear, 1993;Bliss and Lomo, 1973). I performed LTP experiments in two different conditional knockout mice strains for the cannabinoid-receptor 1 (CB1R). The endocannabinoid system is involved in activity-dependent regulation of synaptic plasticity throughout the central nervous system. In addition to well investigated influences on short-term plasticity at excitatory as well as inhibitory synapses (Llano et al., 1991). There is evidence for an endocannabinoid mediated form of long-term LTD in excitatory neurons of the hippocampus, cerebellum and neocortex (Chevaleyre and Castillo, 2003). Here, I investigated the influence of the specific knockout of the CB1 receptor on either all excitatory glutamatergic pyramidal neurons in the hippocampus or all inhibitory GABAergic interneurons on the LTP in pyramidal neurons in the CA1 region.

In a second approach I dealt with a special form of plasticity, adult neurogenesis, and neuronal functional integration in a pre-existing circuit. The subgranular zone of the hippocampus is one of two regions in the brain capable of adult neurogenesis (Eriksson et al., 1998). Recent studies revealed in a subset (type A) of ES cell-derived neuronal precursors (ESNPs) transplanted into organotypic hippocampal slices the typical structure and orientation of intrinsic neurons (Neuser, 2010). A subset of cells carried postsynaptic dendritic spines indicating excitatory input from the neuronal pre-existing circuit. This was previous shown for the hilar region of the dentate gyrus (Benninger et al., 2003). To investigate the functional integration of ESNPs in the CA1 and CA3 region I addressed three questions: First, do transplanted cells of type A are able to generate action potentials and miniature EPSPs and if, are they comparable to neighboring cells? Second, are transplanted type A cells located in the CA3 region capable to receive input from projections of the dentate gyrus via the mossy fibers? Third, do these transplanted cells carry neurotransmitter receptors?

2. Material and Methods

2.1 Equipment

Centrifuge	Sigma – 3K 15
Electrode holder	Biomedical instruments
Incubator	Heraeus – HeraCell 150
Laminar flow hood	BDK-S 1200
Micromanipulator	Leitz
Water bath	Medingen – W12
Cell count chamber	Marienfeld – Neubauer improved
Pico spritzer	Toohey Company
Pipettes	Hirschmann
Tissue Chopper	Mc Illwain
Vertical puller	Narishige – PC-10

2.2 Disposables

Bacteriological dishes 100 mm	Greiner Bio One (633102)
Cannulas 0.60 x 60 mm Sterican®	Braun (4665600)
Cell culture dishes 100 mm, 60 mm	Corning (3073078/3073080)

Cell culture plates 6-well, 12-well	Nunc (140675/150628)
Cell culture plates 6-well, 24-well	TPP (92406/92424)
Cell Strainer 40 µm	BD Falcon (352340)
Coverslips 13 mm	Marienfeld (No.1; 111530)
Cryotubes	Nunc (377267)
Filter for shooting	BD Falcon (353092)
Fluoro-Gel	Electron Microscopy Sciences (17985-10)
Glass capillaries 1.5 mm O.D. x 0.86 mm I.D.	Harward Apparatus (GC150F-10)
Millicell cell culture inserts	Millipore (PICMORG50)
Mycoalert® Mycoplasma detection kit	Lonza (LT-07-108)
Parafilm	Roth (H666.1)
Serological pipettes 2 ml, 5 ml, 10 ml, 25 ml	Sarstedt (86.125-2/3/4/5.001)
Stericup filter unit 250 ml, 500 ml	Millipore (SCGP U02 RE)
Suspension culture dishes 35 mm	Sarstedt (83.1800.002)
Syringes Inject®-F 1 ml	Braun (9166017V)
Tissue tag	Hartenstein (4583)
*Trans*IT®-LT1 Reagent	Mirus Bio (MIR 2300)

2.3 Reagents

Aqua ad iniectabilia	Braun (3703452)
β-Mercaptoethanol	Sigma (M-7522)
B27-Supplement	Invitrogen (17504-044)
BME Medium	Invitrogen (41010-026)
BSA (Bovine serum albumin) - Immuno	Roth (8076.2)
BSA – ES cell culture	Sigma (A-9418)
BrdU (Bromodeoxyuridine)	Roche Diagnostics (10280879001)
Borax Decahydrat	Sigma (B-9876)
Boric acid	Merck (1.00165.0500)
Cytosin-β-D-Arabinofuranosid Hydrochlorid	Sigma (C-6645)
DAPI (4',6-diamidino-2-phenylindole)	Applichem (A4099)
D-Glucose	Applichem (A3666)
DMEM (Dulbeccos modified eagle medium) ES	Invitrogen (21969-035)
DMEM – Müller culture medium	Invitrogen (61965-026)
DMSO (Dimethyl sulfoxid)	Sigma (D-4540)
DTT (Di-thiothreitol)	Applichem (A2948)
EDTA (Ethylen-diamine-tetraactate)	Sigma (E-6511)
F12 Ham’s nutrient mixture	Invitrogen (21765-029)
FCS (fetal calf serum) – differentiation-tested	Invitrogen (10270106)
5-Fluorodeoxyuridine	Sigma (856657)

Fungizone	Invitrogen (15290-018)
Gelatin	Sigma (G-1890)
GlutaMAX (200 mM)	Invitrogen (35050-038)
GS (goat serum)	PAA (B15-035)
HBSS (Hanks balanced salt solution)	Invitrogen (24020-091)
HBSS (10x)	Invitrogen (14065-049)
HS (horse serum), Hyclone	Perbio (SH30074.03)
Human apo-Transferrin	Sigma (T-1147)
Insulin	Sigma (I-6634)
Kynurenic acid	Sigma Fluka (61260)
Laminin	Roche Diagnostics (1243217)
L-Glutamine (200 mM)	Invitrogen (25030-024)
Microcarrier gold	Biorad (165-2262)
Mitomycin C	Sigma (M-0503)
Na-Selenite	Sigma (S-5261)
NB (Neurobasal) medium	Invitrogen (12348-017)
NEAA (nonessential amino acids)	Invitrogen (11140-035)
PBS (Phosphate buffered saline)	Invitrogen (14190-094)
Penicillin/Streptomycin	PAA (P11-010)
PFA (Paraformaldehyde)	Applichem (A3831)
Poly-L-Lysin Hydrobromid	Sigma (P-2636/53K5114)
Poly-Ornithine	Sigma (P-8638)

Progesterone	Sigma (P-8783)
Putrescine	Sigma (P-5780)
PVP (Polyvinylpyrrolidone)	Sigma (P-5288)
Retinoic acid	Sigma (R-2625)
Trypsin-EDTA solution	Sigma (T-3924)
Trypsin-EDTA ES cells	Invitrogen (25300-054)
Trypsin-Powder	Sigma (T-8802)
Uridine	Sigma (U-3750)

2.4 Solutions and media

2.4.1 ES cell culture and differentiation

EB medium (250 ml)

220 ml DMEM with Na-Pyruvat w/o L-Glutamine

25 ml FCS

2.5 ml non-essential amino acids

2.5 ml L-Glutamine

2.5 µl β-Mercaptoethanol

→ Filter sterile using a Stericup filter unit and store in 50 ml aliquots

ES medium (170 ml)

140 ml DMEM with Na-Pyruvat w/o L-Glutamine

25 ml FCS

1.7 ml non-essential amino acids

1.7 ml L-Glutamine

1.7 µl β-Mercaptoethanol

17 µl DTT stock solution (X)

→ Filter sterile using a Stericup filter unit and store in 50 ml aliquots, add LIF directly prior to medium change

2x Cryo medium (80 ml)

39 ml DMEM with Na-Pyruvat w/o L-Glutamine

25 ml FCS

16 ml DMSO (20%)

→ Filter sterile using a Stericup filter unit and store in appropriate aliquots at -20°C; thaw directly before use

N2 medium (50 ml)

25 ml DMEM with Na-Pyruvat w/o L-Glutamine

25 ml F12 (Ham's nutrient mixture)

1.25 ml Human apo-Transferrin stock (50 µg/ml)

250 µl Insulin stock (25 µg/ml)

250 µl BSA stock (50 µg/ml)

50 µl Progesterone stock (20 nM)

50 µl Putrescine stock (100 nM)

500 µl 200mM Glutamine (2 mM)

500 µl Penicillin/Steptomycin 100x

5 µl Sodium Selenite stock (30 nM)

→ Prepare quickly, filter and store in 10 ml aliquots at 4°C

→ Discard when pink

0.2% Gelatin (500 ml)

Add 1 g gelatin to 500 ml aqua ad iniectabilia and autoclave

→ Stir or shake in a warm state to dissolve gelatin and store at 4°C

Poly-Ornithine (0.5 mg/ml)

Dissolve 25 mg in 50 ml 150 mM Na-Borate ("Borax") solution pH 8.3 (adjust with HCl)

→ Filter and store at 4°C for 3 months

→ Dilute 1:5 in aqua ad iniectabilia to obtain a 0.1 mg/ml solution for coating the plate

Laminin (0.5 mg/ml)

→ Dilute 1:250 in PBS using glass pipettes and flask to obtain a working solution of 2 µg/ml Laminin

Mitomycin C (1 mg/ml)

Resuspend 10 mg in 10 ml of 5% DMSO in PBS

→ Filter and store in 1 ml aliquots at 4°C in the dark

→ Dilute 1:100 in dish (10 µg/ml)

Retinoic acid (5 mM)

Dissolve 15 mg in 10 ml DMSO

→ Prepare 100 µl aliquots in a dark bench and store at -20°C

→ Dilute 1:1000 in tube (5 µM) in the dark

4% EDTA in PBS (w/v)

Dissolve 400 mg EDTA in 10 ml PBS as 4% stock solution, filter and store at 4°C

→ Before use dilute 1:100 in PBS to obtain work solution with 0.04% EDTA

0.05% Trypsin in EDTA solution

Aliquot frozen trypsin powder into Eppendorf tubes containing 1-2 mg each

→ Directly before use dissolve 1 mg trypsin in 2 ml 0.04% EDTA in PBS

FCS (inactivated)

Thaw 500 ml bottle over night at 4°C

Heat-inactivate at 55°C for 30 min and store 25 ml aliquots at -20°C

→ Thaw directly before use at room temperature

→ FCS batch has to be tested for a successful completion of the differentiation procedure

Human apo-Transferrin stock solution (2 mg/ml)

Dissolve in H_2O, aliquot and store at -20°C

Insulin stock solution (5 mg/ml)

Dissolve in H_2O acidified with one drop of 25% HCl/10 ml

→ Aliquot and store at -20°C

BSA stock solution (10 mg/ml)

Dissolve in H_2O, aliquot and store at -20°C

Progesterone stock solution (20 µM)

Dilute 1:100 in H_2O to obtain 20 µM solution

→ Aliquot and store at -20°C

Putrescine stock solution (100 µM)

Prepare 100 µM solution in H_2O and store at -20°C

Sodium selenite stock solution (300 µM)

Prepare 300 µM solution in H_2O and store at -20°C

2.4.2 Neuronal cell culture

Müller culture medium (MKM)

100 ml BME-Medium (Invitrogen)

50 ml HBSS (Invitrogen)

50 ml Equine serum

1 ml Glutamax

2 ml Glucose (50%)

Preparation solution

98 ml GBSS

1 ml Kynurenic acid

1 ml Glucose (50 %)

→ Adjust pH to 7.2 using 1 M HCl and filter sterile

GBSS (g/l)

0.22 g $CaCl_2 * 2\ H_2O$

0.37 g KCl

0.03 g KH_2PO_4

0.21 g $MgCl_2 * 6\ H_2O$

0.07 g $MgSO_4 * 7\ H_2O$

8.00 g NaCl

0.227 g Na_2HCO_3

0.12 g Na_2HPO_4

1.00 g D-Glucose

→ Filter sterile and keep at 4°C

Kynurenic acid (5 mM)

Dissolve 946 mg Kynurenic acid in 5 ml 1 M NaOH; add 45 ml MilliQ; filter sterile; prepare 1 ml fractions and store at -20°C

50% Glucose

Dissolve glucose in dH_2O 1:1 while heating, filter sterile in warm state and store 1 ml fractions at -20°C.

Antimitotics

2.422 mg Uridine in 10 ml dH_2O (1 M)

2.797 mg Cytosin-β-D-Arabinofuranosid Hydrochlorid in 10 ml dH_2O (1 M)

2.462 mg 5-Fluoro-2´-Deoxyuridin in 10 ml H_2O (1 M)

→ Mix stock solutions 1:1; filter sterile and freeze in 500 µl fractions

Borate buffer pH 8.5

1.24 g Boric acid

1.90 g Borax

→ Fill to 400 ml using sterile H_2O and adjust pH to 8.5

Poly-L-Lysin stock solution

Dissolve 10 mg/ml in H_2O, store at -20°C

GBSS/Glucose

50 ml GBSS

0.5 ml 50 % Glucose

→ Adjust pH to 7.2 using 1 M HCl and filter sterile

NB++ medium

50 ml NB

125 µl GlutaMAX

1 ml B27 supplement

Serum medium

200 µl inactivated FCS in 10 ml NB

1x HBSS for live imaging

50 ml HBSS 10x

175 mg $NaHCO_3$ (4.17 mM)

147 mg $CaCl_2*2H_2O$ (2 mM)

→ Fill to 500 ml with MilliQ

→ Stir to dissolve and filter sterile, store at 4°C

2.4.3 Electrophysiology

2.4.3.1 Artificial cerebrospinal fluids

Konnerth I (g/l)

7.305 g NaCl

0.186 g KCL

0.172 g $NaH_2PO_4 * H_2O$

0.406 g $MgCl_2 * 6 H_2O$

2.184 g $NaHCO_3$

4.504 g D-Glucose

0.294 *g* $CaCl_2 * 2 H_2O$

Konnerth II (g/l)

7.305 g NaCl

0.186 g KCL

0.172 g $NaH_2PO_4 * H_2O$

0.203 g $MgCl_2 * 6 H_2O$

2.184 g $NaHCO_3$

4.504 g D-Glucose

0.294 *g* $CaCl_2 * 2 H_2O$

2.4.3.2 Intra-electrode solutions

IES I (g/l)

28.11 g K-Gluconate

1.305 g KCL

0.584 g NaCl

2.38 g HEPES

0.190 g EGTA

1.102 g Na-ATP

0.610 g $MgCl_2$

0.147 g $CaCl_2 * 2 H_2O$

➔ Adjust pH to 7.2 with KOH

IES II (g/l)

23.57 g CsCl

2.383 g HEPES

4.184 g EGTA

0.407 g $MgCl_2$

0.147 g $CaCl_2 * 2 H_2O$

➔ Adjust pH to 7.2 with CsOH

2.5 Cell culture techniques

2.5.1 Cultivation and differentiation of mouse embryonic stem cells

All mouse ES cells were cultivated and differentiated as described in the dissertation of F. Neuser (Neuser, 2010) or a protocol by Bibel et al. (Bibel et al., 2004;Bibel et al., 2007), respectively. As ES cells are highly sensitive and the cultivation and differentiation are a complex process the steps will be here described briefly.

Basic ES cell culture

The ES cells were cultivated at 36.5 °C and 7% CO_2 in ES cell culture medium with the addition of leukemia inhibitory factor (LIF) on a layer inactivated mouse embryonic fibroblasts (MEF). This assured that the ES cells remained in an undifferentiated and proliferative state. MEFs were sowed and cultured in EB medium and then mitotically inactivated and used for the ES cell culture after 4 h to 4 days. LIF was produced using COS-7 cells which were cultured in EB medium and transfected with the LIF plasmid ("pCAGGS-LIF" from Y.-A. Barde, Basel, CH). 24 h after transfection the cells started to secrete the expressed LIF to the medium which was harvested after 5 days and frozen at -80 °C.

Differentiation of ES cells into neuronal precursors

The ES cells were deprived of MEFs in a highly proliferating state in LIF-enriched ES medium for 36-72 h in culture. The ES cells were trypsinized and sowed to EB medium where they formed cellular aggregates, embryoid bodies. After six days retinoic acid was added and after eight days in culture the ES cells were carefully trypsinized, filtered and frozen in liquid nitrogen.

Culture of neuronal precursors

ES cell-derived neuronal precursors (ESNPs) were grown on Poly-ornithine and laminin-coated surfaces at 37 °C.

2.6 Slice preparation

2.6.1 Preparation and cultivation of hippocampal organotypic slice cultures

The organotypic cultures were prepared and cultivated as previously described (Stoppini et al., 1991). C57Bl/6 mice at postnatal day 5 were decapitated and the scalp removed medial from the skull. The skull was then opened rostral using a scissor and a micro-scissor and the fragments removed to protect the brain from physical damage. A horizontal caudal starting cut between cerebellum and inferior colliculus was done with a sharpened spatula; the upper part of the brain with the hippocampi was now transferred into ice-cold GBSS. Before separating the hemispheres the cerebellum and colliculi were removed and the accentuated hippocampi flapped over and cut from the cortex at the subiculum. The hippocampi were positioned onto a teflon disk and cut in 400 µm thick slices with a tissue-shopper. The slices were washed carefully into ice-cold GBSS to separate them and then incubated for 20 minutes at 4 °C. For an incubation at 36.5 °C and 5% CO_2 four slices were placed carefully on one cell culture inserts with 1.1 ml MKM medium per well. After 72 h of incubation 15.4 µl antimitotics were added to the cultures. 24 h later the cultures were transferred to a new plate with fresh MKM medium. The MKM medium change was done twice a week for 50% of the medium-volume and additionally 1.25µg/ml Fungizone, 100 U Penicillin and 100 µg/ml Streptomycin.

2.6.2 Preparation of hippocampal acute slices

For the preparation of transversal hippocampal slices, mice were anesthetized with CO_2 and immediately decapitated. The scalp was medially cut and flipped over laterally to dissect the skull. It was opened using a preparation-scissor beginning from the spine and cutting medial-rostral. The dorsal cleared brain was separated from the *bulbus olfactorius* using a spatula and transferred into the ice-cold carbogenated (95% O_2, 5% CO_2) artificial cerebrospinal fluid (ACSF). As this step is crucial for cell survival the maximum duration was always under 90 s.

To minimize the oxidative stress during the following steps the brain was cooled down for three minutes in ACSF.

Always submerged by ice-cold ACSF the brain hemispheres were separated and the hippocampi dissected consecutively by removing the surrounding tissue. First, the *cerebellum* and the frontal part of the cortex were cut off by a razorblade, then using two spatulas the resting tissue was carefully detached beginning medially with the *striatum*. The hippocampus was finally separated from the cortex by cutting the subiculum.

The hippocampi were then cut with a vibratome VT1200S (Leica Microsystems, Germany) into 400 µm thick transversal slices (see Fig. 6). For this the hippocampus was placed upright on the specimen disk fixed with tissue-gluten and leaning with the dentate gyrus to an agar cube. This assembly was rapidly transferred into a buffer tray filled with ice-cold carbogenated ACSF. A high-frequently vibrating razorblade then cut the hippocampus horizontally by moving through the tissue slice after slice. After every cycle the originated slice was transferred with a pipette into a "submerged" like storage chamber filled with carbogenated ACSF at room-temperature adjusted to 22 °C. Before starting with experiments the slice were allowed to recover for minimum 90 min.

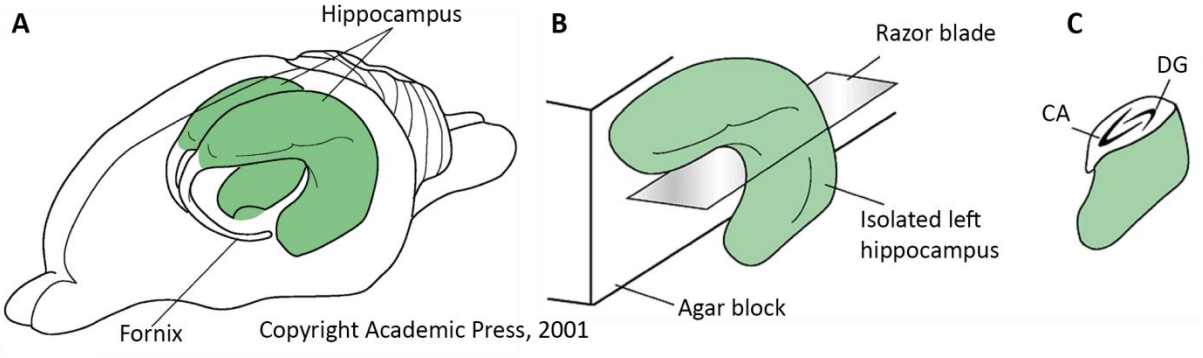

Figure 6: Spatial orientation and cutting procedure of a rodent hippocampus. A: Bilateral orientation of both hippocampi inside the rodent brain. **B:** Principle cutting procedure with the left hippocampus fixed next to agar block for stabilization. **C:** Transversal cutted hippocampus with indicated regions dentate gyrus (DG) and *Cornu Ammonis* (CA). (Hammond, 2001)

2.7 Transplantation of ESNPs into hippocampal slice cultures

Micropipettes were pulled from borosilicate glass-electrodes using a vertical electrode 2-step puller (Narishige, Japan). For a defined tip opening two steps of the heating filament were adjusted to 62.7 and 19. The resulting tip opening size was between 25 and 35 µm. This

size was chosen as a compromise between the ability of passing precursors safely through the tip and a minimum damage of the culture during transplantation. The frozen precursors were centrifuged for five min in 20 ml EB and the pellet carefully resuspended in 100 µl N2 medium. This cell suspension was then transferred to a suspension culture dish and incubated for 30 min in the incubator at 36.5 °C and 5% CO_2. The following steps were done as fast as possible because of their importance for survival of the precursors. The precursors were transferred into the produced micropipettes and microinjected with 10 psi for 0.1 ms using a micro injection device (Pico Spritzer, Toohey Company) into organotypic slice cultures at 5 DIV. During the transplantation the properties of the micropipette may vary or finally clog. Therefore the effective volume was controlled after every cycle as well as the presence of cells in the volume.

2.8 Cell lines

Table 1: Overview of all four cell lines used in this study

Cell line	Origin	Genotype	Source
M22	J1 murine ES cell line	WT, *tau*EGFP transgene	K. Tucker, Basel
MEFs	Bl6 mouse	$Puro^R$/Tbx2 transgene	Y.-A. Barde, Basel
COS7	African green monkey kidney fibroblasts	WT	DSMZ Braunschweig

The M22 ES cell line was created by K.-L. Tucker in the lab of Y.-A. Barde (Basel, CH) by cloning a 8.5 kb fragment from the Mapt (tau) locus and inserted into an EGFP and neomycin resistance (plasmid A) containing plasmid. This plasmid was electroporated in the genome of J1 ES cells as a multiple copy transgene. The fluorescence of the EGFP was relatively higher than in a homologous integration approach.

2.9 Field potential recordings

2.9.1 Setups

The experiments were done on two different experiment setups in parallel, both are here described separately.

2.9.1.1 Setup 1

The experimental setup consists of a vibration isolated table (Spindler & Hoyer, Germany) equipped with a manual micromanipulator (Leitz, Wetzler, Germany), a motor-controlled micromanipulator (Nano-Stepper, Sonnhof, Germany) and a custom made recording-chamber. The chamber was made from V4A steel and enables a temperature regulation of the ACSF via a heated filament from Ni-Cr alloy (Thermocoax, Phillips, Germany) fixed with special gluten (E-Solder, Epoxyprodukte, Fürth, Germany). The heating filament was electrically isolated from the surrounding metal with magnesiumoxid. The temperature in the chamber was adjusted to 32 ± 0.2 °C with a controller (DB100, Mawitherm) which measures the temperature permanently via a sensor inside the chamber. The chamber was perfused by carbonated ACFS at 1 ml / min using a peristaltic pump (Minipuls 3, Gilson, USA) and PVC tubing (Braun, Germany / Ismatec). To ensure a stable level of ACSF in the chamber and avoid pulsations, the chosen tubing for suction was larger than on the sustentative site. An aluminum-foiled headstage was set in direct adjacency to the connected recording electrode to minimize noise. The headstage calculated the potential difference via the current difference between the recording electrode and the indifferent electrode. The signal was then filtered (MPI für biologische Kybernetik, Germany) and amplified (Axoclamp 2B, Axon Instruments, USA). The amplifier was additionally used to determine the tip resistance of the recording electrode by a wheatstone bridge and to adjust the offset of the signal. The monopolar stimulating electrode (WPI, USA) made of tungsten were coated with lacquer and had a resistance of 10 MΩ. The electrode was connected to stimulus-isolator (A360, WPI,

USA) which was controlled by a programmable master trigger (Master 8, A.M.P.I). The signal was monitored in parallel with an oscilloscope (HM507, Hameg, Germany) and a computer.

2.9.1.2 Setup 2

Because the principle operational sequences are the same for the setup two, only the differences are described. The recordings were done on a setup mounted on a vibration isolated Optical Top (Series 780, TMC). For recording the slices were placed in a recording-chamber (RC-22, Warner Instruments). The chamber was perfused by carbonated ACFS at 1 ml / min using a peristaltic pump (Ismatec, Switzerland) and PVC tubing (Braun, Germany / Ismatec). To ensure a stable level of ACSF in the chamber and avoid pulsations, the chosen tubing for suction was larger than on the sustentative site. A combination of two resistors integrated in a platform and a single inline solution heater (SH-27B, Warner Instruments) controlled by a temperature controller (TC-344B, Warner Instruments) assured a stable temperature (+/- 0.2 °C). The recordings were performed at 32 °C. The chamber was placed under a binocular using a platform (PH-1, Warner Instruments) and a manually adjustable micromanipulator (Luigs & Neumann).

The headstage was mounted on a micromanipulator (Unit Mini 3 Axes, Luigs & Neumann) which was guided by a controller (SM-5, Luigs & Neumann) using a remote (Keypad SM-5, Luigs & Neumann). The signals were send to an oscilloscope (HM507, HAMEG) and a computer-interface. The signal was filtered (5 kHz) and amplified by an Axoclamp 2B (Axon Instruments).

2.9.2 Stimulation

With the stimulus-isolator it was possible to adjust the given stimulus strength to up to 200 µA individually for every single slice to elicit field EPSPs in approx. 40% in LTP experiments. For a duration of 20 min a baseline was recorded with 0.1 Hz stimulation to estimate the

vitality of the slice and as a reference. Depending on the different protocols a programmed stimulus was given after a stable baseline for minimum 20 min. For the induction of LTP the "theta-burst stimulation" protocol was used (see Figure 7). It consists of three iterations of ten bursts with an interval of ten seconds. Every burst had four pulses with an interval of 10 ms. Between the bursts there was an inter-train-interval (ITI) of 200 ms. The regulation of the inter-stimulus interval (ISI) between 10 and 160 ms of the paired-pulse facilitation was done manually with the Master 8. The EPSP signal amplitude was determined with different stimulus-strength between 50 and 200 µA at 0.1 Hz.

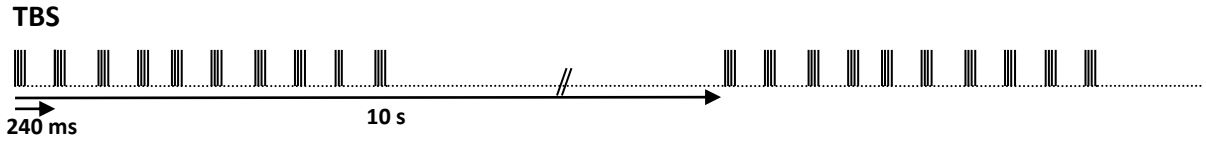

Figure 7: Stimulation protocol for a typical Theta-burst stimulation to induce LTP in hippocampal acute slices

2.9.3 Extracellular recording

The extracellular recordings of hippocampal acute slices were carried out with borosilicate glass electrodes with an outer diameter of 1 mm and an inner diameter of 0.58 mm (Biomedical Instruments, Germany). Electrodes were pulled of capillaries with a horizontal electrode puller (Flaming Brown P-97, Sutter Instruments, USA) to a tip resistances of 5-20 MΩ when filled with 3 M NaCl. The pulled electrodes were attached to an electrode holder which was adjustable with a micromanipulator. The signal was then either amplified 10x in the headstage, lowpass filtered at 10 kHz and 20x amplified in the Axoclamp 2B and Bessel-filtered between 1 and 1000 Hz or 10x amplified in the headstage, Bessel-filtered between 1 and 1700 Hz with a 20x gain in a filter unit (LHBF-48X, npi, Tamm, Germany). The signal was then send to a PC-interface (National Instruments, Austin, USA) which converts the signal into a digital format recorded and live-analyzed by a custom programmed data-acquisition program (Labview, National instruments).

2.9.4 Positioning of electrodes

Due to the specific neuronal cell architecture within a transversal slice of the hippocampus a specific stimulation of different hippocampal pathways is possible and extracellular recordings can be securely performed (see Figure 3). During the preparation the lateral superficial located neurons of the 400 µm thick slice are potentially damaged or dead, this is why for all experiments only neuron-populations situated medially in a depth of 100-150 µm were chosen. The inception of the surface of the tissue was investigated by alterations in the measured resistance. With the used micromanipulators it was possible to access neuron-populations 100-150 µm deep inside the slice. The navigation inside the slice architecture was done using the clearly visible pyramidal cell layer of the slice culture. The stimulus-electrode was based from the *dentate gyrus* placed at the distal end of the CA3-region and medial-apical of the cell body layer to stimulate the *Schaffer collaterals*. The emerging action potentials were conducted to the CA1 region and synapses at the apical dendrites of the pyramidal cells in the CA1 region are excited. The resulting EPSP could be recorded by recording electrode located in this area.

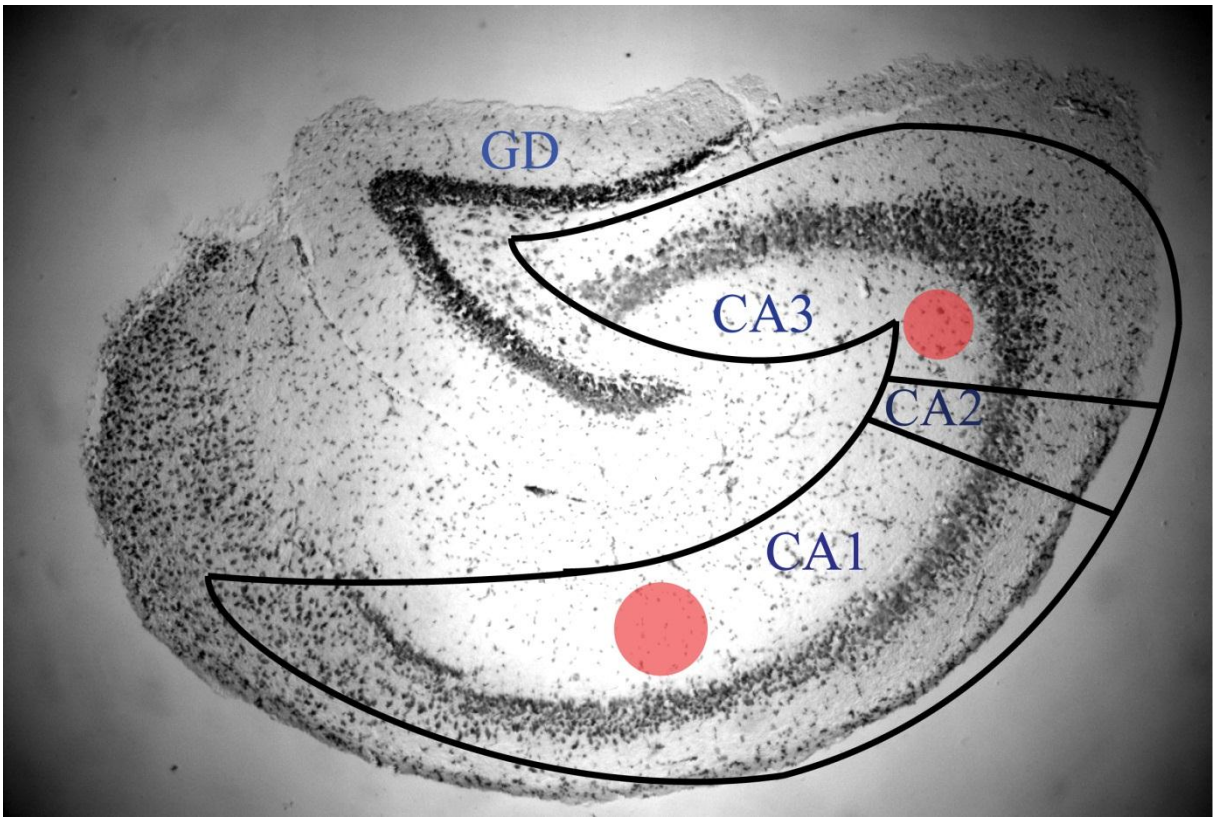

Figure 8: Nissl staining of a transversal hippocampal acute slice. The location of the stimulation electrode in CA3 region and the recording electrode in the CA1 region is indicated by red dots. CA: *Cornu Ammonis*, GD: *Dentate Gyrus*

2.9.5 Excitatory postsynaptic potential

Excitatory postsynaptic potentials (EPSP) are resulting from changes in conductivity of the postsynaptic membrane, which are engendered by presynaptic transmitter release. EPSPs are temporal transient disturbances of the resting membrane potential of the cell, but the often only small potentials can accumulate spatially and temporally. Postsynaptic ion trophic receptors open, after binding of neurotransmitters, ion-channels. The influx of Ca^{2+} und Na^{+} results in a deficit of positive charged ions at the surface of the cell membrane and therefore a depolarizing change in the potential which can be detected by the recording electrode. With increasing stimulus strength from electrodes close to CA3 pyramidal cell axons an increasing frequency of action potentials is generated and more fibers are stimulated with the result that more neurons are recruited. Both have a supporting influence on the amount of released neurotransmitters which influence the number of opened ion channel and their opening period and accordingly the stimulus has strength a direct effect on the size of the

EPSP. The recorded signal is because of its extracellular position not the depolarization of *one* cell but the sum-depolarization of a neuron population and is defined as field potential (fEPSP = field-EPSP).

The shape of the signal in an extracellular recording is formed by the following effects: Due to the stimulus-current of the stimulusisolator a negative stimulus artifact becomes visible 5 ms after triggering. The evoked action potentials at the *Schaffer collaterals* in the CA3 region of the hippocampus cause a depolarization in the pyramidal cells of the CA1 region, the fEPSP. To estimate the size of the evoked fEPSPs the negative slope in a defined integral is calculated.

2.9.6 Data analysis and statistics

All programs used for data analysis were programmed by Martin Korte and Volker Staiger in Labview. The major tasks were the calculation of the size of the negative slope of the fEPSP in a defined integral and the live post-analysis of every signal and its validation. The calculated values were exported into an Excel (Microsoft, USA) compatible format for later manual analysis. During the baseline at 0.1 Hz every six values were averaged and taken as minute-value. The values of the last 20 min before LTP induction were averaged to a 100% reference value. This was done because of the typical variance in signal strength and response of individual neuron populations over all slices, therefore all following values are in relation to this reference value for each individual neuron population.

For the analysis of signals during different stimulus strength (50, 75, 100, 125, 150 and 200 µA) and PPF three signals were averaged and plotted against the corresponding stimulus strength or ISI values.

For all averaged values the standard error of the mean was calculated and plotted as error bar whereas the standard deviation was used in the example experiments.

The statistical analysis was carried out using the student´s t-test in Prism. The confidence interval was set to α=0.05.

2.9.7 Rejection criteria

For the rejection of single experiments from the final results and an objective estimation specific parameters were defined. All experiments which showed unstable signal characteristics were carried out to the end, but rejected from final analysis.

2.10 Patch-clamp experiments

The patch-clamp recordings were done on a setup situated in an isolated dark room electrically protected by a grounded custom made Faraday cage mounted on a vibration isolated Optical Top (Series 780, TMC). For recording, the slice cultures were placed in a recording chamber (RC-22, Warner Instruments) spatially fixed by a slice hold-down (SHD-22CL/15, Warner Instruments). The chamber was perfused by carbonated ACFS at 1 ml / min using a peristaltic pump (Ismatec, Switzerland) and PVC tubing (Braun, Germany / Ismatec). To ensure a stable level of ACSF in the chamber and avoid pulsations, the chosen tubing for suction was larger than on the accommodative site. The recordings of miniature excitatory postsynaptic potentials EPSCs (mEPSCs) and receptor occurrence were performed at room temperature (21-22 °C); all other recordings were done at 32°C. A combination of two resistors integrated in a platform and a single inline solution heater (SH-27B, Warner Instruments) controlled by a temperature controller (TC-344B, Warner Instruments) assured a stable temperature (+/- 0.2 °C). The chamber was placed in the light path of a microscope (Axioskop 2 FS plus, Zeiss) using a platform (PH-1, Warner Instruments) and a manually adjustable micromanipulator (Luigs & Neumann).

For detection of the target cells either fluorescence- or differential interference contrast microscopy was used. An objective with 4x magnification (4x/0.1 Achroplan, Zeiss) was able to give a general overview of the position of target cells. For a detailed view and positioning of the patch electrode a 40x objective (40x/0.8W Achroplan, Zeiss) with an optional DIC filter was used. An infrared sensitive video camera (KP-M2RP, Hitachi Kokusai Electric Inc.) was mounted in the light path of the microscope to send the video to a screen (UM-1213, ENEO).

For all voltage-clamp and current-clamp recordings a low noise amplifier (Axopatch 200B, Axon Instruments) connected to a cooled headstage (CV203 BU, Axon Instruments) was used. The headstage was mounted on a micromanipulator (Unit Mini 3 Axes, Luigs & Neumann) which was guided by a controller (SM-5, Luigs & Neumann) using a remote (Keypad SM-5, Luigs & Neumann). The signals were filtered at 5 kHz at amplifier level and then simultaneously send to a scope (HM507, HAMEG) and a digitizer (Digidata 1322A, Axon Instruments) which was connected to a computer-interface. PCLAMP 9 (Axon Instruments) was used for data acquisition and live analysis, Clampfit 9 (Axon Instruments) for data analysis.

All recordings were done with borosilicate glass capillaries (1.5 mm outer diameter, 0,86mm inner diameter, GC150F-10, Harvard Apparatus). The capillaries were pulled with a vertical electrode puller (PC-10, Narishige, Japan) to a resulting tip resistance of 5-7 MΩ when filled with 10µl intra-electrode solution (see 2.4.3.2). The electrode was tightly connected to an electrode holder containing a chloride silver filament inserted into the solution and a tube for air pressure control. The air pressure was adjusted and controlled using a gauge (GDH200, Greisinger). The slice culture was transferred from an incubator (MIDI 40, Thermo Scientific) to a sterile hood and cut out to fit into the recording chamber. Before driving with the tip of the electrode through the surface of the ACSF the pressure was adjusted to 50 mbar. After immerging the electrode into the ACSF it was possible to adjust the pipette offset to zero. In this condition there is no flowing current between the indifferent bath electrode and the open pipette. A repetitive rectangular voltage-pulse of 5 mV was given to calculate the tip resistance using Ohms Law and estimate the capacitive artifacts to compensate them using the amplifier. The electrode was now placed directly above the target cell and gently lowered to the direct proximity of the tissue. Due to artifacts resulting from the now deeper immerged electrode and the surface tension of the ACSF along the electrode offset and capacitive parameters were adjusted. The pressure was increased to 60 mbar to prevent the pipette from clogging while moving through the tissue. To prevent movement or damage of the cells the pipette was inside the tissue only moved using the Z axis. When reaching the vicinity of the target cell to approximate 250 µm the pressure was reduced to 20 mbar and all further pipette movements were done very accurate. Under permanent visual control the pipette was moved to the cell membrane until a dent was visible evoked from the outflowing intra electrode solution. This is the last time point where

the pipette offset is adjusted. The pressure was now reduced to zero to form the seal and the dent in the membrane disappeared, at the same time the rectangle pulse broke down resulting from the highly increasing resistance at the pipette tip. These indicators for a starting seal forming were supported by gently suction until the rectangle pulse is almost a flat line. In this cell-attached configuration the seal resistance was calculated and permanently checked during the experiments as well as all capacitive artifacts were compensated. At this point a holding potential of -65 mV was given at the pipette to prevent the cell from damage through massive depolarization while and after breaking the membrane. Because all experiments were done in the whole-cell configuration the membrane of the patch under the pipette was broken using a combination of a short high-amplitude alternating current and gentle suction. The new capacitive artifacts resulting from the whole membrane were eliminated and the series resistance calculated and compensated. Cells which were outside of defined values for compensable parameters were excluded.

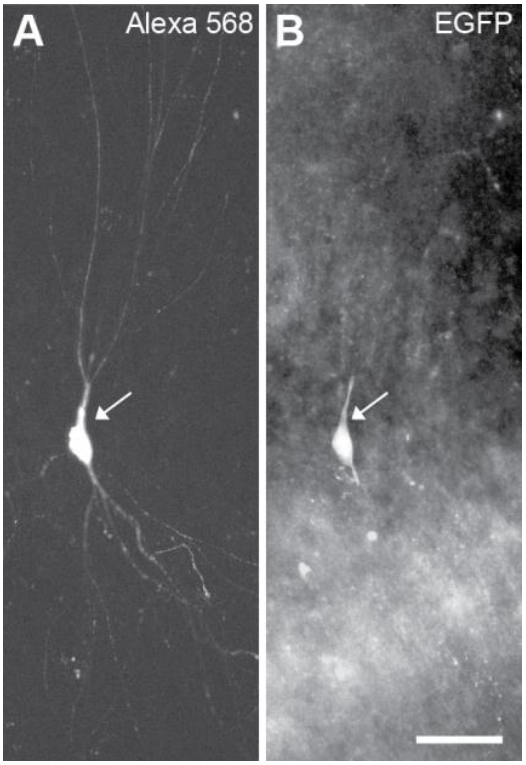

Figure 9: ESN in CA3 region is positive for Alexa 568 (A) and EGFP (B) after the whole-cell recording due to filling via the dye filled recording electrode. EGFP is endogenous expressed. Arrows are at same position indicating the same cell. Bar: 100 µm.

2.10.1 Selection of target cells & exclusion criteria

As described before "the transplantation of a population of ESNPs into the hippocampal slice culture results in a variety of neuronal and glia-like cell shapes, differing in size and complexity […]" (Neuser, 2010). To categorize this heterogeneity of cells the same parameters were chosen for type A and type B ESN cells. Criteria for type A were the following: A pyramidal-shaped cell body must be located in the intrinsic cell body layer as well as the distinguishable morphology of the dendritic tree into an apical and basal compartment. The orientation of the polarization of the type A ESNs had to follow the characteristic intrinsic cytoarchitecture with the apical dendrite in the *stratum radiatum* and the basal dendrites in the *stratum oriens*. Type B ESNs were

characterized by a general more immature morphology in one or more of the criteria. They were located outside the intrinsic cell body layer and often conglomerated superficially on the slice.

While measuring extremely small currents with the patch-clamp technique it is important to monitor possible side effects which may alternate these currents in amplitude, time-constant or length. One of the most important parameter is the series resistance. Breaking up the cell membrane opens the measureable volume to the whole cell. The resting membrane fragments and other cell compartments are sucked next to the pipette opening and this increases the resistance of the pipette-cell volume; the series resistance R_s. At the same time the resistance of the membrane of the whole cell, the membrane resistance R_m, and its parallel arranged capacity C_m were measured as important parameters for excitatory cells. It is of crucial importance that $R_s << R_m$ due to a direct effect on the time until the cell is depolarized by the predetermined holding potential. All experiments were excluded where R_s was higher than 25 MΩ and/or $R_s <= R_m$. The series resistance was compensated using the differential amplifier for 80%. As the series resistance is influenced by biological and variable causes it was monitored at the beginning and the end of all experiments or subexperiments. When the values for R_s, R_m or C_m were aberrated for more than 20 % at the end in comparison to the beginning of the experiment it was rejected. All measured cells were contemporary filled with Alexa 568 while patching. Directly after the experiment the filled cell was examined for morphological parameters. WT cells were identified as characteristically pyramidal neurons, type A ESNs were checked for co-immunofluorescence of Alexa 568 and EGFP and the predefined parameters for type A ESNs (see Fig. 9). During the analysis of spike trains all experiments showing decreasing action potential firing frequencies or decreasing peak amplitude were rejected.

2.10.2 Patch-clamp protocols

For the variety of experiments different protocols were programmed to determine the electrical parameters of the target cells in whole-cell configuration. These protocols are described consecutively.

2.10.2.1 Intra-electrode solutions

Two different intra-electrode solutions were used, IES I for all experiments except of experiments concerning receptor occurrence where potassium is missing totally in the solution (IES II). Both solutions were adjusted to pH 7.2 with KOH or CsOH and had 310 mOsmol · kg^{-1}.

2.10.2.2 Whole-cell current-clamp recordings, general I-V-curve and spike timing

Neurons have natural permanent changes in their electrical potential which are a summation of ion-flow through open ion channels, ion pumps and physically forces between ion concentrations. For a general electrical characterization of the target cells as well as spiking parameters like action potential frequency, amplitude and I-V-curves it is important to determine not the single current flows but the physiological stimulus-pattern of the whole cell. In current-clamp recordings in the whole-cell configuration it is possible to manipulate the cell with a defined current through the membrane and the natural electrical potential stays variable. Figure 10A shows typical current-clamp experiments with hyperpolarizing and depolarizing current steps in whole-cell configuration.

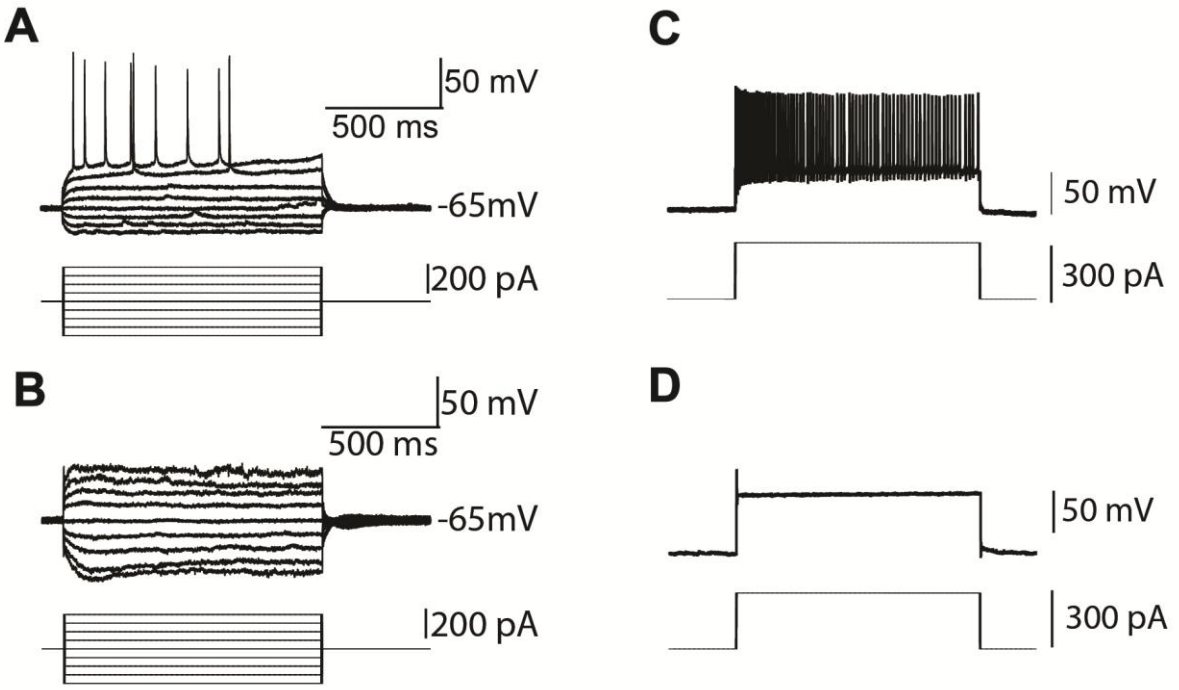

Figure 10: Stimulation protocols and respective signals from type A ES cells (A, C) and type B (B, D) in CA3 region. Depolarizing and hyperpolarizing pulses-steps **(A, B)** with an interval of 50 pA were chosen do characterize action-potential kinetics and threshold, a strong depolarization to evoke a high frequent action-potential burst.

The membrane potential of the cell was calculated without giving any current-injection. Hyperpolarizing and depolarizing currents of 50 – 200 pA in 50 pA steps were given for each 1000 ms. For each of these steps the contemporary monitored resulting current and the resulting potential was calculated at a defined time point on a representative plateau phase of the signal. The resulting potential was calculated as difference between the membrane potential at the beginning of the experiment and resulting membrane potential for each cell. In case of action potentials during the depolarizing current steps a plateau phase between to action potentials was chosen.

To determine the characteristics of action potentials the cells were depolarized with a single stronger injection of 300 pA for 1000 ms. A typical experiment with stimulus protocol and resulting potential is shown in Figure 10.

The characterization of the different parameters of action potentials was done by using common calculations for their kinetics (Figure 11).

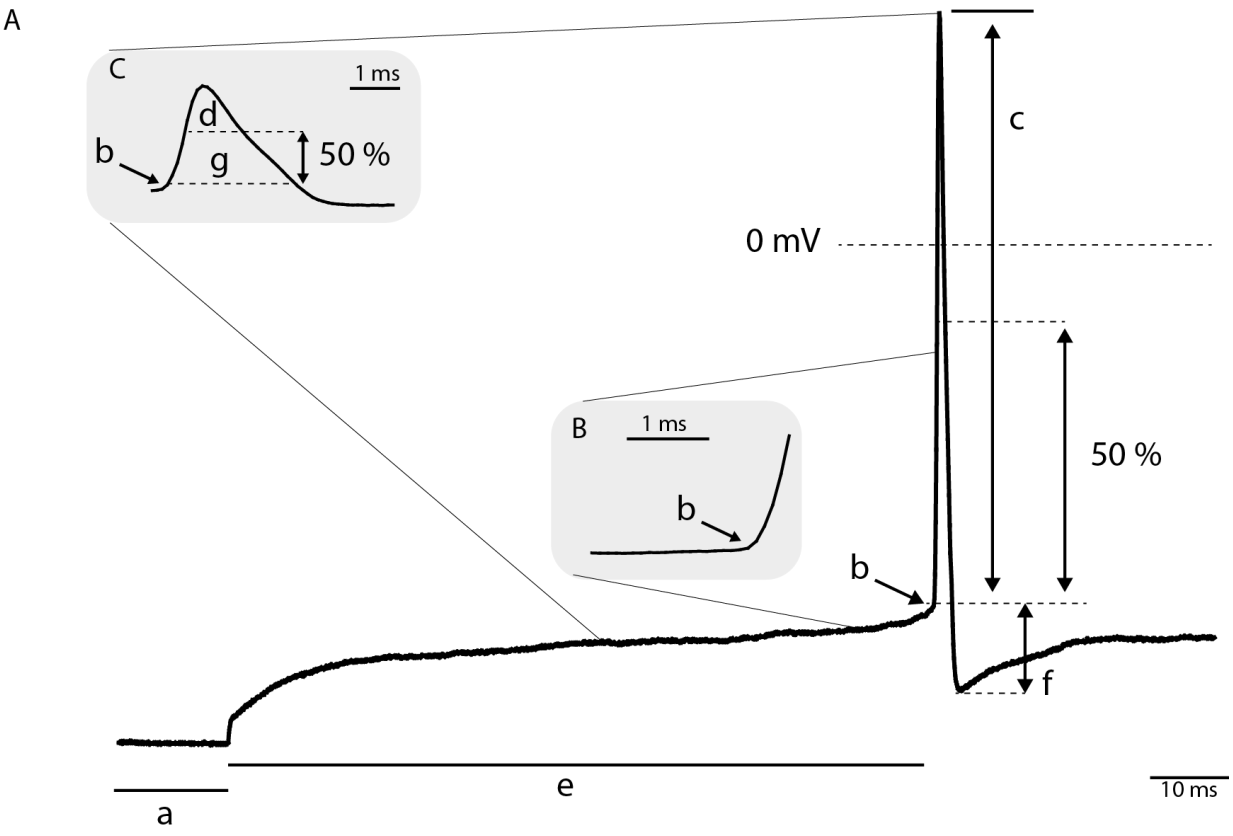

Figure 11: Typical action-potential of a CA3 pyramidal cell with indicated parameters (a-g). A: Complete action potential signal including a: Resting membrane potential, b: Action-potential threshold, c: action-potential peak amplitude, e: time-to-peak duration, f: anti-peak amplitude. **B:** Magnification of interval around AP threshold to visualize the fast depolarization, **C:** Magnification of the AP peak itself to visualize half-width (d) and area (g).

2.10.2.3 Whole-cell voltage-clamp recordings, miniature EPSCs

The excitatory postsynaptic potential (EPSP) is a short depolarization of the postsynaptic membrane potential caused by excitatory postsynaptic currents (EPSC). Ligand-sensitive channels mediate an influx of positively charged ions into the postsynaptic cell. Miniature EPSCs (mEPSCs) have a quantal character (Bernhard Katz, 1951) and are consequently a synaptic response to a release of a single vesicle from the pre-synapse and is an evidence for an intact neuronal connection between two cells via a synapse. Spontaneous EPSCs are in contrast generated by action potential-independent AND –dependent release of neurotransmitters and accordingly do not share the quantal character. The suppression of action-potentials with Tetrodotoxin (TTX) is an established method to focus on mEPSCs. TTX binds repressively to the fast voltage-gated sodium channels which are essential for the initial phase of an action potential and prevent the fast depolarization.

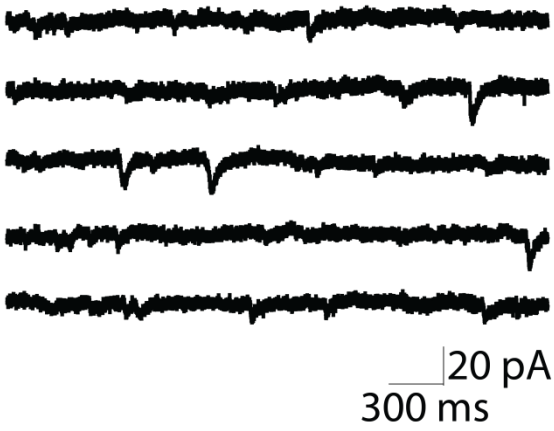

Figure 12: Representative voltage-clamp recording of a CA3 pyramidal neuron with mEPSCs.

Before the wash-in of TTX (0.5 mM) for 10 min the resting potential and the action potential threshold were calculated. Two criteria were assumed for a vital cell: A resting potential between -60 and -70 mV and action potentials caused by a manual depolarization. Figure 12 shows a typical recording of a whole-cell voltage clamp. Single mEPSCs were recorded over 20 min after a wash-in of TTX while the holding potential was adjusted to -65 mV. All recorded EPSCs were handpicked using the *Event Detection Tool* in Clampfit. The baseline of each experiment was corrected manually to correct long-term current fluctuations to afford further analysis. The baseline was manually set at the baseline of the signal and the trigger line was manually set to a level, where all EPSCs were detected under visual control. Search parameters were adjusted to a negative-going event with a noise rejection of 1 ms, a pre- and post-trigger of 1 ms. The detected EPSCs were further handpicked, analyzed and amplitude and frequency calculated.

2.10.2.4 Whole-cell voltage-clamp recordings, stimulation evoked receptor currents

The direct connectivity of neuronal cells can be represented by mEPSCs but the integration of cells in a neuronal network is better shown with stimulation of neuronal pathways. Neurons in the dentate gyrus and the CA3 region are indirectly connected via the mossy fibers. A stimulating electrode was placed into the *dentate gyrus* in a depth of 50 µm. The electrode is connected to a stimulusisolator (SGT 1002, Multi channel systems) which is programmed and controlled via a computer. At the same time a target cell was patched in the CA3 region and cmapled in voltage-clamp mode to -65 mV. The given stimulus over the electrode consisted of monophasic square pulses of 0.2 ms duration with stimulus sizes between 10 and 40 µA, depending on the minimum appearance of the signal and its half-maximum measured over the patched cell in CA3. The interval between two stimulations was ten seconds for five minutes at -65 mV (see Figure 13).

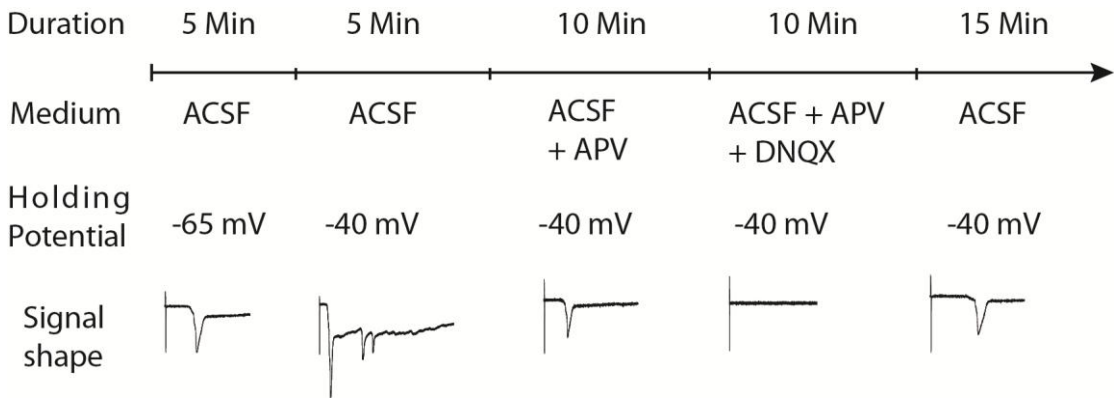

Figure 13: Experimental procedure during a 45 min long experiment. After establishing a stable seal the membrane potential as well as the medium is changed to evoke different receptor mediated currents or block them specifically.

To not only see an AMPA-receptor mediated compound of the signal the holding potential was then set to -40 mV for the rest of the experiment. Now an NMDAR mediated signal became visible and intermingled with the AMPAR compound. Exactly after 5 min a NMDAR antagonist, AP-V, was washed in for 10 min followed by a 10 min wash-in of a combination of AP-V and an AMPAR antagonist DNQX. At the end of the experiment a wash-out of 20 min was done to enable reversible effects of the antagonistic drugs.

The recorded EPSCs were analyzed using the threshold search in Clampfit. For every protocol-section the recorded traces were isolated, the baselines corrected and the peak-amplitudes calculated and averaged.

2.11 Animals

The animals used for preparation of hippocampal organotypic slice cultures in patch-clamp experiments of ESNs and endogenous pyramidal neurons were C57Bl/6 mice.

The mice used for the set of electrophysiological experiments concerning the endocannabinoid system were kindly provided by Prof. Beat Lutz (Department of Physiological Chemistry, Johannes Gutenberg University, Mainz, Germany) and consists of two different lines and their correspondent littermate controls.

Conditional knockout of CB1 in glutamatergic neurons

$CB1^{f/f;NEX\text{-}Cre}$ mice (here called Glu-$CB1^{-/-}$) were obtained by crossing $CB1^{f/f}$ with NEX-Cre mice (Wu et al., 2005). In those mice the Cre recombinase encoding sequence is knocked in the endogenous NEX locus, which is highly expressed in the hippocampus (Kleppisch et al., 2003). NEX is a helix-loop-helix transcription factor which is expressed in glutamatergic but not GABAergic interneurons to assure the deletion in glutamatergic neurons.

Conditional knockout of CB1 in GABAergic neurons

$CB1^{f/f;Dlx5/6\text{-}Cre}$ mice (here called GABA-$CB1^{-/-}$) were produced by crossing Dlx5/6-Cre mice with $CB1^{f/f}$ mice. Dlx5/Dlx6 are homeobox genes which are early expressed and involved in differentiation and migration processes of GABAergic neurons (Zerucha et al., 2000). This ensures an early deletion of the loxP-flanked allele specific in GABAergic neurons.

3. Results

3.1 Electrical characterization of ESNs

It has been shown previously that ES cell-derived neuronal precursors (ESNPs) can be transplanted and mature in organotypic hippocampal slice cultures and morphologically integrate into the pre-existing neuronal circuit (Neuser, 2010;Benninger et al., 2003). What is less clear are the electrophysiological properties of these neurons. Do they form functional synapses and can they produce action potentials and are the passive electrical properties comparable to young or even mature neurons? To further investigate the maturation of ESNPs in organotypic cultures experiments are necessary which directly investigate the major characteristics of neurons and the ability to have distinct electrical parameters and competence in electrical communication with connected neurons. Therefore I performed a set of different experiments to assess the unique properties of the transplanted cells using the patch-clamp technique. So far, comparable experiments were done with non-transplanted ESNs (Bibel et al., 2004), in-vitro expanded neuronal stem cells of the adult subependymal zone (Berninger et al., 2007c), astroglia-derived neurons (Berninger et al., 2007c) or with ESNPs transplanted on the surface of slice cultures (Benninger et al., 2003;Husseini et al., 2008) but these studies were focused on properties of neuronal and glial precursors integrated into the hilar region of the dentate gyrus.

3.1.1 Basic electrical parameters and I-V curves of type A ESNs

As described before the transplanted ESNs were categorized into two groups. Cells with a more mature character with complex cell morphology and orientation and pyramidal neuron comparable phenotype was termed type A. In contrast a lot of transplanted cells had an immature morphology and a reduced neuronal character (Neuser, 2010). In a first approach I characterized the basal electrical properties of type A ESNs in the CA1 and CA3 region of hippocampal slice cultures in comparison to intrinsic pyramidal neurons of the same region. Two important parameters for classification are the membrane potential and the membrane capacitance. The ESNs found in the different compartments of the slice were patched

separately and compared to neighboring cells in the same region. The resting membrane potential of pyramidal neurons is typically between the reversal potential of potassium (- 80 mV) and approximately - 60mV. I found that ESNs in the CA3 (n = 6) and the CA1 region (n = 3) had a typical resting membrane potential which is comparable to the intrinsic pyramidal neurons (n = 5) in both regions (Table 2). In contrast the capacitance of ESNs was significantly increased both in the CA1 ($p = 0.0051$, n = 3) and the CA3 region ($p < 1.45 * E^{-7}$, n = 13) in comparison to CA1 (n = 3) and CA3 region (n = 11) pyramidal neurons.

Table 2: Capacitance and resting membrane potential of ESNs and pyramidal neurons in two different regions.

	CA1	ESN CA1	CA3	ESN CA3
Capacitance (pF)	152.1 ± 19.56	297.33 ± 15.84	48.18 ± 6.45	235.07 ± 18.96
Membrane potential (mV)	-65.4 ± 3.33	-53.33 ± 6.01	-67,8 ± 1,02	-67.5 ± 2.14

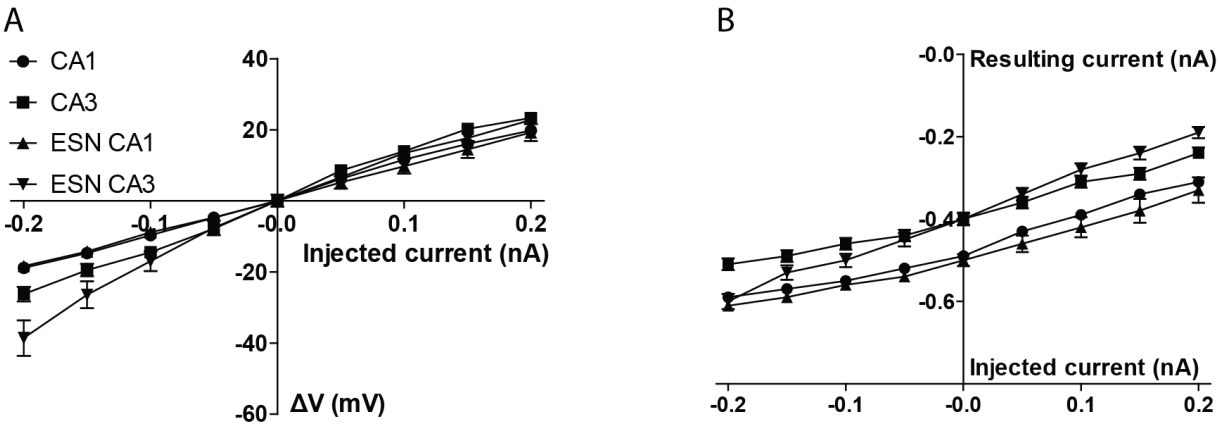

Figure 14: Basal characteristics of ESNs in different regions in comparison to intrinsic WT pyramidal cells. A: Normalized I-V curve of ESNs in the CA1 and the CA3 region of hippocampal slice were plotted the injected currents against the normalized measured voltages. **B:** Current curve, injected currents were plotted against resulting measured resulting currents.

The I-V curve represents a direct answer of cells to manipulation via current injection, here measured as changes in the membrane potential. ESNs in both regions showed responses to positive as well as negative current injections over the whole range comparable to intrinsic pyramidal neurons (Fig. 14A). The resulting measured current to manipulating current injections showed a tendency to be region specific (Fig. 14B). ESNs transplanted in the CA1 region showed answers over the whole range which were comparable to pyramidal cells in the CA1 region, respectively.

Taken together these findings clearly show that ESNs transplanted into the CA1 and CA3 region have comparable basal electrophysiological properties to intrinsic pyramidal neurons concerning the direct electrical reactions on current injections and the resting membrane potential. In contrast to this, the capacitance of ESNs was found to be significantly increased in the CA1 and CA3 region but regarding the low sample size these results may be evaluated as tendency.

3.1.2 Properties of action-potentials in type A ESNs

As a next step, one if not the typical electrical characteristic signal of neurons; action potentials (APs) were evoked by current injections in pyramidal cells as well as ESNs and recorded to analyze defined parameters.

A first approach was the identification of the AP threshold. ESNs in both regions showed values comparable to intrinsic pyramidal cells in the same region (Table 3).

Table 3: Action potential thresholds of ESNs and intrinsic pyramidal neurons in the CA1 and CA3 region

	CA1 (n = 5)	ESN CA1 (n = 3)	CA3 (n = 5)	ESN CA3 (n = 4)
AP threshold (mV)	-29 ± 1.18	-28 ± 4.16	-31.4 ± 1.21	-38.5 ± 2.72

As part of the representation of the number of active voltage gated Na^+ channels the characteristics of the peak (and antipeak) of the action potential itself are relevant. The peak amplitude of ESNs was significantly reduced in the CA1 region compared to intrinsic cells in the same region while in the CA3 region both were comparable (Fig. 15A). In line with previous results and the morphological data of F. Neuser (Neuser, 2010) this shows that the transplanted cells are in general able to evoke action potentials even if ESNs in the CA1 region show significant alterations in the peak amplitude. The spike timing concerning the time to peak was comparable between all four groups (Fig. 15 B). In contrast the amplitude of the antipeak was significantly increased in ESNs found in both regions compared to the corresponding intrinsic pyramidal cells (Fig. 15 C), indicating that K^+ channels during the hyperpolarization-phase may be altered. The half-width of the action potential was

significant faster in CA1 ESNs compared to intrinsic cells (Figure 15 D). The cells transplanted in the CA3 region showed values of the half-width which were comparable (Figure 15 D).

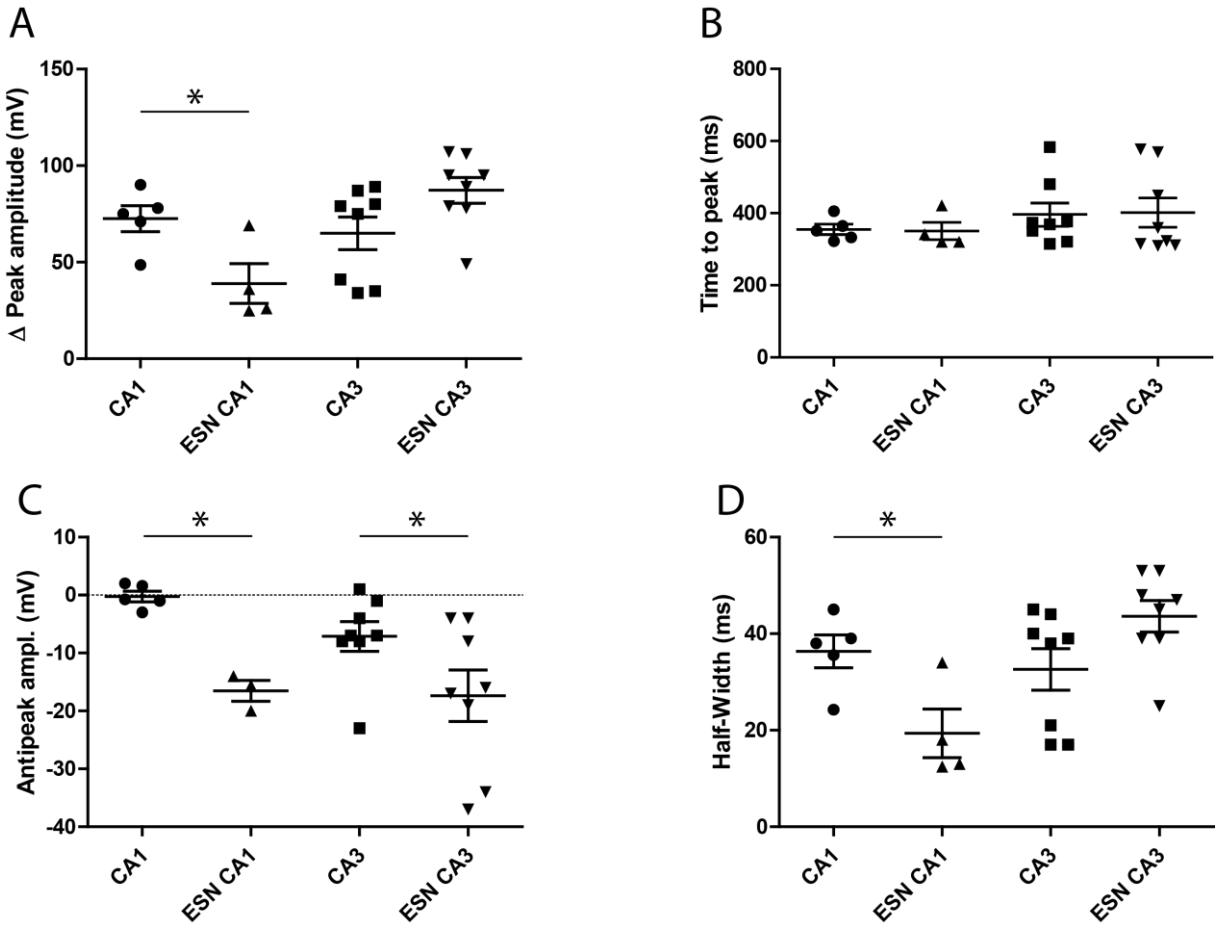

Figure 15: Ambivalent characteristics of recorded action potentials of ESNs and pyramidal neurons in CA1 and CA3 region of a hippocampal organotypic slice culture. A: Comparison of the peak amplitude. ESNs in the CA1 region show a significant reduction compared to the intrinsic cells. ESNs in the CA3 region are comparable to pyramidal cells. **B:** Duration between AP threshold and maximum of peak. ESNs and pyramidal cells show comparable results in both areas. **C:** Comparison of the anti-peak amplitude. ESNs in CA1 and CA3 region show a significant increase in the amplitude of the anti-peak. **D:** Half-Width: Comparable results between intrinsic cells and ESNs in the CA3 region but a significant increased half-width were shown in CA1 region. Two-tailed student's t-test, *$p < 0.05$. (CA1, n = 5; ESN CA1, n = 4; CA3, n = 8; ESN CA3, n = 8).

In addition to the peak and anti-peak itself the depolarization and repolarization phases are important characteristics of the action potential. While Figure 16 shows characteristics during the complete area of both phases Figure 17 excludes the proximal 10 % of the phases for the calculations. Focusing first on Figure 16 all four groups show comparable results in the maximum rise and decay slopes (Fig. 16A, C) and timings (Fig. 16B, D). This finding indicates on the one hand the relatively homogenous characteristics of the intrinsic pyramidal neurons in both regions and on the other hand the mature character for these parameters of the ESNs in both regions.

Taken together, these findings show that ESNs generally are able to evoke action potentials which are altered in amplitude for peak and anti-peak in the CA1 region. ESNs transplanted in the CA1 region showed values where only the peak amplitude is significant lower. The time-to-peak-timings are comparable between the transplanted ESNs and the intrinsic pyramidal neurons.

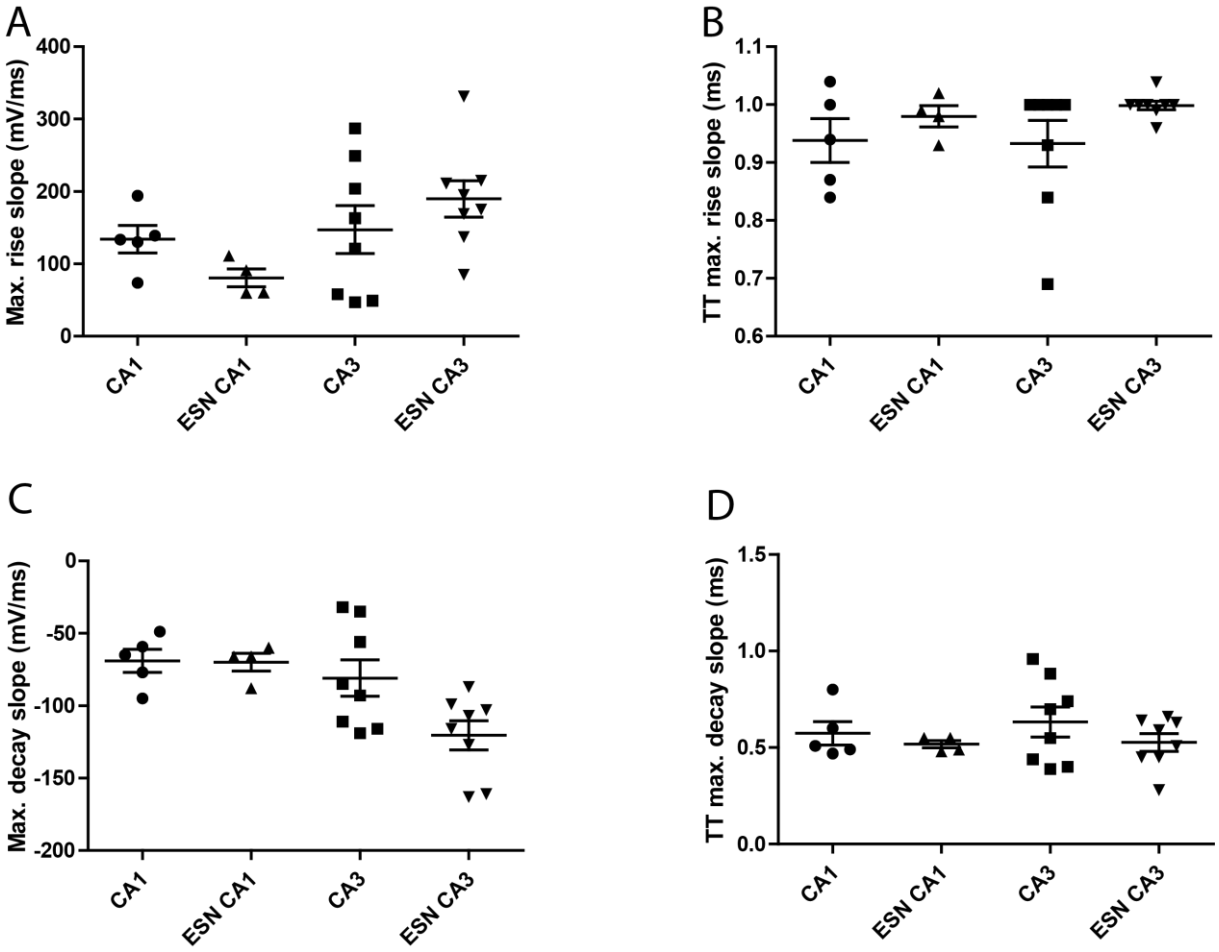

Figure 16: Characteristics of rise and decay timings at an action-potential in ESNs are comparable to intrinsic pyramidal neurons in CA1 and CA3 region of an organotypic hippocampal slice culture. A: The maximum slope on the rising edge and its time point (B) of the action-potential in ESNs are comparable to pyramidal neurons in both regions. **C:** At the falling edge the maximum slope of action-potentials in ESNs is comparable as well as the time to this maximum decay slope (D). (CA1, n = 5; ESN CA1, n = 4; CA3, n = 8; ESN CA3, n = 8).

By focusing on the inner part (10-90% of the phase) of the depolarization and repolarization phase one can exclude calculating artifacts of the proximal parts. The maximum and minimum values und timings of the slopes of the rising and falling edges give details about the membrane conductance. The maximum slope of the rising edge is significantly reduced

in ESNs transplanted in the CA1 region in comparison to intrinsic pyramidal neurons in the CA1 region (Fig. 17 A). In contrast, ESNs located in the CA3 region show comparable values for the maximum rise slope with reduced integral (Fig. 17 A). The maximum decay slope for cells both in the CA1 and CA3 region are comparable to their neighboring pyramidal cells (Fig. 17 C). Not only the total value of the rise and decay slopes are relevant but the time point where this maximum slope is measured. While the time to the maximum rise slope (Fig. 17 B) is comparable between ESNs and the endogenous pyramidal neurons in the same regions, a significant reduction of the time to the maximum decay slopes of the ESNs in the CA1 region arises in the smaller interval (Fig. 17 D).

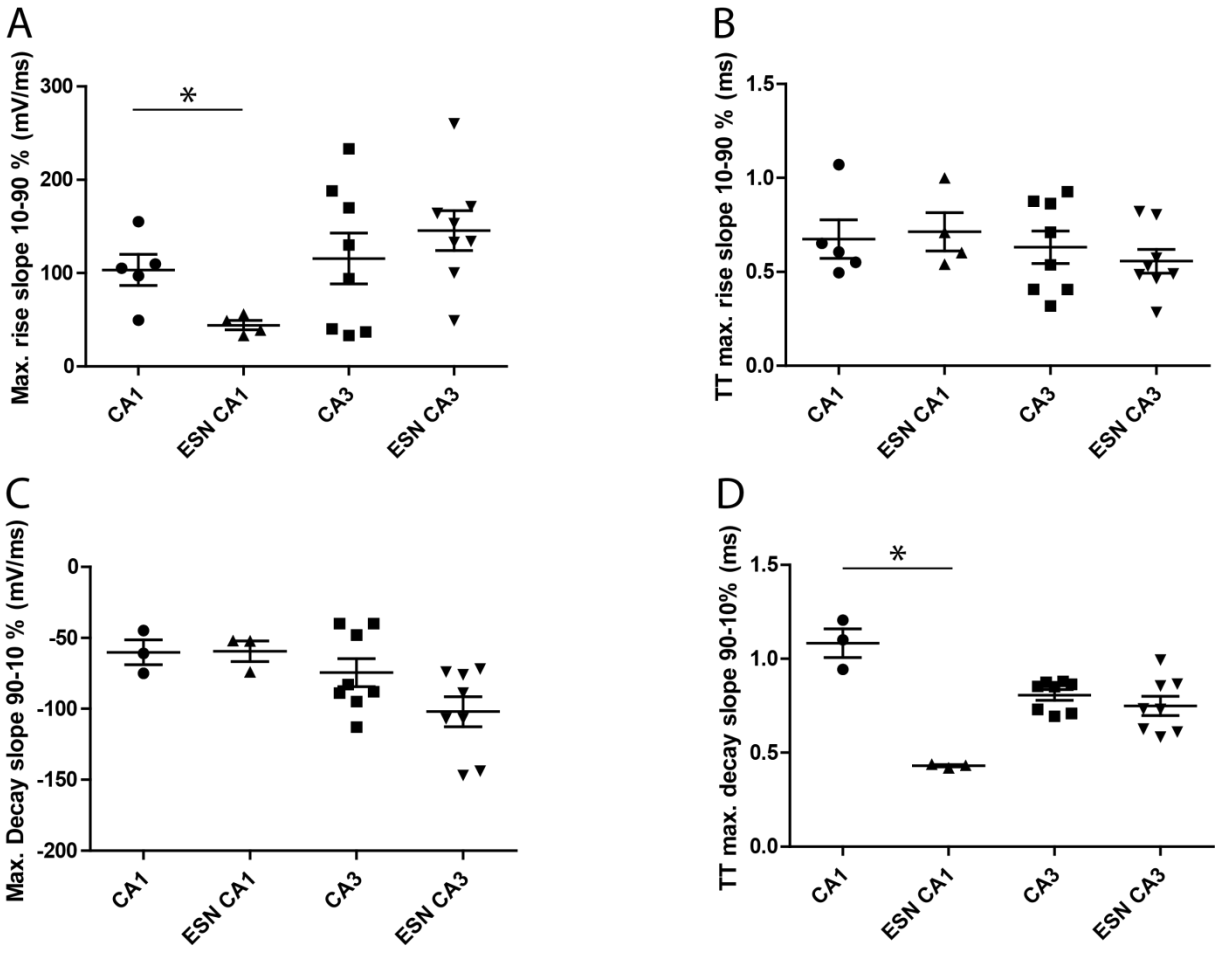

Figure 17: Focusing on a defined interval (10-90%, 90-10%) of the signal reveals differences in rise and decay timings of an action potential for CA1 ESNs. A: CA1 ESNs show a significant reduction of the maximum rise slope between 10 and 90 % of the rising edge while CA3 ESNs are comparable to pyramidal neurons. **B:** The time to the maximum slope is comparable between ESNs and pyramidal neurons as well as for the maximum decay slope (C)**. D:** The time to the maximum decay slope is significantly reduced in CA1 ESNs compared to pyramidal neurons in the same region while ESNs in CA3 region are unaltered. Two-tailed student's t-test, *$p < 0.05$. (CA1, n = 5; ESN CA1, n = 4; CA3, n = 8; ESN CA3, n = 8).

These results indicate that the general slopes and their corresponding timings are generally comparable. Only by focusing on distinct areas of the action potential signal significant differences can be found. Following this, ESNs may have a similar ion channel pattern compared to mature intrinsic pyramidal cells. This ion channel pattern is relevant for the depolarization and repolarization during the AP. The results further indicate that ESNs in the CA1 region have a tendency to faster decay response and maximum rise slopes.

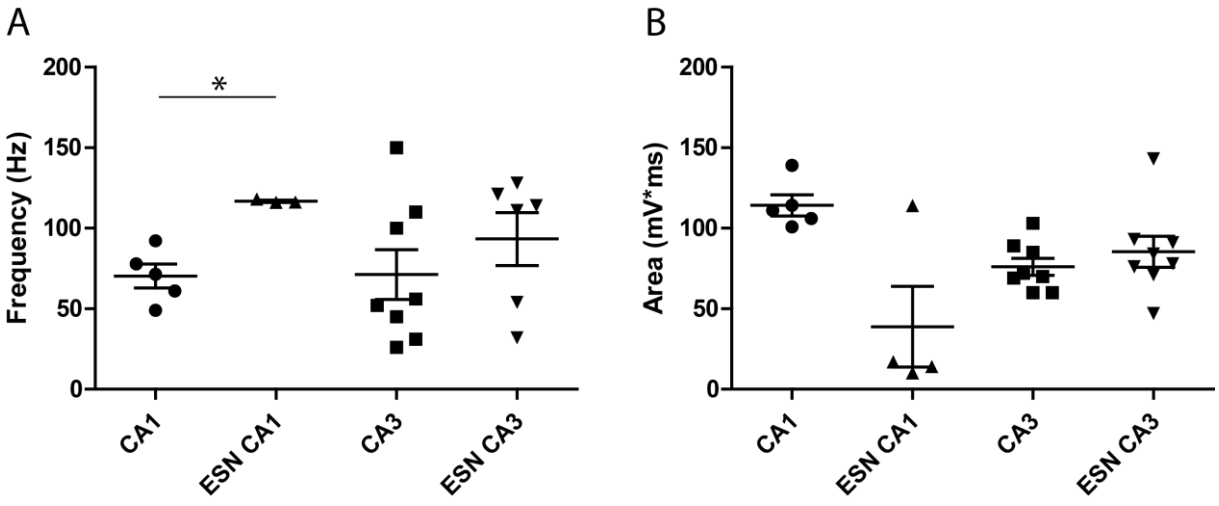

Figure 18: CA1 ESNs show a significant increase in action potential frequency and a tendency to a reduced action potential area. A: Frequency of action potentials evoked by current injection. CA1 ESNs show a significant increase in action potential frequency compared to CA1 pyramidal neurons while CA3 ESNs are comparable to intrinsic cells in the same region. **B:** Total area of action potentials show no significant difference between the ESNs and pyramidal neurons but a tendency to a reduced area in CA1 ESNs compared to intrinsic cells of the same area. Two-tailed student's t-test, *$p < 0.05$. (CA1, n = 5; ESN CA1, n = 4; CA3, n = 8; ESN CA3, n = 8).

The previous findings led to the question if the general action potential shape and/or frequency are affected by the faster and shorter depolarization and repolarization phases. The area under the AP was calculated showing no significant difference for all four groups but a tendency in ESNs transplanted into the CA1 region for a smaller area under the AP (Fig. 18B). The frequency of the APs is significantly increased in ESNs transplanted into the CA1 region in comparison to neighboring cells (Fig. 18 A). ESNs in the CA3 region show no significant difference to their intrinsic controls.

Taken together ESNs are generally able to evoke APs with typical characteristics of neighboring hippocampal pyramidal neurons. In distinct parameters they differ from intrinsic

neurons in the same region. Especially ESNs in the CA1 region have a faster AP firing pattern together with a lower peak amplitude, faster half-width, faster decay slope time and frequency.

3.1.3 Properties of miniature EPSCs in type A ESNs

After showing that ESNs are able to fire APs by injecting currents the next step was to analyze events which are affected by intrinsic triggers. For this purpose, miniature EPSCs were recorded from ESNs and compared to pyramidal neurons in the same region of the hippocampus concerning two important dynamic parameters, amplitude and inter-event interval.

Due to the relatively high number of events (up to 3873 / cell) two different plotting methods were chosen: The cumulative fraction to visualize the high number of events and the averaged display for a statistical analysis.

The cumulative fraction of EPSCs amplitudes shows a tendency of higher amplitudes for the ESNs transplanted in the CA3 region especially between 20 and 30 pA (Fig. 19 A) but a robust decrease of the amplitude for ESNs in the CA1 region until 30 pA (Fig. 19 C). The mEPSC interval of ESNs of both regions is longer (Fig. 19 B), especially the ESNs in the CA1 region showed distinct longer intervals (Fig. 19 D).

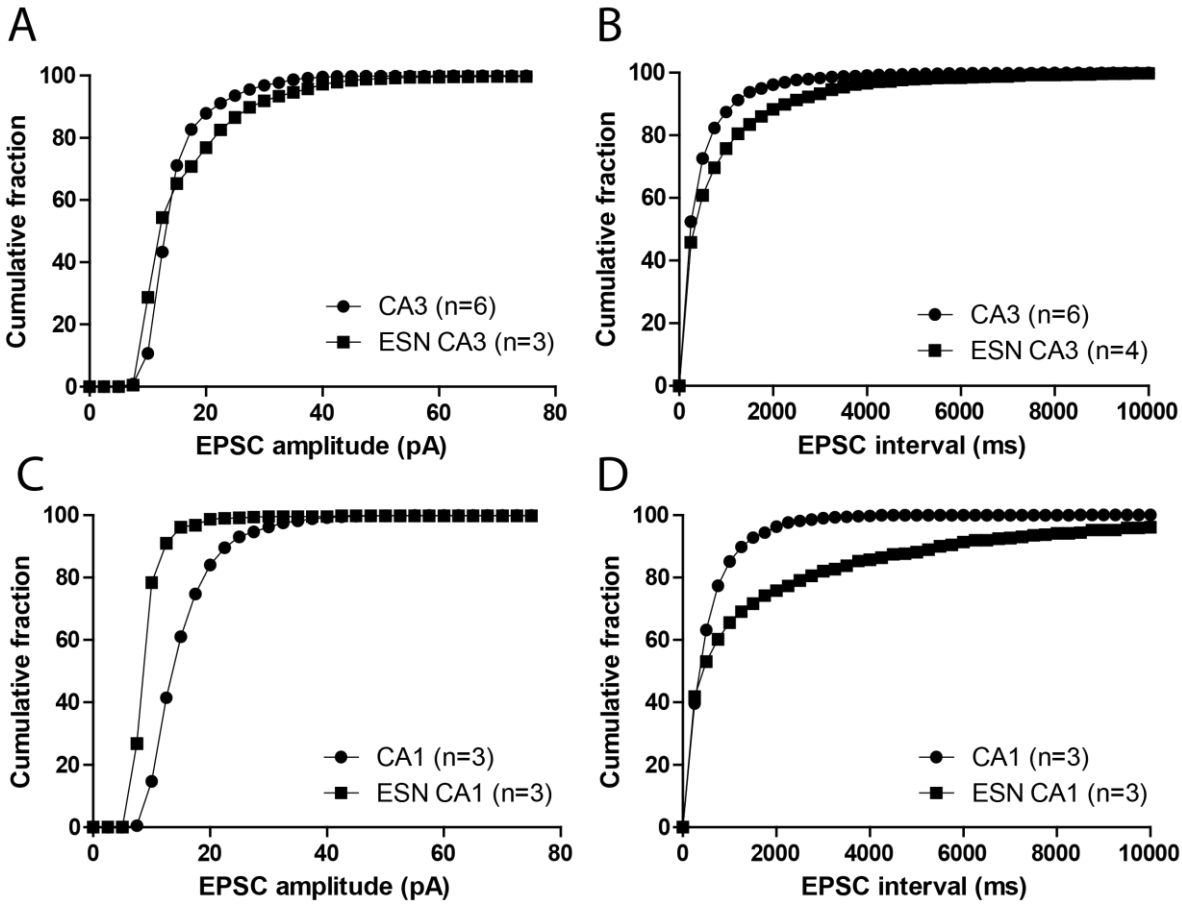

Figure 19: Cumulative fractions of amplitude and interval of miniature EPSCs of ESNs and pyramidal neurons in organotypic hippocampal slice cultures in two different regions. A: ESNs in CA3 region show a tendency to higher mEPSC amplitudes while CA1 ESNs show smaller mEPSC amplitudes (C). **B, D:** ESNs in CA1 and CA3 region showed longer mEPSC intervals in comparison to pyramidal neurons.

A statistical approach was done by using the average of all EPSCs of one cell and therefor reducing the number of experiments to the number of measured cells the previous findings are supported but are not significantly different (Fig. 20).

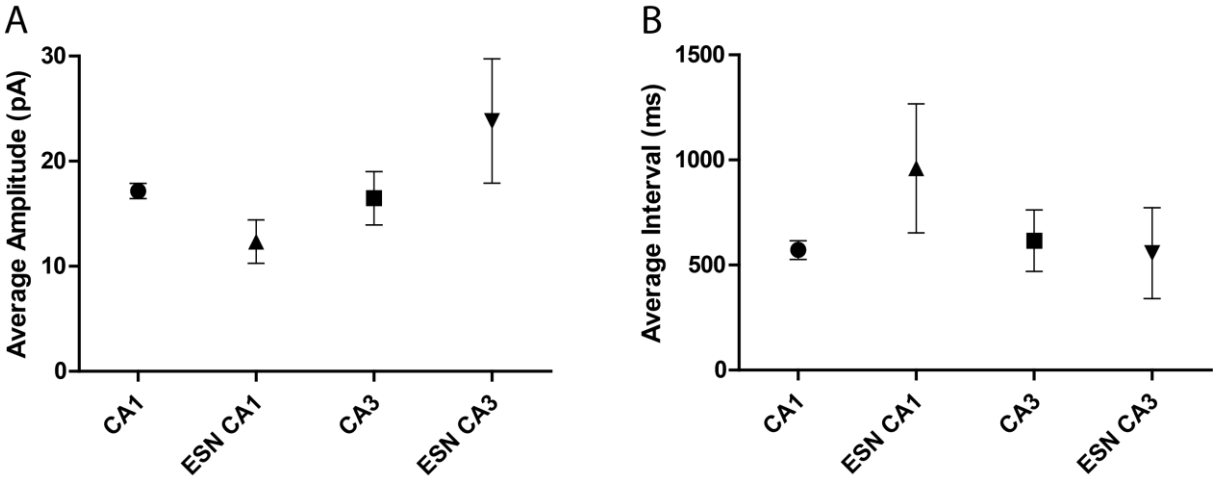

Figure 20: Average amplitude and interval of miniature EPSCs in ESNs and pyramidal neurons is not significantly altered in organotypic hippocampal slice cultures. A: In both regions the average amplitude of the ESNs is comparable to the intrinsic cells. **B:** The average interval of between two mEPSCs is comparable between ESNs in both regions. (CA1, n = 3; ESN CA1, n = 3; CA3, n = 6; ESN CA3, n = 4).

These findings show that ESNs display miniature EPSCs which are comparable to EPSCs in pyramidal neurons with a tendency to have lower amplitudes and longer intervals in ESNs in the CA1 region.

3.1.4 Identification of neurotransmitter receptors in CA3 ESNs via stimulation evoked EPSCs

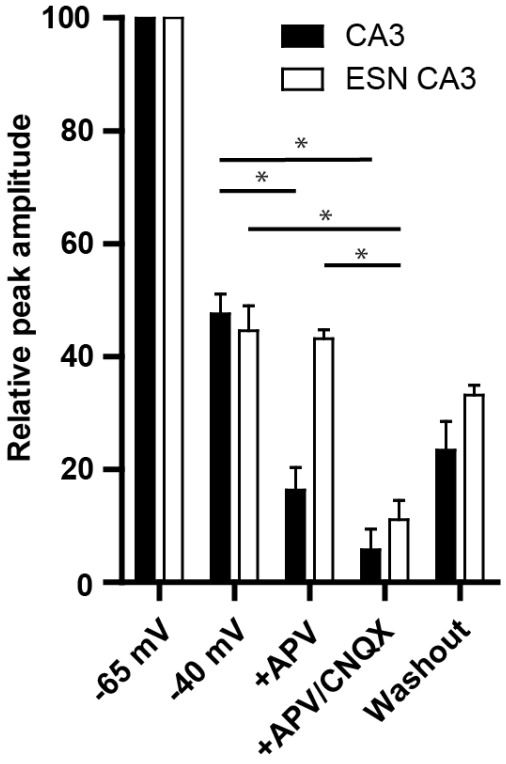

Figure 21: CA3 ESNs form EPSCs with the AMPA, but not NMDA receptor. EPSCs from ESNs in CA3 region are sensitive to CNQX, but not APV. n = 3. Two-tailed student's t-test, *p < 0.05.

The previous findings indicate that ESNs are able to form EPSCs which are potentially evoked by neurotransmitter release and a subsequent activation of transmitter-sensitive ion channels. The next step was to use pharmacological compounds to eliminate specifically EPSC signals mediated by the NMDA- and/or AMPA-receptor.

ESNs in the CA3 region are able to evoke EPSCs after stimulation in the *dentate gyrus* at -65 mV and -40 mV (Fig. 21). The relative peak amplitudes at both holding potentials are comparable to intrinsic pyramidal neurons in the CA3 region of the hippocampus. By the step-wise application of APV and APV + CNQX the signals of the ESNs showed a significant tolerance to APV+CNQX ($p = 0.043$) but not APV alone ($p = 0.83$), while endogenous pyramidal neurons show a significant decrease in the amplitude following both APV ($p = 0.034$) and APV+CNQX ($p = 0.015$). These results suggest that only the AMPAR is responsible for the evoked EPSCs but not the NMDA-receptor or possibly the NMDA-receptor is not present in ESNs in the CA3 region.

3.1.5 Characteristics of type B ESNs

As described by F. Neuser (Neuser, 2010) besides the type A ESNs there is a type B categorized ESN subset. In this study the type B ESNs were morphologically analyzed revealing a degree of maturation that was not comparable to type A ESNs or intrinsic pyramidal cells and they do not carry dendritic spines with some rare exceptions. Staining against presynaptic markers indicate that type B ESNs are a target for excitatory as well as inhibitory projections of intrinsic neurons but the study finally came to the hypothesis that type B cells are missing external input to support maturation equivalent to type A ESNs. Here I was able to show that type B ESNs are reproducible not capable to react to external stimulation in a set of experiments concerning AP and mEPSCs. Figure 22 shows weak responses but missing action potentials (B) even after a robust depolarization (C). In addition miniature EPSCs could never be detected (A).

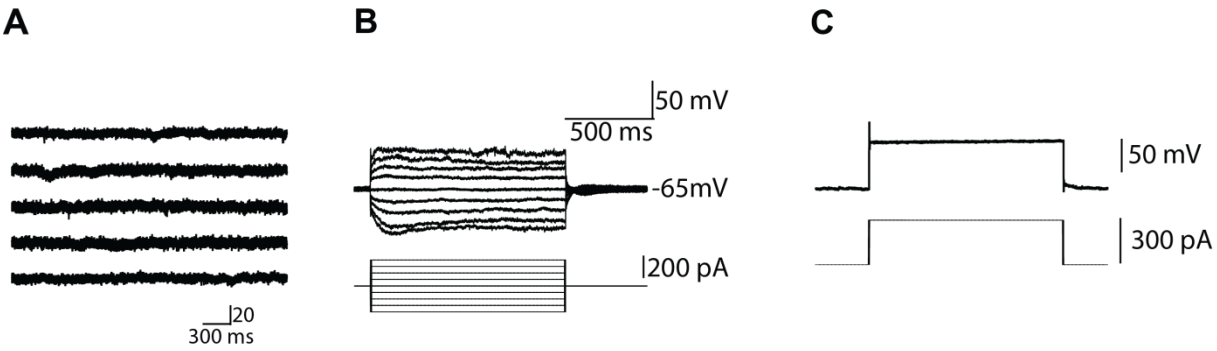

Figure 22: Representative traces of type B ESNs in the organotypic hippocampal slice culture. A: Missing miniature EPSC in a voltage clamp experiment. **B:** Step-wise current-injection showing weak reactions in a type B ESN. **C:** Strong depolarization showing passive reaction with missing action potentials.

3.2 The endocannabinoid receptor 1

The CB1 receptor (CB1R) is one of the widely expressed G-Protein coupled receptors in the CNS and, to date, the only molecularly characterized cannabinoid receptor in the brain (Freund et al., 2003a;Howlett et al., 2002). The CB1R is an important mediator of short-term plasticity through a general depolarization-induced suppression of inhibition (DSI), this is caused by a reduction of GABA-mediated neurotransmission. The CB1R is encoded by the *cnr1* gene and the protein is localized pre-synaptically on both glutamatergic and GABAergic neurons. The opposing inhibitory effects of the CB1R (respectively the cannabinoid release) on both, inhibitory and excitatory neurons may be finally cancelled out effects in the neuronal network. On the other hand it is possible that modulation in the expression of the CB1R or its ligands make it possible to increase or decrease the strength of specific synapses. With the conditional knockouts of the CB1R in glutamatergic or alternatively GABAergic neurons it is possible to discriminate between the role of this receptor for excitatory or inhibitory cells and determine the effect of those CB1R deficient neurons on the hippocampal network, respective in this study of hippocampal pyramidal neurons.

3.2.1 GABA-CB1$^{-/-}$ and functional synaptic plasticity in pyramidal neurons

In a first approach the effect of the knockout of the CB1R of GABAergic neurons was examined in pyramidal hippocampal neurons. It is known that the CB1R inhibits the release of neurotransmitters at the axonterminals. At synapses where the CB1R is missing in GABAergic presynapses one could conclude in an increased GABAergic synaptic transmission and a following hyperpolarizing effect for the post-synapse. This may affect the mechanism for the induction of NMDAR dependent long-term potentiation. In these experiments functional synaptic plasticity was tested using the paradigm of LTP (Fig. 23 A). The summary data of all experiments are shown as mean with a stable baseline (3 ± 1 %). GABA-CB1$^{-/-}$ mice ($n = 10$) showed a significant ($p < 0.05$) decreased potentiation starting from minute four after tetanization until the end of the experiment in comparison to flanked littermate controls ($n = 10$).

Basal transmission was analyzed by modulation of the stimulus strength and the corresponding EPSP size. This allows conclusions on the postsynaptic transmission (Fig. 23 B). The slope is significantly increased at 25 ($p = 0.0008$) and 50 ($p = 0.023$) µA stimulus strength in GABA-CB1$^{-/-}$ mice in comparison to littermate controls. With the application of higher currents the responses of GABA-CB1$^{-/-}$ mice were indistinguishable to controls.

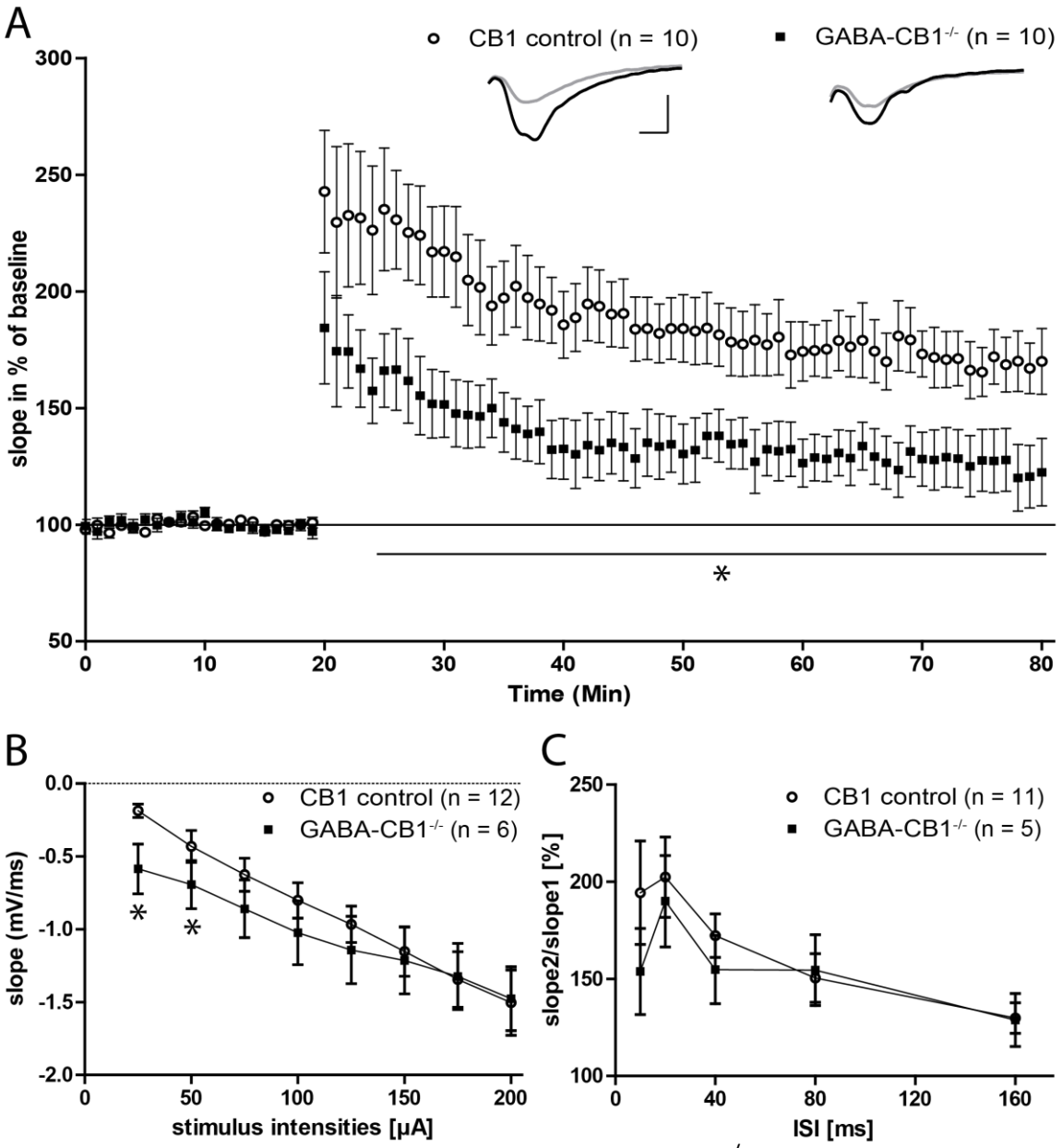

Figure 23: Summary of a set of extracellular fEPSP recordings in GABA-CB1$^{-/-}$ mice. A: LTP with 20 minutes baseline recording, followed by TBS inducing a long lasting potentiation in both phenotypes. GABA-CB1$^{-/-}$ mice show a decreased potentiation, significant from minute 4 after tetanization. **B:** EPSP slopes plotted against stimulus intensities showing significant increased slopes at 25 and 50 µA for GABA-CB1$^{-/-}$ mice. **C:** GABA-CB1$^{-/-}$ mice have a tendency to decreased paired-pulse facilitation ratios at 10 and 20 ms ISI. Two-tailed student's t-test, *$p < 0.05$, insets show original traces of representative individual experiments, vertical scale bar = 1 mV, horizontal scale bar = 4 ms.

The ability of pre-synapses to react adequate to two temporary fast stimuli was tested with paired-pulse facilitation (PPF). The relation between the value of the second slope and the first slope is shown with different inter-stimulus intervals (ISI) in Figure 23 C. Both phenotypes show comparable values with a maximum at 20 ms ISI. There is a tendency for higher values in controls between 10 and 40 ms.

Taken together the results show a strong effect on LTP but decent influences on basal transmission in GABA-CB1$^{-/-}$ mice. To see if this strong effect is reproducible, but in the contrary direction, the next step was to repeat these experiments in Glu-CB1$^{-/-}$ mice.

3.2.2 Glu-CB1$^{-/-}$ and functional synaptic plasticity in pyramidal neurons

In Glu-CB1$^{-/-}$ mice the CB1R is missing specifically at the axon-terminals of glutamatergic neurons. It is known that the CB1R inhibits the release of neurotransmitters at the axon-terminals. At synapses where the CB1R is missing in glutamatergic pre-synapses one could conclude in an increased glutamatergic synaptic transmission and a following depolarizing effect for the post-synapse. This may affect the mechanism for the induction of NMDAR-dependent long-term potentiation. LTP experiments (Fig. 24 A) reveal that the LTP is significantly ($p < 0.05$) increased in Glu-CB1$^{-/-}$ mice ($n = 9$) in comparison to littermate controls ($n = 9$) for the whole range of 60 min after tetanization.

Basal transmission was analyzed by modulation of the stimulus strength and the corresponding EPSP size. This allows conclusions on the postsynaptic transmission (Fig. 24 B). Basal transmission is modulated at higher currents. Comparable at low current values (25-100 µA) the slope values of Glu-CB1$^{-/-}$ mice stay significantly lower at 125 µA ($p = 0.045$), 150 µA ($p = 0.03$), 175 µA ($p = 0.015$) and 200 µA ($p = 0.009$). Paired-pulse facilitation is not altered between both phenotypes at all ISI values (Fig. 24 C).

These results show that the CB1R has an effect on LTP and EPSP sizes in pyramidal neurons but no significant changes in PPF. The LTP results in Glu-CB1$^{-/-}$ mice show an opposed effect to GABA-CB1$^{-/-}$ mice.

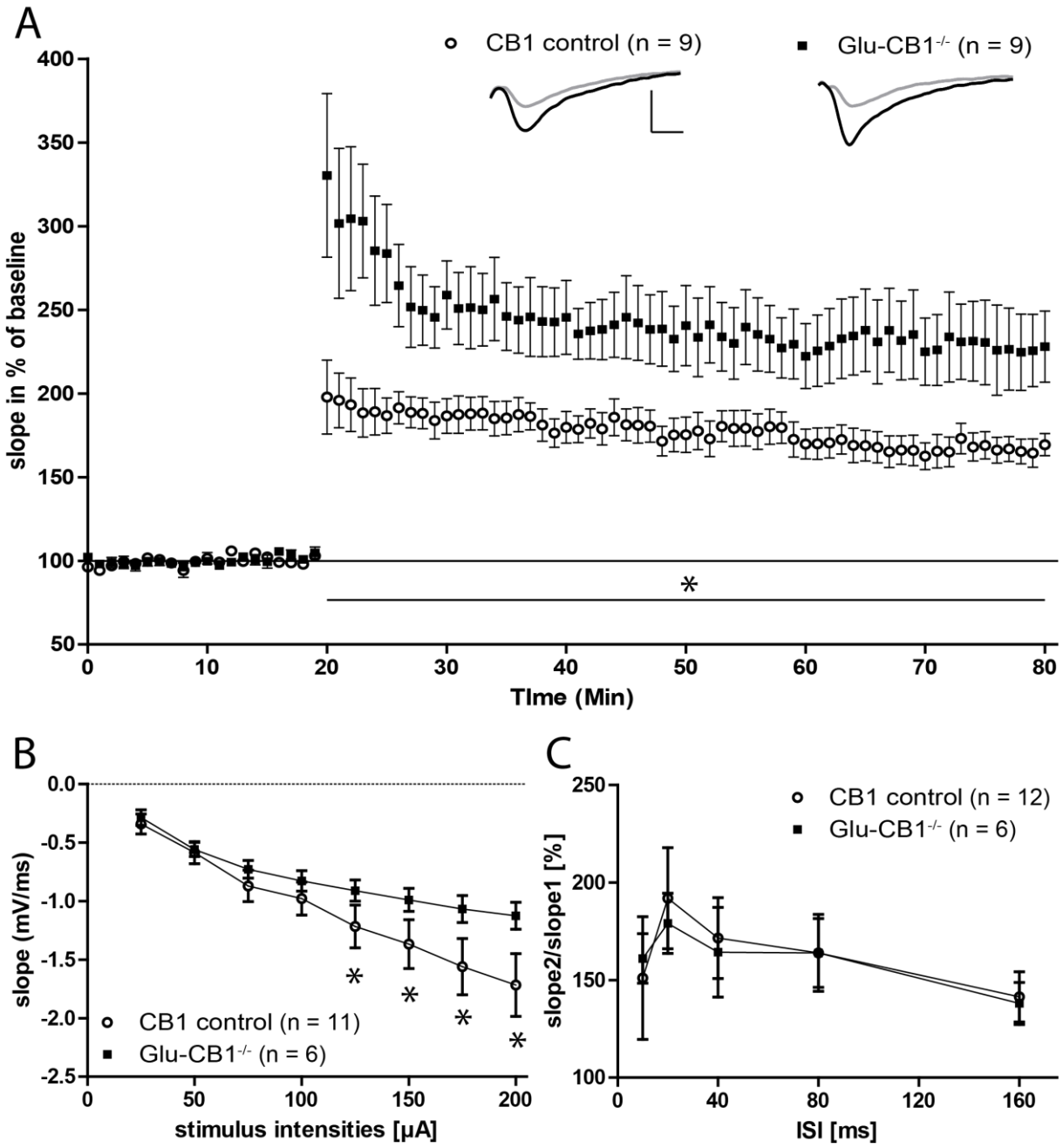

Figure 24: Summary of a set of extracellular fEPSP recordings in Glu-CB1$^{-/-}$ mice. A: LTP with 20 minutes baseline recording, followed by TBS inducing a long lasting potentiation in both phenotypes. Glu-CB1$^{-/-}$ mice show an increased potentiation, significant for 60 minutes after tetanization. **B:** EPSP slopes plotted against stimulus intensities showing significant decreased slopes from 125 to 200 µA for Glu-CB1$^{-/-}$ mice. **C:** Glu-CB1$^{-/-}$ mice show comparable paired-pulse facilitation ratios. Two-tailed student's t-test, *p < 0.05, insets show original traces of representative individual experiments, vertical scale bar = 1 mV, horizontal scale bar = 4 ms.

4. Discussion

4.1 Integration of ESNs into pre-existing neuronal circuits

Already early after the discovery of adult neurogenesis in the human brain the field of recreation from acute injuries inside the central nervous system and progressive neurodegenerative diseases got an additional direction (Bjorklund and Lindvall, 2000). The process of substituting lost neurons or whole neuron population by transplanting neuronal precursors raises various questions and problems: One of them is the fate of a transplanted precursor cell determines if it was transplanted artificially into a defined area? Will the cell be integrated into the pre-existing network consisting of countless intrinsic neurons and glia cells? Which factors are important for a functional and successful integration? These questions particularly show that neuronal integration is not only a field of clinical relevance but also attractive for basic research. While the adult neurogenesis and the integration into neuronal circuits of intrinsic new-born neurons is widely investigated (Lledo et al., 2006); the same processes in transplanted embryonic stem cell derived neurons (ESNs) into neuronal tissue is not completely understood.

In this approach of the present work I was interested in the possible role of functional integration of transplanted ESNs into hippocampal organotypic slice cultures in adult neurogenesis. For this purpose, I established an electrophysiological method to compare electrophysiological parameters of transplanted ESNs in the CA1 and CA3 region of the hippocampus with neighboring intrinsic pyramidal neurons.

As described in the dissertation of F. Neuser (Neuser, 2010) the transplanted precursors were prepared to differentiate into pyramidal neurons in cortex and hippocampus and hippocampal granule cells. Therefore the differentiating procedure was optimized for a predominant expression of the typical protein pattern of Pax6-positive radial glia like nestin, RC2, the brain lipid binding protein (BLBP) and the transcription factor emx2 (Nikoletopoulou et al., 2007). Additionally, there is evidence for Pax6-positive radial glia cells being sensitive to local spinal cord cues, but there was no prevalence to peripheral sensory neuron differentiation found in these lines (Plachta et al., 2004).

4.1.1 Type B ESNs

Using the same transplantation protocol as described in the dissertation of F. Neuser and the studies of M. Bibel (Neuser, 2010;Bibel et al., 2004;Bibel et al., 2007) an apparent effect could be reproduced: EGFP positive ESNs could be separated into two groups by specific criteria concerning position in the hippocampal layers, morphology of the dendritic tree, appearance and distribution of dendritic spines, EGFP signal intensity and nucleus shape (for details see 2.10.1). These groups were termed type A and type B ESNs. Finally, the low number of type A ESNs (3,9 %) appears to be more morphologically developed comparable to intrinsic hippocampal neurons while type B ESNs stay at an immature stage and do occur in large numbers (96,1 %). This may be due to local signals from the pre-existing network which are received by the ESNs and which are maybe crucial to cross the developing step to maturate to type A ESNs. Recent evidence comes from studies showing that hippocampal activity itself can support proliferating progenitors (Tozuka et al., 2005). Additionally, glutamate is capable to increase proliferation through AMPAR (Bai et al., 2003) in the hippocampus of rats. Growth factors like BDNF, CNTF and VEGF support the adult neurogenic proliferation (Katoh-Semba et al., 2002).

My first finding that type B ESNs in the CA1 and CA3 region lack miniature excitatory postsynaptic currents (mEPSCs) supports the hypothesis of missing synaptic input from the surrounding neuronal network. Miniature EPSCs are the synaptic response to the release of a single vesicle from the pre-synapse. From the total absence of mEPSCs might be deduced that postsynaptic ligand-sensitive channels as glutamatergic AMPA (α-amino-3-hydroxy-5-methyl-4-isoxazolepropionic acid) receptors (AMPAR) and NMDA (N-methyl-D-aspartate) receptors (NMDAR) lack in this cell type. There is evidence for a positive interdependency between AMPAR- and NMDAR mediated mEPSCs in hippocampal cultures, indicating a possible absence of both receptors in type B ESNs (Kato et al., 2007). The possible absence of spines or synapses in type B ESNs was questioned in a recent study, which showed the presence of active presynaptic excitatory and inhibitory terminals (Neuser, 2010). Recent studies and later findings in this study give rise to a general ability of developed transplanted cells for the presence of mEPSCs in the hippocampus (Benninger et al., 2003), EPSCs in astroglial precursors (Berninger et al., 2007a), in neurons derived from expanded adult neural stem cells (Berninger et al., 2007d) and in dissociated ES culture (Bibel et al., 2004).

In line with the previous results, type B ESNs in the CA1 and CA3 region never showed action potentials (APs). In a neuronal network EPSPs are the trigger for APs due to summation of depolarization over the threshold at the axon hillock. Although EPSPs are absent in type B ESNs the manipulation of the membrane potential under the AP threshold during voltage-clamp recordings revealed an EPSP-independent lack of APs. The depolarization and repolarization of the membrane during the AP is mainly dependent on voltage-gated Na^+ and K^+ channels. There is evidence for young postnatal and for transplanted cells that they are in general capable to evoke APs (Schmidt-Hieber et al., 2004). It is known that young newly generated granule cells in the adult hippocampus have a high input resistance and a subthreshold Ca^{2+} concentration, which enables them to fire APs with a low threshold (Schmidt-Hieber et al., 2004). Additionally, developed transplanted cells show APs (Benninger et al., 2003;Berninger et al., 2007a;Berninger et al., 2007d;Bibel et al., 2004).

Next, voltage-gated ion channels consist of a specific subunit-compositions depending on the difference in the expression patterns of the single subunits (Pongs, 1999), which may not be the case in type B ESNs due to their immature character. Another possible reason for the lack of APs in type B cells may be provided by a study that showed the influence of Ca^{2+} concentration on APs of hippocampal pyramidal neurons in the CA1 region via Ca^{2+} sensitive K^+ channels (Sah, 1996). Following this, type B ESNs seem to be insensitive for induction of APs due to missing or immature ion channel patterns.

Taken together these findings point to missing input in transplanted type B ESNs from the pre-existing network and underline the important role of external input during maturation of ESNs. Beside the type of external input the source of the input may be important. The surrounding cells are highly complex which results in highly heterogenic arrangement of cell compartments. Transplanted ESNs located in the cell body layer often developed to type A ESNs. In contrast, type B ESNs were often localized superficial or outside the cell body layer (Neuser, 2010). This let me conclude a crucial role for the final location of transplanted ESNs in adult neurogenesis.

4.1.2 Type A ESNs show actions potentials and mEPSCs

Type A ESNs show a more mature morphology comparable to intrinsic pyramidal neurons in the CA1 and CA3 region (Neuser, 2010). In a set of electrophysiological experiments I was able to show that type A ESNs had comparable basal electrical characteristics in an I-V curve to neighboring intrinsic pyramidal neurons (see Fig. 14). The I-V curve represents the currents flow through ion channels to given voltage steps. This allows direct insights into the general conductance of the membrane (HODGKIN et al., 1952). Although the reversal potential of the cells or of distinct ions was not examined in my work, these results show the general ability of the membrane of ESNs transplanted in the CA1 and CA3 region to have a conductance characteristic compared to intrinsic pyramidal neurons. These findings were supported by further experiments concerning injected and total received measured current over the membrane. These results (Fig. 14 B) showed clearly the tendency of ESNs for region specific membrane characteristics in the CA1 and the CA3 region compared to neighboring intrinsic pyramidal neurons in the same region. Additional experiments showed a less complex dendritic morphology in type A ESNs in the CA1 region than the CA3 region (Neuser, 2010). Furthermore, specific electrical properties for glutamatergic receptors differ between the CA1 and the CA3 region (Jonas and Sakmann, 1992). Next, it was found that there are region specific differences in NMDA currents in hippocampal pyramidal neurons (Grishin et al., 2004) and different roles for the CA1 and the CA3 region in memory consolidation (Farovik et al., 2010). This region specific differentiation and the region specific character in comparison to intrinsic neighboring pyramidal neurons suggest the advanced stage of the maturation of transplanted ESNs in both regions probably induced by cues of local hippocampal neuron populations.

The transplanted ESNs in the CA1 and the CA3 region show a typical resting membrane potential for excitable neuronal cells. This crucial ability of the cell to create an electrical potential between the interior and the exterior lumen over the plasma membrane indicates the active und functional interplay between ion channels, ligand-gated channels and ion pumps. The value of the resting membrane potential is expressed by the Goldman equation which is highly depending on the membrane permeability for K^+, Na^+ and Cl^-. Furthermore recent studies showed comparable results in dissociated embryonic stem cells (Bibel et al., 2004), three weeks old transplanted ES cells (Husseini et al., 2008;Benninger et al., 2003),

neurons derived from reprogrammed astroglial ES cells (Berninger et al., 2007b) and ES cells from an embryonic carcinoma cell line (Magnuson et al., 1995). According to these results a high degree of maturation can be concluded for the type A ESNs transplanted in the CA1 and CA3 region to carry ion channel patterns which result in a typical resting membrane potential for intrinsic pyramidal cells and neuronal excitatory cells in general.

In contrast, the capacitance values of the transplanted ESNs in both regions are highly increased in comparison to intrinsic pyramidal neurons. Studies concerning the maturation of developing ES cells found an increasing capacitance over time (Benninger et al., 2003;Husseini et al., 2008), but never to an extend shown in this thesis. The capacitance is directly proportional to the membrane surface area which would point towards an increase in the size of the ESNs. In the dissertation of F. Neuser (Neuser, 2010), however, the morphology of transplanted ESNs in both areas showed a reduced dendritic complexity. In conclusion there is no evidence for a larger membrane surface area of single ESNs. One explanation for the increase in capacitance might reside in an increased direct connection of ESNs to neighboring cells via gap junctions. The expression level of Gap junctions is high during development in several areas of the brain, especially in the developing neocortex and decreases during the maturation of neuronal circuits, for reviews (Bennett and Zukin, 2004;Naus and Bani-Yaghoub, 1998). In line with this, the immature profile of the transplanted ENSs described above might indicate that the expression levels of Gap junction proteins could be still high in these cells. A staining for different gap junction proteins in transplanted slices could help to answer this question.

A different explanation for the increase in capacitance might come from the fact that in her dissertation Franziska Neuser could show at least in some cases a direct cytoplasmic connection of type A ESNs to neighboring cells which could be either ESNs or intrinsic hippocampal cells. This might point to a mechanism of fusion of ESNs with one another or with intrinsic cells. . Further experiments need to be carried out to investigate this possible fusion of ESNs in more detail.

The AP threshold in transplanted ESNs in the CA1 and CA3 region is comparable to intrinsic pyramidal neurons. In line with a recent study in dissociated ES cell cultures (Bibel et al., 2004) this gives evidence for a neuron-typical distribution of voltage-gated Na^+ channels (HODGKIN et al., 1952) in transplanted ESNs in the CA1 and the CA3 region. This is partly

supported by the peak amplitudes reported here which are comparable between ESNs in the CA3 region and neighboring cells and recent studies in neurons during maturation (Esposito et al., 2005) and dissociated ES cells (Bibel et al., 2004).

In contrast, peak amplitudes of APs are reduced in ESNs of the CA1 region indicating differences of voltage-gated ion channels for Na^+ and K^+ between ESNs and intrinsic pyramidal neurons. These channels are directly responsible for the induction and course of APs. In addition with the reduced half-width and the tendency of a reduced AP area in ESNs in the CA1 region this can be explained by a possible modulation of the α- or β-subunits of the voltage-gated K^+ channel resulting in a higher conductance for K^+ and, as a result of this, a lower peak amplitude (Gutman et al., 2005). Additional findings concerning AP slope characteristics in ESNs in the CA1 region and the prolonged activation of a voltage-gated K^+ channel subunit (Guan et al., 2011) support the theory of a modulated subunit composition of the voltage-gated K^+ channel in type A ESNs in the CA1 region.

The influence of the voltage-gated Na^+ channels on the AP in the induction of an AP seems to be minor because of its well investigated subunit $Na_V1.1$. This subunit is crucial for the induction of an AP and modulations of this subunit generally promotes a longer opening probability of the ion channel (Isom, 2001). The higher conductance of the previously described voltage-gated K^+ channel gives additional evidence for the investigated higher after hyperpolarization (AHP) in ESNs of the CA1 and CA3 region: Recently, a study revealed a longer activation of voltage-gated K^+ channels in young post-natal stages in neocortical pyramidal neurons (Guan et al., 2011).

Taken together, these findings indicate an advanced pyramidal cell-like maturation concerning basal electrical parameters and APs in type A ESNs, as reported recently (Benninger et al., 2003;Husseini et al., 2008). In this study I could provide further insight into the region-specific maturation of ESNs in a pre-existing hippocampal network under the possible consideration of local cues.

4.1.3 Type A ESNs are integrated into the pre-existing hippocampal network

As described before (Wernig et al., 2004) ESNs are capable of the successful integration into a local pre-existing circuitry. Miniature EPSCs give rise to a synaptic neurotransmitter-dependent connection between neurons. EPSCs in ES cells were shown before (Bibel et al., 2004;Benninger et al., 2003) but never in the context of a surrounding organotypic neuronal circuit. In this study, the mEPSCs reported for ESNs in the CA1 and the CA3 region provide evidence for transmitter release at functional synapses between ESNs and local hippocampal neuronal populations. No significant differences were found in mEPSCs amplitudes or frequencies both in the CA1 and in the CA3 region. These results suggest the successful integration of ESNs into the local hippocampal circuitry.

4.1.4 Type A ESNs in CA3 show AMPAR- but not NMDAR mediated currents

Further results obtained in this study reveal the absence of NMDAR mediated currents in ESNs in the CA3 region while intrinsic pyramidal neurons in this region show currents of both types of glutamatergic receptors. This was found earlier in similar integration studies (Wernig et al., 2004;Benninger et al., 2003), although the presence of the NMDAR was shown during the entire process of neuronal maturation (Monyer et al., 1994). A contrary study showed in new-born intrinsic granular cells lacking the NMDAR subunit NR1 the generation of functional synaptic spines (Tashiro et al., 2006). The possibility of the coincident presence of the NMDAR but absence of NMDAR mediated currents was discussed in a study that found the inactivation of NMDAR mediated currents by intracellular calcium in hippocampal cultures (Legendre et al., 1993). The results showed here do not directly point to the absence of the NMDAR but its mediated currents, further investigations are necessary in this topic.

Nowadays two different crucial principles in regulating neurogenesis are known: intrinsic programmes and external cues. The external cues investigated in this thesis deal with electrical connection of the ESNs with the neuronal network via NMDAR and AMPAR. The absence of NMDAR mediated currents points to the minor role of NMDAR mediated synaptic plasticity in adult neurogenesis. Recent evidence comes from studies showing that

hippocampal activity itself can support proliferating progenitors (Tozuka et al., 2005). Additionally, glutamate is capable to increase proliferation through AMPAR (Bai et al., 2003) in the hippocampus of rats. In contrast, glutamate decreases the proliferation when acting through the NMDAR (Cameron et al., 1995). This raises the questions if type A ESNs only maturate due to the absence of NMDAR mediated currents. Other external cues may be growth factors like BDNF, CNTF and VEGF support the adult neurogenic proliferation (Katoh-Semba et al., 2002).

The fact that only 3.9 % of the found ESNs were categorized into type A ESNs disproves the predominant role of intrinsic programmes in adult neurogenesis. It was shown that the activation of Ca^{2+} channels plays an important role in neurogenesis (Deisseroth et al., 2004). One more important signaling system during development is the WNT system, which is highly connected to neurogenic proliferation in the adult *dentate gyrus* (Lie et al., 2005).

Recently it was shown that mammalian neural stem cells are not passive elements of their microenvironment. They can re-differentiate into endothelial cells under certain conditions (Wurmser et al., 2004). This suggests that intrinsic programmes and external cues are in a bidirectional interaction. From the results of this study I would conclude that the intrinsic programmes of the ESNs may support the successful adult neurogenesis. However, the final location of the ESN inside the cytoarchitecture of the hippocampal slice may play a crucial role for the support of the intrinsic programmes with external cues from the surrounding network.

4.1.5 Conclusions and Outlook

In the present study I could show that ESNPs transplanted into hippocampal slice cultures mature and integrate into the pre-existing neuronal network. ESNs showed mainly electrophysiological qualities of neighboring intrinsic pyramidal neurons. Additionally, I was able to show AMPAR mediated currents but the absence of NMDAR mediated currents in ESNs in the CA3 region of the hippocampus. This gives evidence for the bidirectional role of intrinsic programmes and external cues in adult neurogenesis. Previous work showed functional integration of ESNs in the hilar region of the dentate gyrus (Benninger et al., 2003). Together with the recent morphological analysis of the transplanted ESNs (Neuser,

2010) and my findings additional future work especially in the electrophysiological field is necessary to examine the functional integration in detail on the synaptic level. The absence of NMDAR mediated currents was shown before (Benninger et al., 2003) but it is known that immature and mature neurons carry the NMDAR with changing subunits, which participate in postsynaptic currents (Cline et al., 1996). Another method to detect the presence of the NMDAR and at the same time test the connectivity between ESNs and the pre-existing circuit may be the induction of NMDAR dependent long-term potentiation via the Schaffer collaterals during patch-clamp experiments. Additionally, induction of the chemical form of LTD by application of the specific NMDAR agonist NMDA (Lee et al., 1998) could reveal more details of the distribution and function of the NMDAR in transplanted ESNs. Furthermore, the combination of calcium imaging techniques, life-imaging, puffing of NMDA could make it possible to investigate on the single-cell level the presence of the NMDAR and its functionality. The composition of the subunits of the NMDAR is crucial for its function (Zhuo, 2009), future investigations could target the composition in type A ESNs, e.g. with immunohistochemical methods (Fritschy et al., 1998).

Despite of that, it would be interesting to investigate if the differentiation to type A ESNs could be further enhanced by stimulation (like the brain-derived neurotropic factor, BDNF) throughout the whole range of the cultivation process. This was shown in the rat hippocampus (Snyder et al., 2009) and in a study investigating the proliferation in the hippocampus (Katoh-Semba et al., 2002).

4.2 The CB1 receptor and its influence on synaptic plasticity

The endocannabinoid receptor 1 (CB1R) is the most highly expressed G protein-coupled receptor in the central nervous system (Herkenham et al., 1990). CB1R expression was amongst others found in hippocampus, basal ganglia, cerebellum, cerebral cortex and amygdala (Freund et al., 2003b;Herkenham et al., 1990;Tsou et al., 1998) consistent with the psychoactive effects of the CB1R ligand THC (Wall et al., 1970). On subcellular level the CB1R was found on axon terminals and its activation leads to a presynaptic inhibition of transmitter release (Schlicker and Kathmann, 2001). The CB1R is located on both excitatory as well as inhibitory cells and so on has influence on the GABAergic- and glutamatergic transmission at the synapse (Laaris et al., 2010;Kawamura et al., 2006). The deletion of the CB1R on cortical and striatal GABAergic interneurons (GABA-CB1$^{-/-}$) and cortical glutamatergic neurons (Glu-CB1$^{-/-}$) helped to investigate the ambivalent role of the CB1R on anxiety (Millan, 2003;Piomelli, 2003), feeding behavior (Bellocchio et al., 2010) and impulsivity (Lafenetre et al., 2009). Together with the finding that the endocannabinoid system (ECS) is an important mediator of different forms of short-term plasticity in various regions in the brain (DSI and DSE) (Llano et al., 1991;Ohno-Shosaku et al., 2002b), these findings gives rise for an additional potential role of the CB1R in long-term plasticity. The ECS mediated depressive form of long-term plasticity (I-LTD) was shown by the use of the theta-burst stimulation protocol (Chevaleyre and Castillo, 2003).

In this approach of the present work I was interested in the influence of the CB1R on both glutamatergic- and GABAergic neurons on synaptic plasticity in the hippocampus and the contribution of each cell type to CB1R mediated processes. For this, I tested long-term potentiation (LTP) and basal electrical properties of pyramidal neurons in the CA1 region in field-EPSP recordings. Previous experiments showed the inhibition of N-type Ca^{2+} channels in the hippocampus by the interaction with the liberated $G_{i/o}$ βγ subunits (Mackie and Hille, 1992) by the CB1R. Additionally, A-type K^{+} channels are positively influenced by the inhibition of adenylyl cyclase and PKA (Ameri, 1999;Howlett et al., 2002;Schlicker and Kathmann, 2001). The calcium conductance of the presynaptic membrane is crucial for neurotransmitter release (Llinas et al., 1981) via the SNARE complex. Considering this I would conclude that the CB1R modulates the neurotransmitter release at inhibitory and

excitatory synapses. In a set of experiments I found opposing effects of this missing inhibition by the CB1R.

4.3.1 Influence of the CB1R on long-term potentiation

In a first approach I investigated the LTP in mice lacking the CB1R on cortical glutamatergic neurons. In those mice the Cre recombinase encoding sequence is knocked in the endogenous NEX locus, which is highly expressed in the hippocampus (Kleppisch et al., 2003). NEX is a helix-loop-helix transcription factor which is expressed in glutamatergic but not GABAergic interneurons to assure the deletion in glutamatergic neurons. In Glu-CB1$^{-/-}$ mice the release of glutamate is no longer inhibited by the ECS following in a hyper-excited neuronal circuit. This is supported by results I found in a set of experiments. LTP is significantly increased in these mice, indicating a general higher excitability of the post-synapse by higher glutamate concentration in the synaptic cleft. This higher concentration would lead to an increased activation of the glutamatergic AMPAR and NMDAR. Those are able to react to increased glutamate concentrations in the synaptic cleft in adequate manner because the dissociation rate of glutamate from the NMDAR and the AMPAR is high enough (Clements et al., 1992). This leads to higher permanent depolarization of the post-synapse. For the induction of LTP there is one more step necessary. The coincidence of the depolarized post-synapse and an additional glutamate release from the post-synapse. This dislocates the Mg^{2+} from the NMDAR with a resulting influx of Ca^{2+} into the post-synaptic cell. This activates mainly kinases (Lynch, 2004): The Calcium/Calmodulin-dependent protein kinase II (CamKII) which is essential (Lisman et al., 2002;Malenka et al., 1989;Malinow et al., 1989) for the induction of LTP. Fast strengthening of the synapse transmission can be explained by the induction of CamKII to insert new AMPARs into the postsynaptic membrane by fast vesicle release from intracellular reservoirs and lateral diffusion and the ability of CamKII to phosphorylate AMPARs, thereby increasing their single-channel conductance (Malinow and Malenka, 2002;Malenka and Nicoll, 1999). Additionally, it was shown that the induction of LTP is dependent on the post-synaptic depolarization (Yoshimura and Tsumoto, 1994).

Taken together this let me conclude the direct influence of the CB1R on the release of glutamate results in a higher depolarization of the post-synaptic neuron. This mediates the

increased induction of LTP via the activation of the NMDAR. On the one hand, the recording of field-EPSPs cannot distinguish between single cells. This left the question open if LTP is increased in all cells or only in those where the threshold for LTP induction was reached. Following this there is still the possibility that the chance for the induction of LTP is increased in Glu-CB1$^{-/-}$ mice. On the other hand it is possible that the depolarization of all cells increased next to the threshold that most of the cells activate the NMDAR. This hypothesis may be supported by findings in this work that the EPSP sizes in Glu-CB1$^{-/-}$ mice are significantly lower at higher stimulation currents, indicating a possible saturation of the excitation of the basal synaptic transmission.

In a second approach I investigated the influence of the CB1R on LTP in mice lacking the CB1R on GABAergic neurons. In GABA-CB1$^{-/-}$ mice the release of the inhibiting neurotransmitter GABA is no longer inhibited by the ECS following in a hypo-excited neuronal circuit. For the induction of LTP the same mechanism are necessary as described previously. In GABA-CB1$^{-/-}$ mice the increased release of GABA resulting in a higher concentration of GABA in the synaptic cleft. GABA binds to the $GABA_A$ receptor and mediates the hyperpolarization of the post-synaptic cell via the influx of Cl^-. The LTP in GABA-CB1$^{-/-}$ mice is significantly decreased supporting the previous described findings for the relevance of a threshold in the post-synapse for the induction of LTP (Yoshimura and Tsumoto, 1994). This is supported by experiments done in this work which show higher EPSP slopes at low stimulus currents. The hyperpolarized post-synapse may be more capable to react on small stimulating currents because it is in a range of polarization where the conductance of the AMPAR is increased. This may be explained by recent findings concerning the depolarization dependent activity of polyamines on AMPAR (Stromgaard and Mellor, 2004).

In addition, recent studies reported heterosynaptic effects of the ECS: Although all forms of endocannabinoid-mediated plasticity share a depressive character, the induction of LTD at inhibitory synapses (I-LTD) results in a LTP at excitatory synapses (Hashimotodani et al., 2007). The increased release of glutamate at excitatory synapses triggers synthesis and release of 2-AG via postsynaptic metabotropic glutamate receptors. Next, 2-AG binds to the CB1Rs at the spatial close GABAergic terminal. The suppressive role of the CB1R on the GABAergic release resulting in a dis-inhibition of the postsynaptic neuron (Chevaleyre and

Castillo, 2003). There is evidence for a link between this GABAergic release and LTP in a study that showed the induction of NMDAR-dependent LTP in the hippocampus is facilitated by the reduction of $GABA_A$ergic IPSCs (Wigstrom and Gustafsson, 1985). Next, the induction of NMDAR-dependent LTP is possible by a stimulus incapable to induce LTP, but DSI. The LTP is endocannabinoid-dependent but occurs only in those cells, which experienced DSI but not neighboring cells (Carlson et al., 2002). This maybe shows a new role of the endocannabinoids in the induction of targeted LTP and a possible link to behavioral learning, where LTP is only induced in a subset of cells, like in the establishment of "place fields" during maze learning in rats (Ekstrom et al., 2001).

4.3.2 Homeostasis and the ECS

Homeostasis is a global principle in biological systems to scale the internal environment and tends to maintain in a stable range. This dynamic range is permanently adjusted to ensure an optimal performance of the system. In the highly modulated system of synaptic connections with permanently strengthening and weakening connections homeostasis plays a key role during development (Turrigiano, 1999). Due to the fact that in the adult nervous system the synaptic strength is modulated during processes of learning and memory homeostasis could be still important. Recent studies revealed mechanism for homeostasis in the hippocampus, using global chemical LTP induction (Roth-Alpermann et al., 2006). One possible mechanism might be the modulation of basal synaptic transmission. A possible candidate could interact with glutamatergic and GABAergic mechanisms to ensure a fine-tuned, fast and bidirectional effect.

It is known that CB1Rs are expressed on both glutamatergic and GABAergic axon terminals inhibiting the release of neurotransmitters (Heifets and Castillo, 2009). Further studies revealed the effect of THC on p70S6K in both Glu-$CB1^{-/-}$ and GABA-$CB1^{-/-}$ mice. P70S6K is a S6 kinase and its phosphorylated form activates the ribosomal protein S6 and therefore indirectly the rate of translation. While GABA-$CB1^{-/-}$ mice showed no increased phosphorylation levels Glu-$CB1^{-/-}$ mice had an increased phosphorylation of p70S6K. In addition, GABA-$CB1^{-/-}$ mice showed no deficits in memory consolidation after application of THC, while Glu-$CB1^{-/-}$ mice where indistinguishable to controls. These results suggest an

important role for the CB1R on GABAergic neurons in the effect of the 10 mg/kg THC (Puighermanal et al., 2009). A recent paper from this year (Ruehle et al., 2011) and unpublished data (personal communication Beat Lutz, Mainz, Germany) revealed a more detailed biphasic influence of THC on the ECS: at a low dose THC has an anxiolytic effect which than changes into an anxiogenic character at high doses. For the anxiolytic effect at low dose the CB1R on glutamatergic terminals is important. At a high dose of THC the CB1R on GABAergic terminals triggers anxiogenic behavior. All these experiments give rise to the role of the CB1R in homeostasis in the excitatory neuronal circuit. It is known that alterations in the influence of inhibitory GABAergic circuits can have profound impact on neuronal excitability and are associated with hyperexcitable states like epilepsy (Fritschy, 2008). On the other side, homeostatic plasticity is well investigated at excitatory components (Pozo and Goda, 2010;Rich and Wenner, 2007). CB1R as an important mediator of glutamatergic and GABAergic transmission may play a role in the homeostasis of this system. The homeostatic regulation of synaptic strength in response to persistent changes of neuronal activity plays an important role in maintaining the overall level of circuit activity within a normal range. Supporting data that gives evidence for the endocannabinoid-dependent homeostatic regulation of inhibitory synapses by mEPSCs was shown recently (Zhang et al., 2009).

4.3.3 Conclusions and Outlook

In the present study I could show that the CB1R restricts functional synaptic plasticity. By using two different mouse lines with a lack of the CB1R on either glutamatergic or GABAergic neurons I was able to show the opposing effects on LTP in the hippocampus. Previous work showed the effect of a full KO on LTP (Bohme et al., 2000) and application of a exogenous antagonists (Slanina et al., 2005). Together with the data of this thesis additionally future work is especially in the electrophysiological field necessary to investigate the role of the CB1R on synaptic transmission and synaptic homeostasis. Until now the role of the CB1R in the late phase of LTP is unknown. In this study it was shown that LTP is altered for up to one hour. In that time window, LTP is independent from gene transcription (Frey et al., 1996) and protein synthesis (Frey et al., 1988b). Further investigations may see an effect of the CB1R

on the late form of LTP. Despite of that, the deletion of the CB1R is very early in development and may affect developmental stages. To circumvent this, stereotaxic uses of a viral induced deletion of the *cnr1* gene in both subpopulations could be possible at later developmental stages or even later to prevent compensating effects of the loss of the CB1R. In addition, the GABAergic and glutamatergic mediated postsynaptic currents and the resting membrane potential in patch-clamp experiments in both subpopulations could give more evidence for the theory of the homeostatic effect of the ECS. In life-imaging experiments with calcium sensitive dyes the crucial role of calcium on the pre- and post-synapse could be further investigated in detail.

5. References

Reference List

1. Adams IB, Martin BR (1996) Cannabis: pharmacology and toxicology in animals and humans. Addiction 91:1585-1614.

2. Altman J, Das GD (1965) Autoradiographic and histological evidence of postnatal hippocampal neurogenesis in rats. J Comp Neurol 124:319-335.

3. Alvarez P, Zola-Morgan S, Squire LR (1994) The animal model of human amnesia: long-term memory impaired and short-term memory intact. Proc Natl Acad Sci U S A 91:5637-5641.

4. Ambrogini P, Lattanzi D, Ciuffoli S, Agostini D, Bertini L, Stocchi V, Santi S, Cuppini R (2004) Morpho-functional characterization of neuronal cells at different stages of maturation in granule cell layer of adult rat dentate gyrus. Brain Res 1017:21-31.

5. Ameri A (1999) The effects of cannabinoids on the brain. Prog Neurobiol 58:315-348.

6. Bacci A, Huguenard JR, Prince DA (2004) Long-lasting self-inhibition of neocortical interneurons mediated by endocannabinoids. Nature 431:312-316.

7. Bai F, Bergeron M, Nelson DL (2003) Chronic AMPA receptor potentiator (LY451646) treatment increases cell proliferation in adult rat hippocampus. Neuropharmacology 44:1013-1021.

8. Basavarajappa BS (2007) Neuropharmacology of the endocannabinoid signaling system-molecular mechanisms, biological actions and synaptic plasticity. Curr Neuropharmacol 5:81-97.

9. Begg M, Pacher P, Batkai S, Osei-Hyiaman D, Offertaler L, Mo FM, Liu J, Kunos G (2005) Evidence for novel cannabinoid receptors. Pharmacol Ther 106:133-145.

10. Bellocchio L, Lafenetre P, Cannich A, Cota D, Puente N, Grandes P, Chaouloff F, Piazza PV, Marsicano G (2010) Bimodal control of stimulated food intake by the endocannabinoid system. Nat Neurosci 13:281-283.

11. Bennett MV, Zukin RS (2004) Electrical coupling and neuronal synchronization in the Mammalian brain. Neuron 41:495-511.

12. Benninger F, Beck H, Wernig M, Tucker KL, Brustle O, Scheffler B (2003) Functional integration of embryonic stem cell-derived neurons in hippocampal slice cultures. J Neurosci 23:7075-7083.

13. Berninger B, Costa MR, Koch U, Schroeder T, Sutor B, Grothe B, Gotz M (2007a) Functional properties of neurons derived from in vitro reprogrammed postnatal astroglia. J Neurosci 27:8654-8664.

14. Berninger B, Costa MR, Koch U, Schroeder T, Sutor B, Grothe B, Gotz M (2007b) Functional properties of neurons derived from in vitro reprogrammed postnatal astroglia. J Neurosci 27:8654-8664.

15. Berninger B, Guillemot F, Gotz M (2007c) Directing neurotransmitter identity of neurones derived from expanded adult neural stem cells. Eur J Neurosci 25:2581-2590.

16. Berninger B, Guillemot F, Gotz M (2007d) Directing neurotransmitter identity of neurones derived from expanded adult neural stem cells. Eur J Neurosci 25:2581-2590.

17. Bibel M, Richter J, Lacroix E, Barde YA (2007) Generation of a defined and uniform population of CNS progenitors and neurons from mouse embryonic stem cells. Nat Protoc 2:1034-1043.

18. Bibel M, Richter J, Schrenk K, Tucker KL, Staiger V, Korte M, Goetz M, Barde YA (2004) Differentiation of mouse embryonic stem cells into a defined neuronal lineage. Nat Neurosci 7:1003-1009.

19. Bienenstock EL, Cooper LN, Munro PW (1982) Theory for the development of neuron selectivity: orientation specificity and binocular interaction in visual cortex. J Neurosci 2:32-48.

20. Bjorklund A, Lindvall O (2000) Parkinson disease gene therapy moves toward the clinic. Nat Med 6:1207-1208.

21. Bliss TV, Collingridge GL (1993) A synaptic model of memory: long-term potentiation in the hippocampus. Nature 361:31-39.

22. Bliss TV, Lomo T (1973) Long-lasting potentiation of synaptic transmission in the dentate area of the anaesthetized rabbit following stimulation of the perforant path. J Physiol 232:331-356.

23. Bohme GA, Laville M, Ledent C, Parmentier M, Imperato A (2000) Enhanced long-term potentiation in mice lacking cannabinoid CB1 receptors. Neuroscience 95:5-7.

24. Bolshakov VY, Siegelbaum SA (1994) Postsynaptic induction and presynaptic expression of hippocampal long-term depression. Science 264:1148-1152.

25. Bredt DS, Nicoll RA (2003) AMPA receptor trafficking at excitatory synapses. Neuron 40:361-379.

26. Brenowitz SD, Regehr WG (2003) Calcium dependence of retrograde inhibition by endocannabinoids at synapses onto Purkinje cells. J Neurosci 23:6373-6384.

27. Brindle PK, Montminy MR (1992) The CREB family of transcription activators. Curr Opin Genet Dev 2:199-204.

28. Brown SP, Brenowitz SD, Regehr WG (2003) Brief presynaptic bursts evoke synapse-specific retrograde inhibition mediated by endogenous cannabinoids. Nat Neurosci 6:1048-1057.

29. Cadas H, di TE, Piomelli D (1997) Occurrence and biosynthesis of endogenous cannabinoid precursor, N-arachidonoyl phosphatidylethanolamine, in rat brain. J Neurosci 17:1226-1242.

30. Cadas H, Gaillet S, Beltramo M, Venance L, Piomelli D (1996) Biosynthesis of an endogenous cannabinoid precursor in neurons and its control by calcium and cAMP. J Neurosci 16:3934-3942.

31. Cameron HA, McEwen BS, Gould E (1995) Regulation of adult neurogenesis by excitatory input and NMDA receptor activation in the dentate gyrus. J Neurosci 15:4687-4692.

32. Carlson G, Wang Y, Alger BE (2002) Endocannabinoids facilitate the induction of LTP in the hippocampus. Nat Neurosci 5:723-724.

33. Chevaleyre V, Castillo PE (2003) Heterosynaptic LTD of hippocampal GABAergic synapses: a novel role of endocannabinoids in regulating excitability. Neuron 38:461-472.

34. Chevaleyre V, Takahashi KA, Castillo PE (2006) Endocannabinoid-mediated synaptic plasticity in the CNS. Annu Rev Neurosci 29:37-76.

35. Clements JD, Lester RA, Tong G, Jahr CE, Westbrook GL (1992) The time course of glutamate in the synaptic cleft. Science 258:1498-1501.

36. Cline HT, Wu GY, Malinow R (1996) In vivo development of neuronal structure and function. Cold Spring Harb Symp Quant Biol 61:95-104.

37. Cravatt BF, Giang DK, Mayfield SP, Boger DL, Lerner RA, Gilula NB (1996) Molecular characterization of an enzyme that degrades neuromodulatory fatty-acid amides. Nature 384:83-87.

38. Cummings JA, Mulkey RM, Nicoll RA, Malenka RC (1996a) Ca2+ signaling requirements for long-term depression in the hippocampus. Neuron 16:825-833.

39. Cummings JA, Mulkey RM, Nicoll RA, Malenka RC (1996b) Ca2+ signaling requirements for long-term depression in the hippocampus. Neuron 16:825-833.

40. Davies SN, Pertwee RG, Riedel G (2002) Functions of cannabinoid receptors in the hippocampus. Neuropharmacology 42:993-1007.

41. Deisseroth K, Singla S, Toda H, Monje M, Palmer TD, Malenka RC (2004) Excitation-neurogenesis coupling in adult neural stem/progenitor cells. Neuron 42:535-552.

42. Deng W, Aimone JB, Gage FH (2010) New neurons and new memories: how does adult hippocampal neurogenesis affect learning and memory? Nat Rev Neurosci 11:339-350.

43. Devane WA, Dysarz FA, III, Johnson MR, Melvin LS, Howlett AC (1988) Determination and characterization of a cannabinoid receptor in rat brain. Mol Pharmacol 34:605-613.

44. Devane WA, Hanus L, Breuer A, Pertwee RG, Stevenson LA, Griffin G, Gibson D, Mandelbaum A, Etinger A, Mechoulam R (1992) Isolation and structure of a brain constituent that binds to the cannabinoid receptor. Science 258:1946-1949.

45. Di M, V, Deutsch DG (1998) Biochemistry of the endogenous ligands of cannabinoid receptors. Neurobiol Dis 5:386-404.

46. Dudek SM, Bear MF (1993) Bidirectional long-term modification of synaptic effectiveness in the adult and immature hippocampus. J Neurosci 13:2910-2918.

47. Ekstrom AD, Meltzer J, McNaughton BL, Barnes CA (2001) NMDA receptor antagonism blocks experience-dependent expansion of hippocampal "place fields". Neuron 31:631-638.

48. Elphick MR, Egertova M (2001) The neurobiology and evolution of cannabinoid signalling. Philos Trans R Soc Lond B Biol Sci 356:381-408.

49. Eriksson PS, Perfilieva E, Bjork-Eriksson T, Alborn AM, Nordborg C, Peterson DA, Gage FH (1998) Neurogenesis in the adult human hippocampus. Nat Med 4:1313-1317.

50. Esposito MS, Piatti VC, Laplagne DA, Morgenstern NA, Ferrari CC, Pitossi FJ, Schinder AF (2005) Neuronal differentiation in the adult hippocampus recapitulates embryonic development. J Neurosci 25:10074-10086.

51. Farovik A, Dupont LM, Eichenbaum H (2010) Distinct roles for dorsal CA3 and CA1 in memory for sequential nonspatial events. Learn Mem 17:12-17.

52. Freund TF, Katona I, Piomelli D (2003a) Role of endogenous cannabinoids in synaptic signaling. Physiol Rev 83:1017-1066.

53. Freund TF, Katona I, Piomelli D (2003b) Role of endogenous cannabinoids in synaptic signaling. Physiol Rev 83:1017-1066.

54. Frey U, Frey S, Schollmeier F, Krug M (1996) Influence of actinomycin D, a RNA synthesis inhibitor, on long-term potentiation in rat hippocampal neurons in vivo and in vitro. J Physiol 490 (Pt 3):703-711.

55. Frey U, Krug M, Reymann KG, Matthies H (1988a) Anisomycin, an inhibitor of protein synthesis, blocks late phases of LTP phenomena in the hippocampal CA1 region in vitro. Brain Res 452:57-65.

56. Frey U, Krug M, Reymann KG, Matthies H (1988b) Anisomycin, an inhibitor of protein synthesis, blocks late phases of LTP phenomena in the hippocampal CA1 region in vitro. Brain Res 452:57-65.

57. Fritschy JM (2008) Epilepsy, E/I Balance and GABA(A) Receptor Plasticity. Front Mol Neurosci 1:5.

58. Fritschy JM, Weinmann O, Wenzel A, Benke D (1998) Synapse-specific localization of NMDA and GABA(A) receptor subunits revealed by antigen-retrieval immunohistochemistry. J Comp Neurol 390:194-210.

59. Gage FH, Coates PW, Palmer TD, Kuhn HG, Fisher LJ, Suhonen JO, Peterson DA, Suhr ST, Ray J (1995) Survival and differentiation of adult neuronal progenitor cells transplanted to the adult brain. Proc Natl Acad Sci U S A 92:11879-11883.

60. Galiegue S, Mary S, Marchand J, Dussossoy D, Carriere D, Carayon P, Bouaboula M, Shire D, Le FG, Casellas P (1995) Expression of central and peripheral cannabinoid receptors in human immune tissues and leukocyte subpopulations. Eur J Biochem 232:54-61.

61. Ge S, Goh EL, Sailor KA, Kitabatake Y, Ming GL, Song H (2006) GABA regulates synaptic integration of newly generated neurons in the adult brain. Nature 439:589-593.

62. Giuffrida A, Parsons LH, Kerr TM, Rodriguez de FF, Navarro M, Piomelli D (1999) Dopamine activation of endogenous cannabinoid signaling in dorsal striatum. Nat Neurosci 2:358-363.

63. Grishin AA, Gee CE, Gerber U, Benquet P (2004) Differential calcium-dependent modulation of NMDA currents in CA1 and CA3 hippocampal pyramidal cells. J Neurosci 24:350-355.

64. Guan D, Horton LR, Armstrong WE, Foehring RC (2011) Postnatal development of A-type and Kv1- and Kv2-mediated potassium channel currents in neocortical pyramidal neurons. J Neurophysiol 105:2976-2988.

65. Gutman GA, Chandy KG, Grissmer S, Lazdunski M, McKinnon D, Pardo LA, Robertson GA, Rudy B, Sanguinetti MC, Stuhmer W, Wang X (2005) International Union of Pharmacology. LIII. Nomenclature and molecular relationships of voltage-gated potassium channels. Pharmacol Rev 57:473-508.

66. Hashimotodani Y, Ohno-Shosaku T, Kano M (2007) Endocannabinoids and synaptic function in the CNS. Neuroscientist 13:127-137.

67. Hashimotodani Y, Ohno-Shosaku T, Tsubokawa H, Ogata H, Emoto K, Maejima T, Araishi K, Shin HS, Kano M (2005) Phospholipase Cbeta serves as a coincidence detector through its Ca2+ dependency for triggering retrograde endocannabinoid signal. Neuron 45:257-268.

68. Hastings NB, Gould E (1999) Rapid extension of axons into the CA3 region by adult-generated granule cells. J Comp Neurol 413:146-154.

69. Heifets BD, Castillo PE (2009) Endocannabinoid signaling and long-term synaptic plasticity. Annu Rev Physiol 71:283-306.

70. Herkenham M (1991) Characterization and localization of cannabinoid receptors in brain: an in vitro technique using slide-mounted tissue sections. NIDA Res Monogr 112:129-145.

71. Herkenham M, Lynn AB, Johnson MR, Melvin LS, De Costa BR, Rice KC (1991) Characterization and localization of cannabinoid receptors in rat brain: a quantitative in vitro autoradiographic study. J Neurosci 11:563-583.

72. Herkenham M, Lynn AB, Little MD, Johnson MR, Melvin LS, de Costa BR, Rice KC (1990) Cannabinoid receptor localization in brain. Proc Natl Acad Sci U S A 87:1932-1936.

73. Hill MN, Hunter RG, McEwen BS (2009) Chronic stress differentially regulates cannabinoid CB1 receptor binding in distinct hippocampal subfields. Eur J Pharmacol 614:66-69.

74. Hillard CJ, Jarrahian A (2000) The movement of N-arachidonoylethanolamine (anandamide) across cellular membranes. Chem Phys Lipids 108:123-134.

75. Hodgkin AL, Huxley AF (1952) A quantitative description of membrane current and its application to conduction and excitation in nerve. J Physiol 117:500-544.

76. HODGKIN AL, HUXLEY AF, Katz B (1952) Measurement of current-voltage relations in the membrane of the giant axon of Loligo. J Physiol 116:424-448.

77. Honore T, Lauridsen J, Krogsgaard-Larsen P (1982) The binding of [3H]AMPA, a structural analogue of glutamic acid, to rat brain membranes. J Neurochem 38:173-178.

78. Howlett AC, Barth F, Bonner TI, Cabral G, Casellas P, Devane WA, Felder CC, Herkenham M, Mackie K, Martin BR, Mechoulam R, Pertwee RG (2002) International Union of Pharmacology. XXVII. Classification of cannabinoid receptors. Pharmacol Rev 54:161-202.

79. Hrabetova S, Sacktor TC (1996) Bidirectional regulation of protein kinase M zeta in the maintenance of long-term potentiation and long-term depression. J Neurosci 16:5324-5333.

80. Husseini L, Schmandt T, Scheffler B, Schroder W, Seifert G, Brustle O, Steinhauser C (2008) Functional analysis of embryonic stem cell-derived glial cells after integration into hippocampal slice cultures. Stem Cells Dev 17:1141-1152.

81. Isokawa M, Alger BE (2005) Retrograde endocannabinoid regulation of GABAergic inhibition in the rat dentate gyrus granule cell. J Physiol 567:1001-1010.

82. Isom LL (2001) Sodium channel beta subunits: anything but auxiliary. Neuroscientist 7:42-54.

83. Johnston D, Williams S, Jaffe D, Gray R (1992) NMDA-receptor-independent long-term potentiation. Annu Rev Physiol 54:489-505.

84. Jonas P, Sakmann B (1992) Glutamate receptor channels in isolated patches from CA1 and CA3 pyramidal cells of rat hippocampal slices. J Physiol 455:143-171.

85. Kaplan MS, Hinds JW (1977) Neurogenesis in the adult rat: electron microscopic analysis of light radioautographs. Science 197:1092-1094.

86. Kato K, Sekino Y, Takahashi H, Yasuda H, Shirao T (2007) Increase in AMPA receptor-mediated miniature EPSC amplitude after chronic NMDA receptor blockade in cultured hippocampal neurons. Neurosci Lett 418:4-8.

87. Katoh-Semba R, Asano T, Ueda H, Morishita R, Takeuchi IK, Inaguma Y, Kato K (2002) Riluzole enhances expression of brain-derived neurotrophic factor with consequent proliferation of granule precursor cells in the rat hippocampus. FASEB J 16:1328-1330.

88. Katona I, Sperlagh B, Magloczky Z, Santha E, Kofalvi A, Czirjak S, Mackie K, Vizi ES, Freund TF (2000) GABAergic interneurons are the targets of cannabinoid actions in the human hippocampus. Neuroscience 100:797-804.

89. Katona I, Sperlagh B, Sik A, Kafalvi A, Vizi ES, Mackie K, Freund TF (1999) Presynaptically located CB1 cannabinoid receptors regulate GABA release from axon terminals of specific hippocampal interneurons. J Neurosci 19:4544-4558.

90. Kauderer BS, Kandel ER (2000) Capture of a protein synthesis-dependent component of long-term depression. Proc Natl Acad Sci U S A 97:13342-13347.

91. Kawamura Y, Fukaya M, Maejima T, Yoshida T, Miura E, Watanabe M, Ohno-Shosaku T, Kano M (2006) The CB1 cannabinoid receptor is the major cannabinoid receptor at excitatory presynaptic sites in the hippocampus and cerebellum. J Neurosci 26:2991-3001.

92. Kelleher RJ, III, Govindarajan A, Tonegawa S (2004) Translational regulatory mechanisms in persistent forms of synaptic plasticity. Neuron 44:59-73.

93. Kleppisch T, Wolfsgruber W, Feil S, Allmann R, Wotjak CT, Goebbels S, Nave KA, Hofmann F, Feil R (2003) Hippocampal cGMP-dependent protein kinase I supports an age- and protein

synthesis-dependent component of long-term potentiation but is not essential for spatial reference and contextual memory. J Neurosci 23:6005-6012.

94. Kornack DR, Rakic P (1999) Continuation of neurogenesis in the hippocampus of the adult macaque monkey. Proc Natl Acad Sci U S A 96:5768-5773.

95. Kreitzer AC, Regehr WG (2001a) Cerebellar depolarization-induced suppression of inhibition is mediated by endogenous cannabinoids. J Neurosci 21:RC174.

96. Kreitzer AC, Regehr WG (2001b) Retrograde inhibition of presynaptic calcium influx by endogenous cannabinoids at excitatory synapses onto Purkinje cells. Neuron 29:717-727.

97. Krug M, Lossner B, Ott T (1984) Anisomycin blocks the late phase of long-term potentiation in the dentate gyrus of freely moving rats. Brain Res Bull 13:39-42.

98. Kuhn HG, Dickinson-Anson H, Gage FH (1996) Neurogenesis in the dentate gyrus of the adult rat: age-related decrease of neuronal progenitor proliferation. J Neurosci 16:2027-2033.

99. Laaris N, Good CH, Lupica CR (2010) Delta9-tetrahydrocannabinol is a full agonist at CB1 receptors on GABA neuron axon terminals in the hippocampus. Neuropharmacology 59:121-127.

100. Lafenetre P, Chaouloff F, Marsicano G (2009) Bidirectional regulation of novelty-induced behavioral inhibition by the endocannabinoid system. Neuropharmacology 57:715-721.

101. Lee HK, Kameyama K, Huganir RL, Bear MF (1998) NMDA induces long-term synaptic depression and dephosphorylation of the GluR1 subunit of AMPA receptors in hippocampus. Neuron 21:1151-1162.

102. Legendre P, Rosenmund C, Westbrook GL (1993) Inactivation of NMDA channels in cultured hippocampal neurons by intracellular calcium. J Neurosci 13:674-684.

103. Lie DC, Colamarino SA, Song HJ, Desire L, Mira H, Consiglio A, Lein ES, Jessberger S, Lansford H, Dearie AR, Gage FH (2005) Wnt signalling regulates adult hippocampal neurogenesis. Nature 437:1370-1375.

104. Ling DS, Benardo LS, Serrano PA, Blace N, Kelly MT, Crary JF, Sacktor TC (2002) Protein kinase Mzeta is necessary and sufficient for LTP maintenance. Nat Neurosci 5:295-296.

105. Lisman J (1989) A mechanism for the Hebb and the anti-Hebb processes underlying learning and memory. Proc Natl Acad Sci U S A 86:9574-9578.

106. Lisman J, Schulman H, Cline H (2002) The molecular basis of CaMKII function in synaptic and behavioural memory. Nat Rev Neurosci 3:175-190.

107. Liu X, Wang Q, Haydar TF, Bordey A (2005) Nonsynaptic GABA signaling in postnatal subventricular zone controls proliferation of GFAP-expressing progenitors. Nat Neurosci 8:1179-1187.

108. Liu YB, Lio PA, Pasternak JF, Trommer BL (1996) Developmental changes in membrane properties and postsynaptic currents of granule cells in rat dentate gyrus. J Neurophysiol 76:1074-1088.

109. Llano I, Leresche N, Marty A (1991) Calcium entry increases the sensitivity of cerebellar Purkinje cells to applied GABA and decreases inhibitory synaptic currents. Neuron 6:565-574.

110. Lledo PM, Alonso M, Grubb MS (2006) Adult neurogenesis and functional plasticity in neuronal circuits. Nat Rev Neurosci 7:179-193.

111. Llinas R, Steinberg IZ, Walton K (1981) Relationship between presynaptic calcium current and postsynaptic potential in squid giant synapse. Biophys J 33:323-351.

112. Lois C, Alvarez-Buylla A (1993) Proliferating subventricular zone cells in the adult mammalian forebrain can differentiate into neurons and glia. Proc Natl Acad Sci U S A 90:2074-2077.

113. Lynch MA (2004) Long-term potentiation and memory. Physiol Rev 84:87-136.

114. Maass W, Zador AM (1999) Dynamic stochastic synapses as computational units. Neural Comput 11:903-917.

115. Maccarrone M, van der Stelt M, Rossi A, Veldink GA, Vliegenthart JF, Agro AF (1998) Anandamide hydrolysis by human cells in culture and brain. J Biol Chem 273:32332-32339.

116. Mackie K, Hille B (1992) Cannabinoids inhibit N-type calcium channels in neuroblastoma-glioma cells. Proc Natl Acad Sci U S A 89:3825-3829.

117. Maejima T, Hashimoto K, Yoshida T, Aiba A, Kano M (2001) Presynaptic inhibition caused by retrograde signal from metabotropic glutamate to cannabinoid receptors. Neuron 31:463-475.

118. Magnuson DS, Morassutti DJ, Staines WA, McBurney MW, Marshall KC (1995) In vivo electrophysiological maturation of neurons derived from a multipotent precursor (embryonal carcinoma) cell line. Brain Res Dev Brain Res 84:130-141.

119. Malenka RC (2003) The long-term potential of LTP. Nat Rev Neurosci 4:923-926.

120. Malenka RC, Kauer JA, Perkel DJ, Mauk MD, Kelly PT, Nicoll RA, Waxham MN (1989) An essential role for postsynaptic calmodulin and protein kinase activity in long-term potentiation. Nature 340:554-557.

121. Malenka RC, Kauer JA, Zucker RS, Nicoll RA (1988) Postsynaptic calcium is sufficient for potentiation of hippocampal synaptic transmission. Science 242:81-84.

122. Malenka RC, Nicoll RA (1999) Long-term potentiation--a decade of progress? Science 285:1870-1874.

123. Malinow R, Malenka RC (2002) AMPA receptor trafficking and synaptic plasticity. Annu Rev Neurosci 25:103-126.

124. Malinow R, Schulman H, Tsien RW (1989) Inhibition of postsynaptic PKC or CaMKII blocks induction but not expression of LTP. Science 245:862-866.

125. Manahan-Vaughan D, Kulla A, Frey JU (2000) Requirement of translation but not transcription for the maintenance of long-term depression in the CA1 region of freely moving rats. J Neurosci 20:8572-8576.

126. Martin SJ, Grimwood PD, Morris RG (2000) Synaptic plasticity and memory: an evaluation of the hypothesis. Annu Rev Neurosci 23:649-711.

127. Matsuda LA, Lolait SJ, Brownstein MJ, Young AC, Bonner TI (1990) Structure of a cannabinoid receptor and functional expression of the cloned cDNA. Nature 346:561-564.

128. Mayer ML, Westbrook GL, Guthrie PB (1984) Voltage-dependent block by Mg2+ of NMDA responses in spinal cord neurones. Nature 309:261-263.

129. Mayr B, Montminy M (2001) Transcriptional regulation by the phosphorylation-dependent factor CREB. Nat Rev Mol Cell Biol 2:599-609.

130. Millan MJ (2003) The neurobiology and control of anxious states. Prog Neurobiol 70:83-244.

131. Ming GL, Song H (2005) Adult neurogenesis in the mammalian central nervous system. Annu Rev Neurosci 28:223-250.

132. Monyer H, Burnashev N, Laurie DJ, Sakmann B, Seeburg PH (1994) Developmental and regional expression in the rat brain and functional properties of four NMDA receptors. Neuron 12:529-540.

133. Mulkey RM, Herron CE, Malenka RC (1993) An essential role for protein phosphatases in hippocampal long-term depression. Science 261:1051-1055.

134. Munro S, Thomas KL, Abu-Shaar M (1993) Molecular characterization of a peripheral receptor for cannabinoids. Nature 365:61-65.

135. Nagerl UV, Eberhorn N, Cambridge SB, Bonhoeffer T (2004) Bidirectional activity-dependent morphological plasticity in hippocampal neurons. Neuron 44:759-767.

136. Natarajan V, Reddy PV, Schmid PC, Schmid HH (1982) N-Acylation of ethanolamine phospholipids in canine myocardium. Biochim Biophys Acta 712:342-355.

137. Naus CC, Bani-Yaghoub M (1998) Gap junctional communication in the developing central nervous system. Cell Biol Int 22:751-763.

138. Neuser F (2010) Integration of ES cell-derived neurons into pre-existing neuronal curcuits.

139. Nikoletopoulou V, Plachta N, Allen ND, Pinto L, Gotz M, Barde YA (2007) Neurotrophin receptor-mediated death of misspecified neurons generated from embryonic stem cells lacking Pax6. Cell Stem Cell 1:529-540.

140. Nowak L, Bregestovski P, Ascher P, Herbet A, Prochiantz A (1984) Magnesium gates glutamate-activated channels in mouse central neurones. Nature 307:462-465.

141. Ohno-Shosaku T, Shosaku J, Tsubokawa H, Kano M (2002a) Cooperative endocannabinoid production by neuronal depolarization and group I metabotropic glutamate receptor activation. Eur J Neurosci 15:953-961.

142. Ohno-Shosaku T, Tsubokawa H, Mizushima I, Yoneda N, Zimmer A, Kano M (2002b) Presynaptic cannabinoid sensitivity is a major determinant of depolarization-induced retrograde suppression at hippocampal synapses. J Neurosci 22:3864-3872.

143. Otani S, Abraham WC (1989) Inhibition of protein synthesis in the dentate gyrus, but not the entorhinal cortex, blocks maintenance of long-term potentiation in rats. Neurosci Lett 106:175-180.

144. Pacher P, Batkai S, Kunos G (2006) The endocannabinoid system as an emerging target of pharmacotherapy. Pharmacol Rev 58:389-462.

145. Pastalkova E, Serrano P, Pinkhasova D, Wallace E, Fenton AA, Sacktor TC (2006) Storage of spatial information by the maintenance mechanism of LTP. Science 313:1141-1144.

146. Pertwee RG (2006) The pharmacology of cannabinoid receptors and their ligands: an overview. Int J Obes (Lond) 30 Suppl 1:S13-S18.

147. Piomelli D (2003) The molecular logic of endocannabinoid signalling. Nat Rev Neurosci 4:873-884.

148. Pitler TA, Alger BE (1992) Postsynaptic spike firing reduces synaptic GABAA responses in hippocampal pyramidal cells. J Neurosci 12:4122-4132.

149. Plachta N, Bibel M, Tucker KL, Barde YA (2004) Developmental potential of defined neural progenitors derived from mouse embryonic stem cells. Development 131:5449-5456.

150. Pongs O (1999) Voltage-gated potassium channels: from hyperexcitability to excitement. FEBS Lett 452:31-35.

151. Pozo K, Goda Y (2010) Unraveling mechanisms of homeostatic synaptic plasticity. Neuron 66:337-351.

152. Puighermanal E, Marsicano G, Busquets-Garcia A, Lutz B, Maldonado R, Ozaita A (2009) Cannabinoid modulation of hippocampal long-term memory is mediated by mTOR signaling. Nat Neurosci 12:1152-1158.

153. Rich MM, Wenner P (2007) Sensing and expressing homeostatic synaptic plasticity. Trends Neurosci 30:119-125.

154. Ronesi J, Gerdeman GL, Lovinger DM (2004) Disruption of endocannabinoid release and striatal long-term depression by postsynaptic blockade of endocannabinoid membrane transport. J Neurosci 24:1673-1679.

155. Roth-Alpermann C, Morris RG, Korte M, Bonhoeffer T (2006) Homeostatic shutdown of long-term potentiation in the adult hippocampus. Proc Natl Acad Sci U S A 103:11039-11044.

156. Ruehle S, Aparisi RA, Remmers F, Lutz B (2011) The endocannabinoid system in anxiety, fear memory and habituation. J Psychopharmacol.

157. Safo PK, Regehr WG (2005) Endocannabinoids control the induction of cerebellar LTD. Neuron 48:647-659.

158. Sah P (1996) Ca(2+)-activated K+ currents in neurones: types, physiological roles and modulation. Trends Neurosci 19:150-154.

159. Sajikumar S, Navakkode S, Frey JU (2005a) Protein synthesis-dependent long-term functional plasticity: methods and techniques. Curr Opin Neurobiol 15:607-613.

160. Sajikumar S, Navakkode S, Sacktor TC, Frey JU (2005b) Synaptic tagging and cross-tagging: the role of protein kinase Mzeta in maintaining long-term potentiation but not long-term depression. J Neurosci 25:5750-5756.

161. Savinainen JR, Saario SM, Laitinen JT (2011) The serine hydrolases MAGL, ABHD6 and ABHD12 as guardians of 2-arachidonoylglycerol signalling through cannabinoid receptors. Acta Physiol (Oxf).

162. Schlicker E, Kathmann M (2001) Modulation of transmitter release via presynaptic cannabinoid receptors. Trends Pharmacol Sci 22:565-572.

163. Schmidt-Hieber C, Jonas P, Bischofberger J (2004) Enhanced synaptic plasticity in newly generated granule cells of the adult hippocampus. Nature 429:184-187.

164. Scoville WB, Milner B (1957) Loss of recent memory after bilateral hippocampal lesions. J Neurol Neurosurg Psychiatry 20:11-21.

165. Sjostrom PJ, Turrigiano GG, Nelson SB (2003) Neocortical LTD via coincident activation of presynaptic NMDA and cannabinoid receptors. Neuron 39:641-654.

166. Skrede KK, Westgaard RH (1971) The transverse hippocampal slice: a well-defined cortical structure maintained in vitro. Brain Res 35:589-593.

167. Slanina KA, Roberto M, Schweitzer P (2005) Endocannabinoids restrict hippocampal long-term potentiation via CB1. Neuropharmacology 49:660-668.

168. Snyder JS, Choe JS, Clifford MA, Jeurling SI, Hurley P, Brown A, Kamhi JF, Cameron HA (2009) Adult-born hippocampal neurons are more numerous, faster maturing, and more involved in behavior in rats than in mice. J Neurosci 29:14484-14495.

169. Stanfield BB, Trice JE (1988) Evidence that granule cells generated in the dentate gyrus of adult rats extend axonal projections. Exp Brain Res 72:399-406.

170. Steiner MA, Marsicano G, Wotjak CT, Lutz B (2008) Conditional cannabinoid receptor type 1 mutants reveal neuron subpopulation-specific effects on behavioral and neuroendocrine stress responses. Psychoneuroendocrinology 33:1165-1170.

171. Stella N, Piomelli D (2001) Receptor-dependent formation of endogenous cannabinoids in cortical neurons. Eur J Pharmacol 425:189-196.

172. Stella N, Schweitzer P, Piomelli D (1997) A second endogenous cannabinoid that modulates long-term potentiation. Nature 388:773-778.

173. Stromgaard K, Mellor I (2004) AMPA receptor ligands: synthetic and pharmacological studies of polyamines and polyamine toxins. Med Res Rev 24:589-620.

174. Tashiro A, Sandler VM, Toni N, Zhao C, Gage FH (2006) NMDA-receptor-mediated, cell-specific integration of new neurons in adult dentate gyrus. Nature 442:929-933.

175. Tozuka Y, Fukuda S, Namba T, Seki T, Hisatsune T (2005) GABAergic excitation promotes neuronal differentiation in adult hippocampal progenitor cells. Neuron 47:803-815.

176. Tsou K, Brown S, Sanudo-Pena MC, Mackie K, Walker JM (1998) Immunohistochemical distribution of cannabinoid CB1 receptors in the rat central nervous system. Neuroscience 83:393-411.

177. Turrigiano GG (1999) Homeostatic plasticity in neuronal networks: the more things change, the more they stay the same. Trends Neurosci 22:221-227.

178. Turu G, Varnai P, Gyombolai P, Szidonya L, Offertaler L, Bagdy G, Kunos G, Hunyady L (2009) Paracrine transactivation of the CB1 cannabinoid receptor by AT1 angiotensin and other Gq/11 protein-coupled receptors. J Biol Chem 284:16914-16921.

179. van PH, Schinder AF, Christie BR, Toni N, Palmer TD, Gage FH (2002) Functional neurogenesis in the adult hippocampus. Nature 415:1030-1034.

180. Varma N, Carlson GC, Ledent C, Alger BE (2001) Metabotropic glutamate receptors drive the endocannabinoid system in hippocampus. J Neurosci 21:RC188.

181. Vautrin J, Barker JL (2003) Presynaptic quantal plasticity: Katz's original hypothesis revisited. Synapse 47:184-199.

182. Wall ME, Brine DR, Brine GA, Pitt CG, Freudenthal RI, Christensen HD (1970) Isolation, structure, and biological activity of several metabolites of delta-9-tetrahydrocannabinol. J Am Chem Soc 92:3466-3468.

183. Wang J, Ueda N (2009) Biology of endocannabinoid synthesis system. Prostaglandins Other Lipid Mediat 89:112-119.

184. Wang J, Zucker RS (2001) Photolysis-induced suppression of inhibition in rat hippocampal CA1 pyramidal neurons. J Physiol 533:757-763.

185. Wernig M, Benninger F, Schmandt T, Rade M, Tucker KL, Bussow H, Beck H, Brustle O (2004) Functional integration of embryonic stem cell-derived neurons in vivo. J Neurosci 24:5258-5268.

186. Whitlock JR, Heynen AJ, Shuler MG, Bear MF (2006) Learning induces long-term potentiation in the hippocampus. Science 313:1093-1097.

187. Wigstrom H, Gustafsson B (1985) Facilitation of hippocampal long-lasting potentiation by GABA antagonists. Acta Physiol Scand 125:159-172.

188. Wu SX, Goebbels S, Nakamura K, Nakamura K, Kometani K, Minato N, Kaneko T, Nave KA, Tamamaki N (2005) Pyramidal neurons of upper cortical layers generated by NEX-positive progenitor cells in the subventricular zone. Proc Natl Acad Sci U S A 102:17172-17177.

189. Wurmser AE, Nakashima K, Summers RG, Toni N, D'Amour KA, Lie DC, Gage FH (2004) Cell fusion-independent differentiation of neural stem cells to the endothelial lineage. Nature 430:350-356.

190. Yasuda H, Barth AL, Stellwagen D, Malenka RC (2003) A developmental switch in the signaling cascades for LTP induction. Nat Neurosci 6:15-16.

191. Yoshimura Y, Tsumoto T (1994) Dependence of LTP induction on postsynaptic depolarization: a perforated patch-clamp study in visual cortical slices of young rats. J Neurophysiol 71:1638-1645.

192. Yuste R, Bonhoeffer T (2001) Morphological changes in dendritic spines associated with long-term synaptic plasticity. Annu Rev Neurosci 24:1071-1089.

193. Zerucha T, Stuhmer T, Hatch G, Park BK, Long Q, Yu G, Gambarotta A, Schultz JR, Rubenstein JL, Ekker M (2000) A highly conserved enhancer in the Dlx5/Dlx6 intergenic region is the site of cross-regulatory interactions between Dlx genes in the embryonic forebrain. J Neurosci 20:709-721.

194. Zhang SY, Xu M, Miao QL, Poo MM, Zhang XH (2009) Endocannabinoid-dependent homeostatic regulation of inhibitory synapses by miniature excitatory synaptic activities. J Neurosci 29:13222-13231.

195. Zhao C, Teng EM, Summers RG, Jr., Ming GL, Gage FH (2006) Distinct morphological stages of dentate granule neuron maturation in the adult mouse hippocampus. J Neurosci 26:3-11.

196. Zhou Q, Homma KJ, Poo MM (2004) Shrinkage of dendritic spines associated with long-term depression of hippocampal synapses. Neuron 44:749-757.

197. Zhuo M (2009) Plasticity of NMDA receptor NR2B subunit in memory and chronic pain. Mol Brain 2:4.

6. Supplement

Acknowledgements

Mein größter Dank gilt meinem Doktorvater Professor Dr. Martin Korte, für die Möglichkeit meine Promotion in der Arbeitsgruppe durchführen zu können. Er konnte mir die Widrigkeiten des wissenschaftlichen Alltags und ihre Umschiffung näher bringen.

Ich danke Herrn Prof. Dr. Reinhard Köster für die freundliche Übernahme des Koreferats sowie Herrn Prof. Ralf-Rainer Mendel für den Vorsitz der Prüfungskommission. Weiterhin danke ich Prof. Beat Lutz für die freundliche Bereitstellung der CB1-Tiere.

Dr. Franziska Neuser danke ich für die Arbeit, die sie in das Transplantationsprojekt gesteckt hat, ohne Sie wären die Messungen nicht in dieser Art möglich gewesen. Dr. Kristin Michaelsen-Preusse danke ich für die letzten Jahre voller wissenschaftlicher Erfahrungen im Labor und zoologischen Erlebnissen auf Helgoland und in der Oberlausitz. Für alle Hilfen in Lehre und dem Laboralltag danke ich Dr. Martin Rothkegel. Dr. Marta Zagrebelsky-Holz danke ich für Ihre kritische Einstellung zu ziemlich jedem Sachverhalt. Den promovierten Kreis schließt Dr. Andrea Delekate, die mit mir die letzten Jahre sowohl Büro, als auch Setups geteilt hat. Wir haben eine Menge Kabel gesteckt, Geräte programmiert und Brummen beseitigt.

Mein besonderer Dank gilt Diane Mundil. Die Mischung aus absoluter professioneller Routine und gleichzeitigem Drang nach Neuem haben mich beeindruckt und ohne sie würde der AG eine Menge Menschlichkeit fehlen. Reinhard Huwe danke ich dafür immer für alle technischen Anfragen Zeit zu haben. Außerdem für unzählige Frühstückspausen, surreale Diskussionen und die Zeit, die ich während Studium und Dissertation im Feld mit ihm verbringen durfte. Ebenfalls danke ich Angela Traudt für die Unterstützung in den letzten Jahren hinsichtlich Ozeanen an frischer ACSF und für meterweise Goldfäden.

Weiterhin bedanke ich mich bei Anita Remus für die Übernahme der BDNF-Zucht und die Zeit, die sie darin investiert hat. Ich durfte mit vielen jungen Wissenschaftlern zusammen arbeiten, denen ich hiermit alles Gute auf dem weiteren Weg wünsche: Dr. Claudia Bohner, Dr. Nicole Fanselow, Dr. Susanne Kilian, Dr. Daniel Minge, Arne Buschler, Michael Kintscher, Ulrike Herrmann, Melissa O´Brien und Stefanie Schweinhuber. Eine weitere Instanz im Zoologischen Institut ist Frau Ursula Behrendt, ohne sie würde die Bürokratie über die Wissenschaft siegen. Aber natürlich danke ich auch allen anderen Mitgliedern der Arbeitsgruppe für jegliche Unterstützung.

Sabine danke ich für die schönen, glücklichen und erleuchtenden letzten 2 Jahre, die wir in und außerhalb des Labors verbracht haben. Danke.

CURRICULUM VITAE

PERSONAL DATA

Name:	Martin Polack
Date of birth:	October 23th, 1979 in Wolfenbuettel, Germany

EDUCATION

Since 11/2006	PhD-Student at the Institute of Technology, TU Braunschweig, Zoological Institute, Division of Cellular Neurobiology in the group of Professor Dr. Martin Korte. Topic: "Functional plasticity in the brain. Neuronal integration of ES cell-derived neurons in the hippocampus and the influence of the endocannabinoid system on synaptic plasticity"
10/2001 - 10/2006	Studies of Biology at the TU Braunschweig Diploma thesis: "Electrophysiological survey about the potentially influence of Nogo-A on synaptic plasticity in the mouse hippocampus" in the group of Prof. Korte.
08/2000 – 06/2001	Civilian service at "Paritaetischer Dienst" in Wolfenbuettel
08/1995 – 06/2000	Attendance at academic high school "Theodor-Heuss Gymnasium"; Qualification: university-entrance diploma "Abitur"

PUBLICATIONS

Biosynthesis and processing of endogenous BDNF: CNS neurons store and secrete BDNF, not pro-BDNF
Matsumoto, T., Rauskolb, S., Polack, M., Klose, J., Kolbeck, R., Korte, M., Barde, Y.-A.
Nature Neuroscience 11 (2), pp. 131-133

Neurotrophin receptors TrkB.T1 and p75NTR cooperate in modulating both functional and structural plasticity in mature hippocampal neurons
Michaelsen, K., Zagrebelsky, M., Berndt-Huch, J., Polack, M., Buschler, A., Sendtner, M., Korte, M.
European Journal of Neuroscience 32 (11), pp. 1854-1865